

**MODELLING AND CONTROL  
OF A CO-CURRENT SUGAR DRYER**

By  
Benoit Lacave

Submitted in fulfilment of the requirements for the degree of Master of Science in Engineering  
in the school of Chemical Engineering, University of Natal, Durban

Durban  
November 2001

*A mes parents,  
ma soeur*

## ABSTRACT

The drying of sugar is the last step in the recovery of solid sugar from sugar-cane. To ensure that the sugar can be transported and stored, the final moisture content leaving the sugar mill must be carefully controlled.

Data spanning periods of normal plant operation were collected at the Tongaat-Hulett Ltd Darnall sugar mill. These measurements were reconciled to achieve instantaneous mass and energy balances across the sugar dryer.

Using these measurements, a general model has been developed to simulate the sugar drying. It includes ten compartments through which the sugar and drying air flow, with a mass and energy balance in each compartment. It was assumed that a "film" around the sugar crystal is supersaturated, and that crystallisation is still occurring. A sorption isotherm determining the equilibrium moisture content of the sugar, at which point mass transfer ceases, was included. The model has been matched to process measurements by adjusting the heat and mass transfer coefficients.

A Dynamic Matrix Controller was developed and tested off-line on the model, using the reconciled measurement sequences. The controller manipulated the inlet air temperature in order to control the exit sugar moisture content. The model predictive control format successfully dealt with the large process dead-time (5 minutes).

## PREFACE

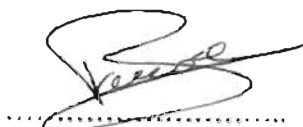
Tongaat-Hulett Sugar Ltd initiated this project to have access to heat and mass transfer coefficients in the process of drying sugar in a co-current rotary dryer, and to investigate improved control algorithms for exit moisture content.

The investigation required data collected from the Damall sugar mill, in the North coast of Kwazulu-Natal. Other studies were made in the postgraduate offices of the School of Chemical Engineering at the University of Natal, Durban under the supervision of Professor Michael Mulholland.

The following courses were completed with the corresponding credits and results achieved:

DNC4DC1	Process Dynamics and Control	(16.0)	64%
DNC5RT1	Real Time Process Data Analysis	(16.0)	70%

I hereby declare that this dissertation is my own work, unless stated to the contrary in the text, and that it has not been submitted for a degree to any other university or institution.



B. Lacave

2002.06.12

Date

As the candidate's supervisor I have / ~~have not~~ approved this dissertation for submission

Signed: m. mulholland Name: m. MULHOLLAND Date: 2002.06.12

## ACKNOWLEDGEMENTS

I would like to express my sincere gratitude to the following people:

My supervisor, Professor Michael Mulholland. He helped me so many times in my work and my stay in South Africa.

The National Research Foundation of South Africa and the Centre National de Recherche Scientifique of France for their financial assistance and co-operation for this project.

The University of Natal and the Ecole Nationale Supérieure d'Ingénieurs de Génie Chimique (France) for having settled an agreement allowing my study here.

Professor Marie-Véronique Le Lann in France. She did everything to make my stay here possible.

The Tongaat-Hulett Sugar Ltd company for having purposed and funded this project. Farouk Ahmed for having been a great intermediary between Natal University and Tongaat-Hulett Ltd. People from the Darnall sugar mill for their help when I was collecting the data.

Mr Raoul Lionnet from the Sugar Milling Research Institute for having made things easier with his French.

My colleagues and friends from the School of Chemical Engineering and from all around the world for their support.

My family who have believed in me when I decided to leave.

# TABLE OF CONTENTS

<b>Abstract</b>	<b>iii</b>
<b>Preface</b>	<b>iv</b>
<b>Acknowledgments</b>	<b>v</b>
<b>Table of contents</b>	<b>vi</b>
<b>List of Figures</b>	<b>x</b>
<b>List of tables</b>	<b>xii</b>
<b>List of Symbols</b>	<b>xiii</b>
<b><i>Chapter 1 Introduction</i></b>	<b><i>1-1</i></b>
1.1 LAYOUT OF THIS DISSERTATION	1-1
1.2 DRYING	1-1
1.2.1 Process	1-1
1.2.2 Dryers	1-2
1.3 SUGAR DRYING	1-4
1.3.1 Different types of moisture	1-4
1.3.2 Drying process	1-4
1.3.3 Drying Model	1-4
1.4 CRYSTALLISATION	1-6
1.5 DATA RECONCILIATION	1-7
1.6 CONTROL	1-7
1.6.1 Predictive Control	1-7
1.6.2 Dynamic Matrix Control	1-7
1.7 DRYER CONTROL	1-8
<b><i>Chapter 2 The dryer considered in this study</i></b>	<b><i>2-1</i></b>
2.1 THE PLANT	2-1
2.1.1 Description of the equipment	2-1
2.1.2 Description of the process	2-2
2.1.3 The instrumentation	2-2
2.1.4 Pictures of the dryer	2-3
<b><i>Chapter 3 Data collection</i></b>	<b><i>3-1</i></b>
3.1 ON - LINE DATA COLLECTION	3-1

3.1.1	Air flow	3-1
3.1.2	Sugar flow	3-1
3.1.3	Moisture in the air at the entrance	3-2
3.2	DATA TREATMENT	3-3
3.2.1	Relation between $H_A$ and $W_A$	3-3
3.2.2	Balances	3-3
3.2.3	Transformation to obtain suitable $W_{S0}$	3-8
3.2.4	Final reconciled data set	3-9
3.2.5	Discussion	3-15
	3.2.5.1 Temperature	3-15
	3.2.5.2 Moisture	3-16
	<b>Chapter 4 Model</b>	<b>4-1</b>
4.1	MODEL OF THE DRYER	4-1
4.1.1	Theory	4-1
4.1.2	The model	4-2
	4.1.2.1 Partial pressure drying force from moisture content	4-3
	4.1.2.2 Sugar hold up volume fraction $h_s$	4-4
	4.1.2.3 Crystallisation	4-4
	4.1.2.4 Air flow	4-5
	4.1.2.5 Discretisation of spatial derivatives	4-6
4.2	AXIAL DISPERSION	4-7
4.2.1	Theory	4-7
4.2.2	Comparison of theoretical and modelled axial dispersion	4-9
	4.2.2.1 Improved convections	4-9
	4.2.2.2 Results	4-11
4.3	MOISTURE CONTENT - ISOTHERM	4-13
4.4	THE HEAT AND MASS TRANSFER COEFFICIENT	4-16
4.4.1	Results	4-16
4.4.2	Discussion	4-22
	4.4.2.1 Moisture content	4-22
	4.4.2.2 Temperature	4-22
	4.4.2.3 Dissolved sucrose $S_{Fn}$	4-22

## **Chapter 5 Adaptive control** **5-1**

5.1	DYNAMIC MATRIX CONTROL THEORY	5-1
-----	-------------------------------	-----

5.1.1	Definition	5-1
5.1.2	Theory	5-1
5.2	APPLICATION TO EXIT MOISTURE CONTROL	5-6
5.3	THE STRUCTURE OF THE PROGRAM	5-8
5.3.1	Initialisation	5-8
5.3.2	Model	5-8
	5.2.3.1 Present operating conditions	5-8
	5.2.3.2 Heat and mass transfer coefficients	5-8
	5.2.3.3 Determination of the vector flow $f_A$	5-9
	5.2.3.4 Initialisation of $X$ and $U$	5-9
	5.2.3.5 Control computations	5-9
	5.2.3.6 Axial Convection	5-9
	5.2.3.7 Tuning of A and B matrices	5-9
	5.2.3.8 Integration	5-9
5.3.3	Control	5-9
	5.3.3.1 Dynamic matrix control	5-9
5.3.4	Plotting	5-10
5.4	RESULTS AND DISCUSSION	5-10
5.4.1	Off-line	5-10
5.4.2	As on-line	5-12
5.4.3	Effect of $W$ the penalty weight on squared deviation $W_{sn}$ from set-point	5-14
5.4.4	Advantages	5-14
<b>Chapter 6 Conclusions</b>		<b>6-1</b>
6.1	CONCLUSIONS	6-1
<b>REFERENCES</b>		<b>R-1</b>
<b>APPENDIX A</b>	<b>Heat Loss</b>	<b>A-1</b>
<b>APPENDIX B</b>	<b>CM Matrix</b>	<b>B-1</b>
<b>APPENDIX C</b>	<b>Parameter values</b>	<b>C-1</b>
C1	GENERAL	C-1
C11	Dryer design	C-1
C12	Sugar crystal properties	C-1
C13	Air properties	C-2



<b>APPENDIX D</b>	<b>Graphs</b>	<b>D-1</b>
D1	GRAPHS FROM THE MATLAB <sup>®</sup> PROGRAM	
D11	Temperature and moisture content profiles along the dryer	D-1
D12	Comparison between the data from the plant and the data from the model	D-3
D13	Closed loop response	D-5
<b>APPENDIX E</b>	<b>Program</b>	<b>E-1</b>

# LIST OF FIGURES

## Chapter 1

<i>Figure 1-1: Drying diagram (Van der Poel <i>et al.</i>, 1998)</i>	1-2
<i>Figure 1-2: Temperature profiles along the dryer (Lipták, 1998)</i>	1-3
<i>Figure 1-3: Co-current rotary dryer control (Lipták, 1998)</i>	1-9
<i>Figure 1-4: Control scheme (Savaresi <i>et al.</i>, 2001)</i>	1-11

## Chapter 2

<i>Figure 2-1: Schematic view of the sugar dryer</i>	2-1
<i>Figure 2-2: Measurement instruments around the sugar dryer</i>	2-2
<i>Figure 2-3: Picture of the dryer</i>	2-3
<i>Figure 2-4: Picture of the sugar coming in the dryer</i>	2-4
<i>Figure 2-5: Picture of the sugar crystals at the end of the dryer</i>	2-4

## Chapter 3

<i>Figure 3-1: Determination of sugar flow</i>	3-1
<i>Figure 3-2: Sugar flow</i>	3-2
<i>Figure 3-3: Profiles of sugar moisture contents when <math>W_{sn}</math> is fixed on equilibrium</i>	3-7
<i>Figure 3-4: Profiles reconciled of sugar moisture contents</i>	3-9
<i>Figure 3-5: Data set from the 29 August 2000</i>	3-10
<i>Figure 3-6: Data set from the 16 October 2000</i>	3-11
<i>Figure 3-7: Data set from the 18 October 2000 (part I)</i>	3-12
<i>Figure 3-8: Data set from the 18 October 2000 (part II)</i>	3-13
<i>Figure 3-9: Data from the 13 December 2000</i>	3-14
<i>Figure 3-10: Hypothetical temperature profiles along the dryer</i>	3-16

## Chapter 4

<i>Figure 4-1: Illustration of a general compartment</i>	4-3
<i>Figure 4-2: Illustration of the airflow design in the sugar dryer</i>	4-5
<i>Figure 4-3: Axial dispersion in a duct</i>	4-8
<i>Figure 4-4: Grid analysis for the discrete model</i>	4-10
<i>Figure 4-5: Increase of temperature</i>	4-10
<i>Figure 4-6: Graphs representing axial dispersion</i>	4-12
<i>Figure 4-7: Sorption isotherms of white sugar for different temperatures (Schindler and</i>	

Juncker, 1993)	4-13
Figure 4-8: Sorption isotherm results from the model	4-15
Figure 4-9: Comparison between data plant and data model for 29 August 2000	4-17
Figure 4-10: Comparison between data plant and data model for 16 October 2000	4-18
Figure 4-11: Comparison between data plant and data model for 18 October 2000 (I)	4-19
Figure 4-12: Comparison between data plant and data model for 18 October 2000 (II)	4-20
Figure 4-13: Comparison between data plant and data model for 13 December 2000	4-21

## Chapter 5

Figure 5-1: Rotary dryer with exit moisture and temperature determined by air temperature and water addition	5-1
Figure 5-2: Step responses for a 2-input 2-output system	5-2
Figure 5-3: Model Predictive Control configuration	5-4
Figure 5-4: Continuously updated step response from parallel solutions of real-time model	5-7
Figure 5-5: Program diagram	5-8
Figure 5-6: Response from the controller for $W_{Sn}$	5-11
Figure 5-7: Controller effect on $W_{An}$ , $T_{Ao}$ , $T_{Sn}$ , $T_{An}$	5-11
Figure 5-8: Zoom on the controller response	5-12
Figure 5-9: Response from the controller for $W_{Sn}$ with data plant	5-12
Figure 5-10: Controller effect on $W_{An}$ , $T_{Ao}$ , $T_{Sn}$ , $T_{An}$ compared with the data	5-13
Figure 5-11: Closed-loop response for $W_{Sn}$ with plant data and $W = 6000000$	5-14
Figure 5-12: Closed-loop response for $W_{Sn}$ with plant data and $W = 4000000$	5-14
Figure 5-13: Closed-loop response for $W_{Sn}$ with plant data and $W = 2000000$	5-14

## Appendix D

Figure D-1: Temperature profile along the dryer at different times	D-1
Figure D-2: Moisture content profile along the dryer at different times	D-2
Figure D-3: Temperatures and moisture contents profiles along the dryer for $t = t_{end}$	D-2
Figure D-4: Air and sugar temperature from the model	D-3
Figure D-5: Air and sugar moisture content from the model	D-3
Figure D-6: Comparison of sugar temperature from the plant and the model	D-4
Figure D-7: Comparison of air temperature from the plant and the model	D-4
Figure D-8: Comparison of air moisture content from the plant and the model	D-5
Figure D-9: Control influence on the inlet air temperature	D-5
Figure D-10: Control response on the exit sugar moisture content	D-6

# LIST OF TABLES

## ***Chapter 1***

<i>Table 1-1:</i> Comparison of heat and mass transfer coefficient	1-6
--	-----

## ***Chapter 3***

<i>Table 3-1:</i> Average temperature values from the trials	3-15
--	------

<i>Table 3-2:</i> Average moisture values from the trials	3-16
---	------

## ***Chapter 4***

<i>Table 4-1:</i> Nomenclature recall	4-1
---------------------------------------	-----

<i>Table 4-2:</i> Heat and mass transfer coefficient values for each trial	4-16
--	------

## ***Chapter 5***

<i>Table 5-1:</i> Translator from theory to program	5-10
---	------

## ***Appendix A***

<i>Table A-1:</i> Overview of CM Matrix	A-1
---	-----

## ***Appendix B***

<i>Table B-1:</i> Dryer design values	B-1
---------------------------------------	-----

<i>Table B-2:</i> Sugar crystal properties	B-1
--	-----

<i>Table B-3:</i> Air properties	B-2
----------------------------------	-----

# LIST OF SYMBOLS

## Alphabet

$a$	Interfacial area	$\text{m}^2.\text{m}^{-3}$
$A$	Sugar dryer section	$\text{m}^2$
$[A]$	Matrix containing coefficients for a linear system of ordinary differential equations	
$[AC]$	Matrix containing coefficients for the Euler integration	
$[B]$	Matrix containing coefficients for a linear system of ordinary differential equations	
$[BC]$	Matrix containing coefficients for the Euler integration	
$B_{OL}$	Matrix	
$B_0$	Matrix	
$[CM]$	Matrix containing coefficients to built $[A]$ and $[B]$	
$[CC]$	Matrix containing coefficients to built $[AC]$ and $[BC]$	
$C_{pA}$	Heat capacity for air	$\text{kJ}.\text{kg}^{-1}.\text{°C}^{-1}$
$C_{pS}$	Heat capacity for sugar	$\text{kJ}.\text{kg}^{-1}.\text{°C}^{-1}$
$C_{pvap}$	Heat capacity for vapor	$\text{kJ}.\text{kg}^{-1}.\text{°C}^{-1}$
$D_A$	Diffusivity coefficient for air	$\text{m}.\text{s}^{-1}$
$D_S$	Diffusivity coefficient for sugar	$\text{m}.\text{s}^{-1}$
$e_{CL}$	Closed-loop error	
$e_{OL}$	Open-loop error	
$E_a$	Activation energy	$\text{kJ}.\text{mol}^{-1}$
<i>Error</i>	Function	
$f_A$	Air flow	$\text{kg}.\text{s}^{-1}$
$f_S$	Sugar flow	$\text{kg}.\text{s}^{-1}$
<i>Funct B</i>	Function	
<i>Fubct b</i>	Function	
$F_w$	Flow of water added	$\text{kg}.\text{s}^{-1}$
$G$	Crystallisation growth rate	$\text{m}.\text{s}^{-1}$
$H$	Enthalpy	$\text{kJ}$
$h_S$	Sugar hold up volume fraction	$\text{kg}.\text{kg}^{-1}$
$h_i$	Heat transfer coefficient	$\text{kW}.\text{m}^{-2}.\text{K}^{-1}$

$I$	Impurity	$\text{kg.kg}^{-1}$
$k$	Coefficient	
$K_0$	Crystallisation parameter	
$K_1$	Crystallisation parameter	
$K_2$	Crystallisation parameter	
$K_3$	Crystallisation parameter	
$k_g$	Mass transfer coefficient	$\text{kg.m}^{-2}.\text{s}^{-1}.\text{Pa}^{-1}$
$L_H$	Latent heat of vaporisation of water	$\text{kJ.kg}^{-1}$
$M_{Crystal}$	Mass of crystal	$\text{kg}$
$M_{Impurity}$	Mass of impurity	$\text{kg}$
$M_{Sucrose}$	Mass of sucrose	$\text{kg}$
$M_{Total}$	Mass total	$\text{kg}$
$M_{Water}$	Mass of water	$\text{kg}$
$M_{Waterf}$	Mass of water in the feed	$\text{kg}$
$p$	Pressure	$\text{Pa}$
$p^\circ$	Pressure reference	$\text{Pa}$
$p_{bp}$	Partial pressure of air at the boiling point	$\text{Pa}$
$pur$	Purity	$\%$
$p_{100}$	Partial pressure of air at $T = 100^\circ\text{C}$	$\text{Pa}$
$RH$	Relative humidity	$\%$
$SC$	Solubility coefficient	
$S_F$	kg sucrose dissolved in film per kg of dry sugar crystal	$\text{kg.kg}^{-1}$
$SOL$	Mass percent of sucrose	$\%$
$SS$	Supersaturation in the film	
$t$	Time	$\text{s}$
$T$	Temperature	$^\circ\text{C}$
$T^\circ$	Temperature reference	$^\circ\text{C}$
$T_{absolute}$	Temperature absolute	$^\circ\text{C}$
$T_{Bp}$	Boiling point temperature	$^\circ\text{C}$
$T_{dry}$	Dry bulb temperature	$^\circ\text{C}$
$T_{wet}$	Wet bulb temperature	$^\circ\text{C}$
$\bar{U}$	Vector containing the bounding conditions	
$W$	Penalty weight on squared set-point deviation	
$W$	Moisture	$\text{kg.kg}^{-1}$
$W_{SAT}$	Moisture in the sugar at saturation	$\text{kg.kg}^{-1}$

$W_{snequilibrium}$	Moisture in the sugar at equilibrium	kg.kg <sup>-1</sup>
$x_{CL}$	Closed-loop response	
$x_{OMEAS}$	Present measurement	
$x_{OL}$	Open-loop response	
$x_{SP}$	Set point	
$\bar{X}$	Vector containing the unknown	
$y_A$	Fraction of moisture in the air	
$\%Water$	Mass percentage of water in the sugar	%

### Subscript

$A$	Air
$A0$	Inlet air
$An$	Outlet air
$S$	Sugar
$S_{equilibrium}$	Sugar at equilibrium
$S0$	Inlet sugar
$S0_{corrected}$	Corrected value of inlet sugar
$S0_{fixed}$	Fixed value of inlet sugar
$Sn$	Outlet sugar
$Sn_{equilibrium}$	Outlet sugar at equilibrium

### Greek letters

$\alpha$	Function	
$\beta$	Function	
$\chi$	Filter parameter	
$\gamma$	Filter parameter	
$\rho_A$	Air density	kg.m <sup>-3</sup>
$\rho_S$	Sugar density	kg.m <sup>-3</sup>
$\Delta m$	Vector move	
$\Delta m_{UQO}$	Vector unbounded quadratic optimum control move	
$\Delta m_{PAST}$	Vector past input	
$\Delta P$	Pressure difference	Pa
$\Delta W_s$	Sugar moisture content difference	kg.kg <sup>-1</sup>
$\Delta x$	Interval	m

$\lambda$	Penalty weight on the control move
$\xi$	Function
$\psi$	Function



# CHAPTER 1

## INTRODUCTION

### 1.1 LAYOUT OF THIS DISSERTATION

---

In Chapter 1, the background of drying technology and drying control are developed. A brief presentation of the co-current sugar dryer considered is made in Chapter 2. The techniques used to reconcile the data collected from the plant are explained in Chapter 3. Then these data were used to construct a model able to simulate the drying process in a co-current sugar dryer. The theoretical development is described in Chapter 4. Chapter 5 deals with the arrangement and properties of the controller, and how the program for model and controller was built. In Chapter 6, conclusions and recommendations end the thesis.

### 1.2 DRYING

---

#### 1.2.1 Process

Van der Poel *et al.* (1998) defined the drying process as a thermal separation process: the volatile liquid is vaporised from the solid. A drying agent reduces external vapour pressure, and carries the vaporised liquid away. In their book, they describe the drying process. The moisture in the solid is noted as  $X$  and measured in kg of water per kg of dry solid. The drying rate  $m$  is determined by measuring the change in water content with the time,

$$m = -\frac{m_{s,dry}}{A} \cdot \frac{dX}{dt} \quad (1.1)$$

where  $m_{s,dry}$  is the mass of the dry solid

$A$  is the surface area in contact with the drying agent

The temperature, the pressure and the velocity of the drying agent, and the temperature and the velocity of the solid influence the drying conditions. The drying curve is defined as the relation between the drying rate and the water content under constant drying conditions.

The drying rate is mostly constant in the first part of the drying. The water is taken from the liquid on the surface and carried by the drying agent, say air. (Fig. 1-1, Section I). The surface of the solid dries out when the water content goes down to a value called the critical value  $X_{cr1}$ .

In the second drying period: the drying rate drops with the decreasing water content of solid (Fig. 1-1, Section II).

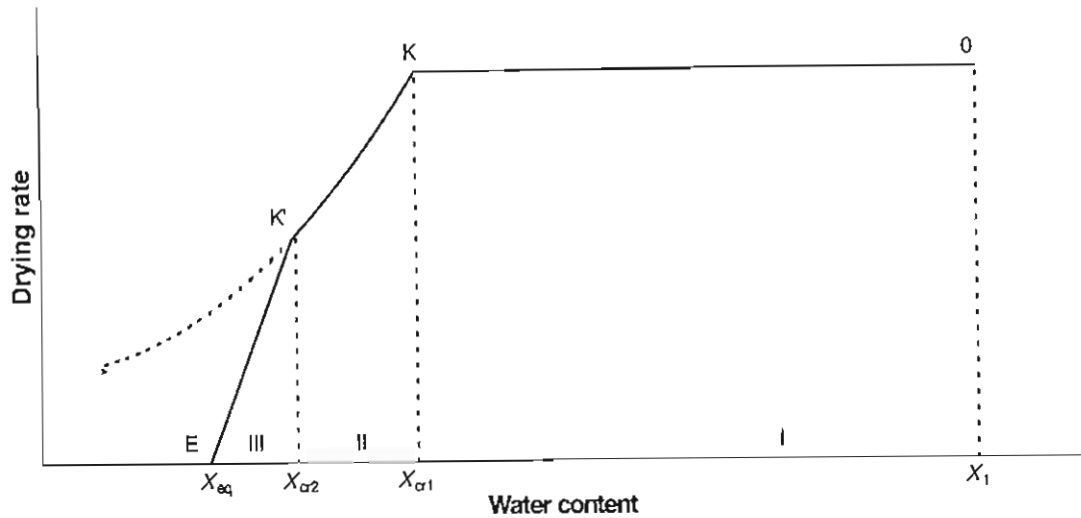


Figure 1-1: Drying diagram (Van der Poel *et al.*, 1998)

The residual water is bound to the solid by sorption. The drying rate decreases rapidly with the decreasing water content and tends to zero as the hygroscopic equilibrium water content  $X_{eq}$  is approached. The regime between the maximum hygroscopic water content  $X_{\alpha 2}$  and the equilibrium value of  $X_{eq}$  is designated as the third drying period. (Fig. 1-1, Section III)

Liptak (1998) defined the drying process in four steps, adding a preheating step:

- Preheating : the particle is heated up to the drying temperature.
- Constant drying rate (Fig. 1-1, Section I) : the moisture is removed by evaporation from the surface of the solid.
- Falling drying rate (Fig. 1-1, Section II) : the particle is dried.
- Falling drying rate (Fig. 1-1, Section III) : the water within the film diffuses to the surface and then is evaporated.

### 1.2.2 Dryers

Different types of dryers exist to dry different materials. Two main types can be distinguished: batch dryer, and continuous dryer. For any drying operation, a dryer must have a source of heat, a way of removing the liquid vaporized from the surface of the solid, a mechanism to mix the solid and the drying agent. In his paper, Lipták (1998) drew up an exhaustive list of batch dryers (atmospheric tray types, tunnel dryers, vacuum and freeze dryers, batch kilns, fluidised-bed

dryers), and continuous dryers (co-current, counter-current). The sugar dryer studied in the present work is a co-current dryer. It is interesting to note in this case that the sugar itself provides much of the heat for evaporation.

Typical continuous dryer temperature profiles are as in Fig. 1-2. The different zones of the drying process are represented along the dryer. A-B describes the pre-heating zone. In the zone B-C, the material is dried at constant rate. Then in the zone C-D-E, the drying rate drops, the temperature increases. The sugar temperature follows the same profile in the both co-current and counter-current configurations. However, the profile is not the same for the air temperature. Often, with the counter current dryers, it is necessary to add cool air at the exit to decrease the sugar temperature. An interesting phenomenon will be observed in the present work on a co-current dryer where the exit sugar temperature exceeds the exit air temperature.

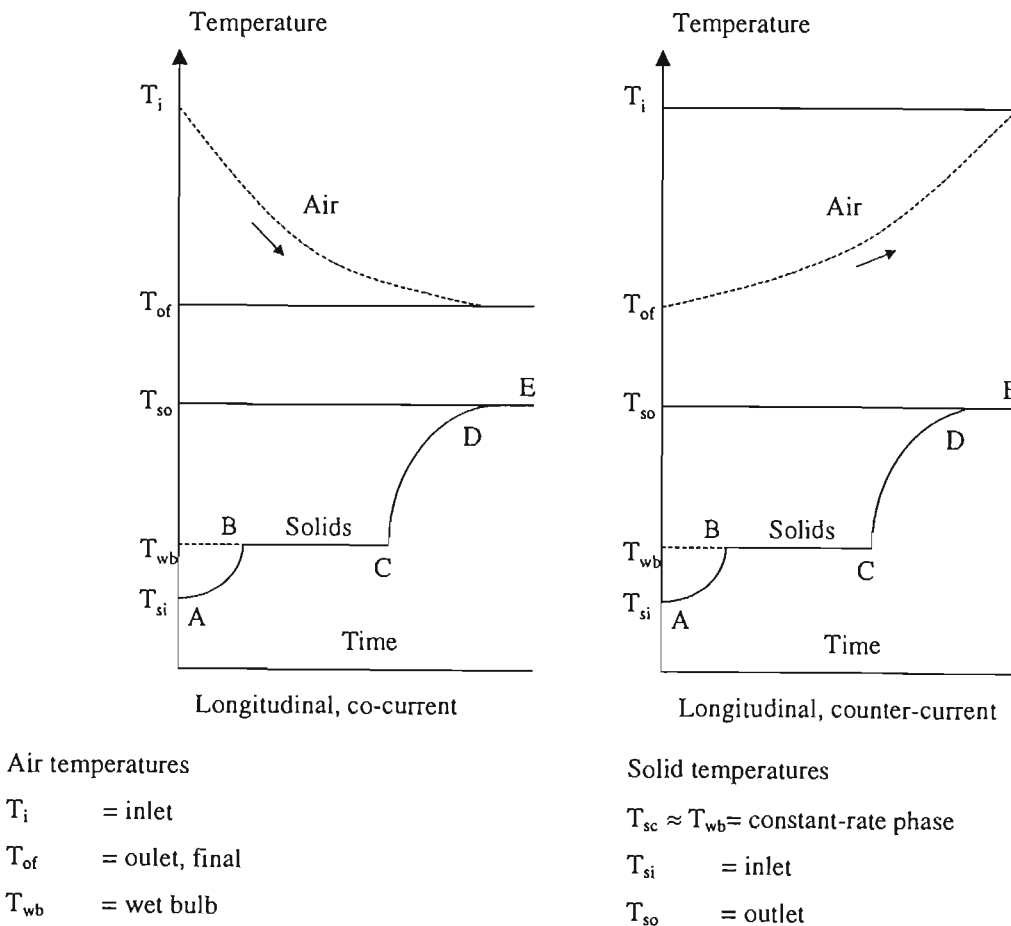


**Figure 1-1: Temperature profiles along the dryer (Lipták, 1998)**

## 1.3 SUGAR DRYING

---

### 1.3.1 Different types of moisture

Sugar moisture is an issue in the conditioning of sugar. If sugar crystals are not dried enough, caking can occur. Moist crystals in contact go on crystallising, and the crystals agglomerate into a cake.

Marijnissen and de Bruijn (1996) note that there are three different kinds of water in a sugar crystal.

- *Free moisture* : this is considered as the water at the surface of the crystal in contact with the surrounding air.
- *Bound water* : this water is trapped inside a thin sucrose film around the sugar crystal. It results from too quick removal of water at the surface of the crystal.
- *Inner, inherent or internal water* : here the water is trapped inside the sugar crystal lattice.

In the case where raw sugar is being dried, only the free moisture is removed. Raw sugar contains a lot of impurities (ash, fructose and glucose, colour) that do not allow the formation of bound water.

### 1.3.2 Drying process

Sugar drying follows the general process of drying explained in part (1.2.1). According to Thompson (1998), white sugar is a hygroscopic material that needs to be stored in a place where the relative humidity is below 65%. A high level of impurities and small crystal size increase the moisture content at equilibrium, but a high temperature decreases it. So the sugar is usually dried with hot air. However, Thompson drew attention to the following possibility, assuming that the wet sugar coming from centrifugals had enough energy to dry itself: he suggested then that hot air was not necessary since cold air was needed to cool the sugar at the exit of the dryer.

Savaresi *et al.* (2001) defined two modes of drying sugar. The first is the “standard-mode”. It is assumed that everywhere in the sugar dryer, the moisture content is always reasonably above zero. The second is the “over-dried mode”: a possible moisture content close to zero in the sugar at the exit characterizes this mode.

### 1.3.3 Drying Model

Tait *et al.* (1994) proposed a model for a counter-current sugar dryer. They based their model on a mass and energy balance with the assumption that crystallisation is still occurring inside the

sugar dryer. When the drying process is looked at from a sugar crystal point of view, the mechanism of evaporating water from the film surrounding the crystal appears more complicated. The film contains sucrose, water and impurity. The partial pressure of the water is reduced due to the presence of sucrose and impurity. As the water is taken from the film, it becomes more and more saturated so that crystallisation can occur. In the model, the sugar dryer is divided into several equal compartments. It is assumed that the sugar and air leaving the compartment are at equilibrium.

Shardlow *et al.* (1996) proposed another sugar drier model based on the above model of Tait *et al.* (1994). They made modifications to improve it. The diffusion of water through the film around the sugar crystals is accounted for using Fick's law of diffusion in the calculation of the partial pressure of the water. They decided as well to decrease the crystallisation rate by 40% in the film.

Rastikian *et al.* (1999) designed a model for a counter current cascading rotary sugar dryer. They preferred to work with the convective heat transfer coefficient in the gas film  $h_g a$  and the convective mass transfer coefficient in the gas film  $k_g a$  rather than with the overall heat and mass transfer coefficients, because they were able to estimate a good value for the interfacial surface area. They did not estimate the phenomenon of axial diffusion, dispersion or back mixing of the solid. According to them, the resistance to the heat transfer lies only in the gas film. The film of sucrose solution surrounding the sugar crystals is supposed to remain supersaturated for the whole drying process. So this implies that the drying rate depends on the driving force in the gas film not on the water remaining in the film around the crystals.

Savaresi *et al.* (2001) based their work on a first principles model similar to Tait *et al.* (1994), optimising the time and spatial discretisation using two separate models of vapour/air and sugar/moisture transport. Working at lower sugar moisture contents, they found that their model could not accurately simulate the moisture contents, but it could predict the temperatures well. They developed guidelines for a controller, including their model as a black box which could be switched from the "standard mode" drying mechanism to the "over-dried mode" drying mechanism.

Table 1-1 illustrates the different values found in the literature for the heat and mass transfer coefficients. These values can be separated into two groups. Tait *et al.* (1994), Shardlow *et al.* (1996), and Savaresi *et al.* (2001) have more or less the same results characterising data coming from Australia. Rastikian *et al.* (1999) have worked with data coming from France. The origin of the sugar might have an effect on the heat and mass transfer coefficients.

**Table 1-1: Comparison of heat and mass transfer coefficient**

	Heat transfer coefficient (kW.m <sup>-2</sup> .K <sup>-1</sup> )	Mass transfer coefficient (kg water.m <sup>-2</sup> .s <sup>-1</sup> .Pa <sup>-1</sup> )
Tait <i>et al.</i> (1994)	0,3000	72 × 10 <sup>-9</sup>
Shardlow <i>et al.</i> (1996)	0,0036	7,9 × 10 <sup>-9</sup>
Rastikian <i>et al.</i> (1999)	0,0019	27 × 10 <sup>-9</sup>
Savaresi <i>et al.</i> (2001)		
“Standard mode”	0,0030	2,7 × 10 <sup>-9</sup>
“Over-dried mode”	0,0038	4,05 × 10 <sup>-9</sup>

## 1.4 CRYSTALLISATION

Tait *et al.* (1994) worked with the following equations for the crystallisation rate:

$$G = 2,060 \cdot 10^{-6} (SS - 1,0046) \exp \left( FT - 1,75 \frac{\text{impurity}}{W_s} \right) \quad (1.2)$$

where

$$FT = \frac{-E_{act}}{1,987 \cdot 10^{-3}} \left( \frac{1}{273,16 + T_s} - \frac{1}{333,16} \right)$$

$$E_{act} = 15,0 - 0,2(T_s - 60)$$

*SS* is the supersaturation of the film that is calculated from *SOL* the mass percent of sucrose in a saturated film without impurities and *SC* the solubility coefficient correcting for the impurity level. *SOL*, *SC*, *SS* are given by Tait *et al.* (1994).

$$SOL = 64,407 + 0,07251 T_s + 0,0020569 T_s^2 - 9,035 \times 10^{-6} T_s^3 \quad (1.3)$$

$$SC = 1,0 - 0,088 \frac{I}{W_s} \quad (1.4)$$

$$SS = \frac{S}{W_s} \frac{100 - SOL}{SOL \cdot SC} \quad (1.5)$$

More information was found in the PhD thesis of Love (2001). Using Wright and White's (1974) equation for the sucrose crystal growth for impure aqueous solution, Love (2001) brought more interpretations of the equation parameters, and corrects them for Kwazulu-Natal cane processing.

$$G = K_1 \cdot (SS - (1 + K_0)) \cdot \exp(K_2 - K_3 \cdot IW) \quad (1.6)$$

- $K_0$  is a constant to take account of the threshold of growth at lower saturation.
- $K_1$  is the major proportionality constant relating to the degree of over saturation.
- $K_2$  is used to describe the extent to which growth rate varies with temperature.
- $K_3$  describes the dependence of growth rate on the level of impurities present.

$K_2$  behaves according to an Arrhenius law type:

$$K_2 = -\frac{Ea}{R} \left( \frac{1}{273,16 + T_s} - \frac{1}{333,16} \right) \quad (1.7)$$

where  $Ea$  is the activation energy in  $\text{kJ.mol}^{-1}$

$R$  is the universal gas constant

The parameters found by Love (2001) result from his study of the modelling and control of a pan boiling crystalliser.

Ben-Yoseph *et al.* (2000) described some of the influences on the crystal growth of the film. When a crystal grows, sucrose is taken from the film to become sugar crystal so the concentration of sucrose decreases. This phenomenon generates heat that raises the film temperature. So the film temperature can be higher than the air temperature.

## 1.5 DATA RECONCILIATION

Bazin *et al.* (1998) worked with data collected from a zinc concentrate rotary dryer. They wanted to illustrate the problems linked to the calculation of non-measured variables arising from error in the data measured. Their paper shows how errors can be propagated from a simple calculated variable such as the gas flow rate, through the mass and energy balance.

## 1.6 CONTROL

### 1.6.1 Predictive Control

The problem with control of a sugar crystalliser is dealing with dead time and huge model order. Clarke *et al.* (1987) explained how a predictive control algorithm was found to improve control in the face of these difficulties. The idea is to use a moving time horizon within which to predict the plant behaviour to determine optimal control actions.

### 1.6.2 Dynamic Matrix Control

Dynamic Matrix Control is one of the techniques using Predictive Control. García *et al.* (1989) studied the family of Predictive Control algorithms. They give an overview of DMC and

MAC (Model Algorithmic Control). They concluded that even if it works well, some progress still needed to be made in the field of linear and especially non-linear systems.

In 1997, Aitchison and Mulholland obtained very good results with the control of a concentric tube heat exchanger using an adaptive control based on Dynamic Matrix Control. A similar scheme, based on an accurate non-linear model, is used in the control of this sugar dryer.

## 1.7 DRYER CONTROL

Shinsky determined the moisture content by (1.8), where any consistent units may be used for any kind of dryable material:

$$w_p = \frac{w_c F_a C_p}{AH_w \zeta} \ln \frac{(T_i - T_w)}{(T_o - T_w)} \quad (1.8)$$

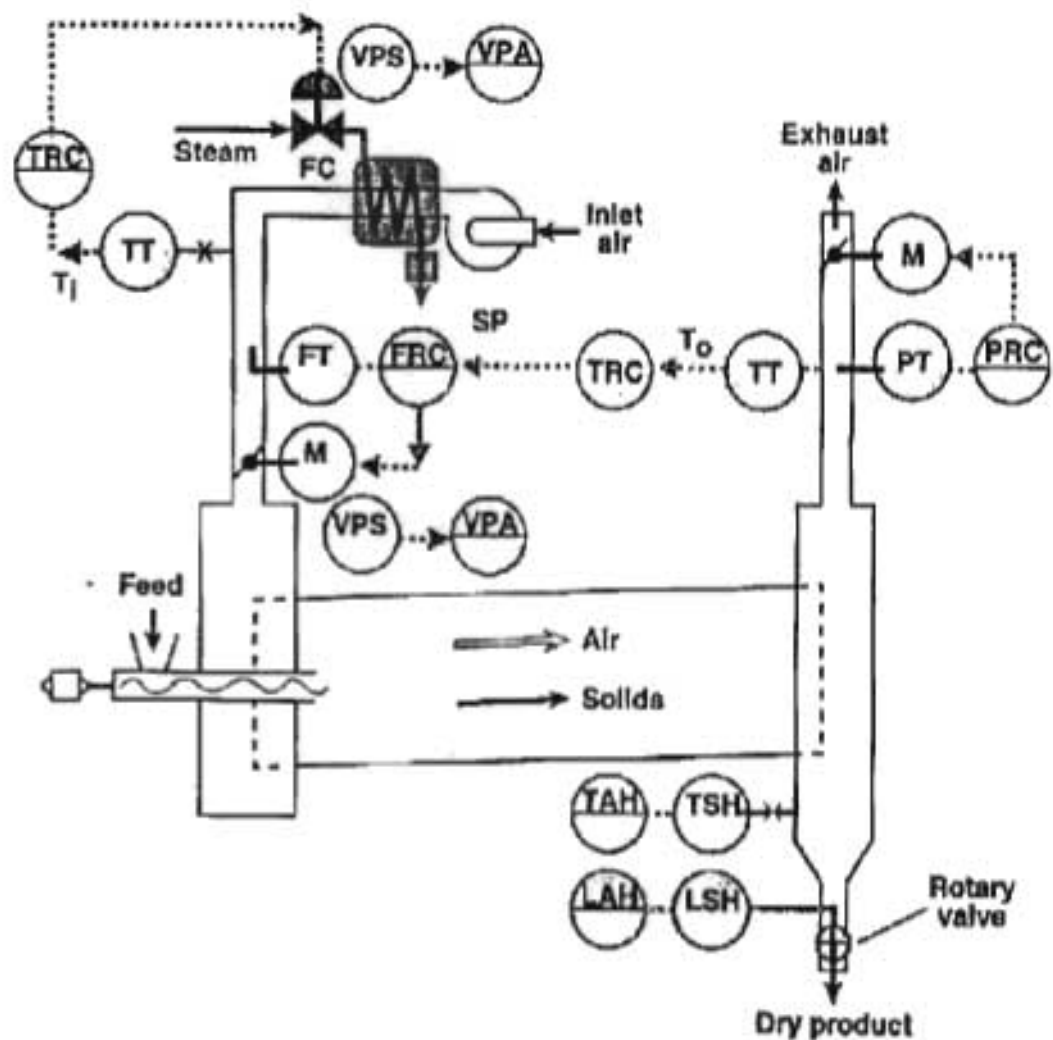
A	= Solid surface area	T <sub>w</sub>	= Air wet bulb temperature
C <sub>p</sub>	= Specific heat of air	ζ	= Mass transfer coefficient
F <sub>a</sub>	= Air flow	w <sub>c</sub>	= Critical moisture content of the dried product
H <sub>w</sub>	= Latent heat of water	w <sub>p</sub>	= Moisture point
T <sub>i</sub>	= Air inlet temperature		
T <sub>o</sub>	= Air outlet temperature		

To control  $w_p$  the two ratios  $\frac{w_c F_a C_p}{AH_w \zeta}$  and  $\frac{(T_i - T_w)}{(T_o - T_w)}$  need to be kept constant. The first ratio can

be assumed constant because the change of the air flow or the solid surface area that depends on the crystal size are compensated by the mass transfer coefficient. Concerning the second ratio, in an adiabatic dryer,  $T_w$  is supposed constant along the dryer. So the control should be done on the air temperature.

Trelea *et al.* (1996) developed a strategy to control a mixed flow corn dryer. The moisture content of the corn or the exhaust air is usually the controlled variable. The manipulated variable can be the air temperature, the gas flow in the burner or the residential time of the product in the dryer. They worked with two control strategies: PI (Proportional Integral) control and LQG (Linear Quadratic Gaussian) control. It was found that the PI control furnished almost as good results as the sophisticated LQG control.





FC = Fail closed  
 FT = Flow transmitter  
 FRC = Flow recording controller  
 LAH = Level alarm high  
 LSH = Level switch high  
 M = Motor  
 PRC = Pressure recording controller

PT = Pressure transmitter  
 $T_o$  = Outlet air temperature  
 $T_i$  = Inlet air temperature  
 TT = Temperature transmitter  
 TRC = Temperature recording controller  
 VPA = Valve position alarm  
 VPS = Valve position switch

**Figure 1-1: Co-current rotary dryer control (Lipták, 1998)**

Lipták (1998) described in Fig.1-3 a conventional way of controlling a co-current rotary dryer. In this kind of control, the optimum inlet air temperature is the maximum that the product can tolerate. If high temperature can degrade the product, a high temperature alarm is needed (TAH). If the steam and air valve are fully open, the product moisture cannot be controlled, so alarms are placed to detect these situations.

Pérez-Correa *et al.* (1998) chose the following manipulated and controlled variables: the inlet gas temperature as a manipulated variable and the solid moisture content measured on-line. They worked with two control schemes: a PID control, and an extended horizon self-tuning regulator. The PID controller was able to control the dryer but it needed periodic tuning, and presented a small overshoot in the response. The self-tuning controller responded with better results: smaller overshoots, and better settling times.

Dryer efficiency is defined as the ratio between the theoretical energy required for evaporation and the actual energy consumed. Clarke (2000) presented figures suggesting that the average dryer efficiency is around 40-60%. It may even go down to 10% for old machines. It is obvious that control is needed. In the UK, most of the dryers use single loop temperature control that gives good results with, however, lots of limitations. The ideal solution would be to measure directly the product moisture content but this remains still very expensive. They proposed then a system able to determine the moisture content simply by measuring two temperature. Their system called the “Delta T” algorithm has given good results.

Temple and van Boxtel (2000) developed a strategy to control a fluidised bed tea dryer. Similarities exist between sugar drying and tea drying. They first tried to work with a direct moisture content feed-back. It provided good results but showed some limitations because of dead-time from the heater system. They worked then with an intermediate exhaust temperature that can be converted into moisture value. This gave good control without requiring expensive instrumentation.

Savaresi *et al.* (2001) proposed a very simple way of controlling the sugar dryer just with the output sugar temperature measurement which is easier than measuring the output sugar moisture content – see Fig. 1-4 . The basic idea of the control scheme was to inject an impulse at regular intervals to excite the system (signal ①) in order to detect the current operating condition of the system. Signal ② was the output sugar temperature response. It was obtained as the difference between the real temperature and its average value calculated from the low pass filter. Signal ③ was the result from the multiplication of delayed signal ① and signal ②. The time delay  $r_t$  had to equal the residence time of the sugar in the dryer because the effect of the impulse appeared only  $r_t$  minutes later. Signal ④, after being transformed by the non-linear static characteristic,

was re-balanced giving an adjusted moisture content response. The time delay  $\Psi$

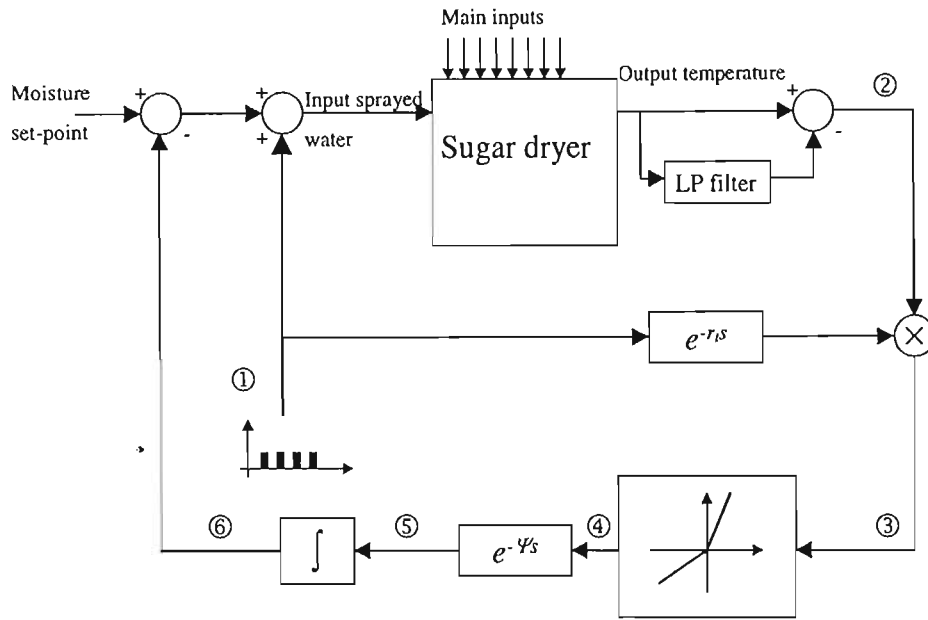


**Figure 1-2: Control scheme** (Savaresi *et al.*, 2001)

which was bigger than  $r_1$  was used to avoid interferences between injection and controller output. With signal ⑥, the integration provided a permanent adjustment to the amount of sprayed water until the next injection. The signal is then adjusted with the moisture set-point. The original point in this work was to control the sugar drying by adding water to the sugar before it was dried.

## CHAPTER 2

### THE DRYER CONSIDERED IN THIS STUDY

#### 2.1 THE PLANT

---

##### 2.1.1 Description of the equipment

The Darnall Sugar Mill (Tongatt Hulett Sugar Ltd) uses a rotary drum dryer as the last stage in the raw sugar milling process. The dryer operates in continuous co-current mode.

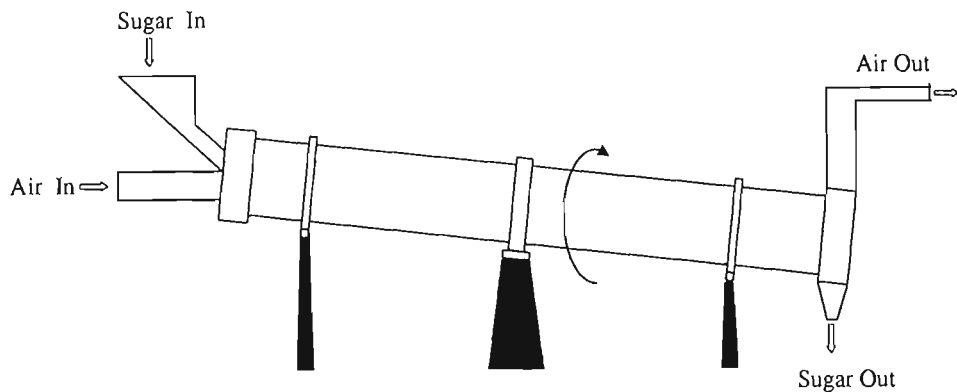


**Figure 2-1: Schematic view of the sugar dryer**

It consists of a large drum (12,5 m long and with internal diameter of about 1,75 m), set at a slight angle, about  $3^\circ$ , in order to let the sugar move slowly under gravity from the inlet to the outlet. The average residential time of the sugar in the dryer is about 5 minutes. The drum slowly rotates around its longitudinal axis (about 10 revolutions per minute), in order to expose the sugar to the air continuously, and to mix the sugar. To this end, the internal surface of the drum is entirely covered with concave louvers (usually called “flights”), which lift the sugar in the drum. The inlet wet/hot sugar passes through the dryer, moving co-current with air flow, and out at the lower end. It is dropped onto a conveyor that takes the dried/cooled sugar to the sugar hopper.

### 2.1.2 Description of the process

After the centrifugation, in which the sugar crystals are separated from the mother liquid, they are then dried in the rotary dryer. They have a size ranging from 0,4 to 0,7 mm. The average value used in the model was obtained from a technician at the Darnall sugar mill as 0,57 mm. At the entrance of the sugar dryer, the sugar moisture content is around 1%, it is dried down to a value of 0,1% (mass/mass). In the general working conditions, the feed sugar flow rate is  $10 \text{ kg.s}^{-1}$  at a temperature of  $55^\circ\text{C}$ . For the air, the temperature is around  $80^\circ\text{C}$ , and the air to sugar ratio is between 0,2 and  $0,7 \text{ kg air.kg sugar}^{-1}$ .

### 2.1.3 The instrumentation

Six temperature sensors have been used to collect data from the plant. They are mineral insulated Pt100 sensors Class B with Tc1 Ptx1-Oop 0-150  $^\circ\text{C}$  head mount transmitters.

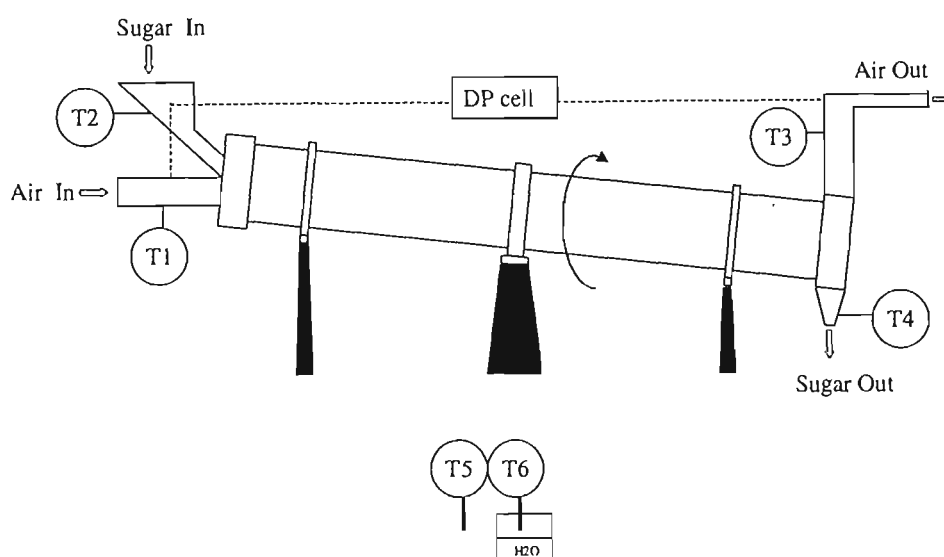


**Figure 2-1: Measurement instruments around the sugar dryer**

The temperature sensors were placed at different locations on the sugar dryer to measure the inlet air (T1) and the inlet sugar (T2) temperatures, the outlet air (T3) and the outlet sugar (T4) temperatures, and the dry bulb (T5) and wet bulb (T6) temperatures. The inlet sugar temperature sensor was placed at the bottom of a bucket elevator that carries the sugar to the entrance of the dryer. This sensor was continuously in contact with the sugar crystals. The outlet sugar temperature sensor measures the temperature intermittently because the sensor was placed in a

discharge hopper at the exit of the dryer. This hopper collects the dried sugar up to a set load, then dumps it onto a product conveyor. The period of this cycle varies inversely with production rate.

A 0-4 kPa DP cell was used to gauge the air flow rate at the entrance of the drier.

A 4-20 mA driver board drove these circuits and provided an input voltage for an A/D converter scanned by a laptop PC SCADA system

The temperature sensors were calibrated by the following procedure: the working range of temperature is between 30°C-90°C. Thus the temperature sensors were calibrated using a point at 20°C and a point at 100°C using water in a thermos flask.

#### *2.1.4 Pictures of the dryer*

The photographs shown in Fig. 2-3 to 2-5 were taken on 29<sup>th</sup> June, 2000.

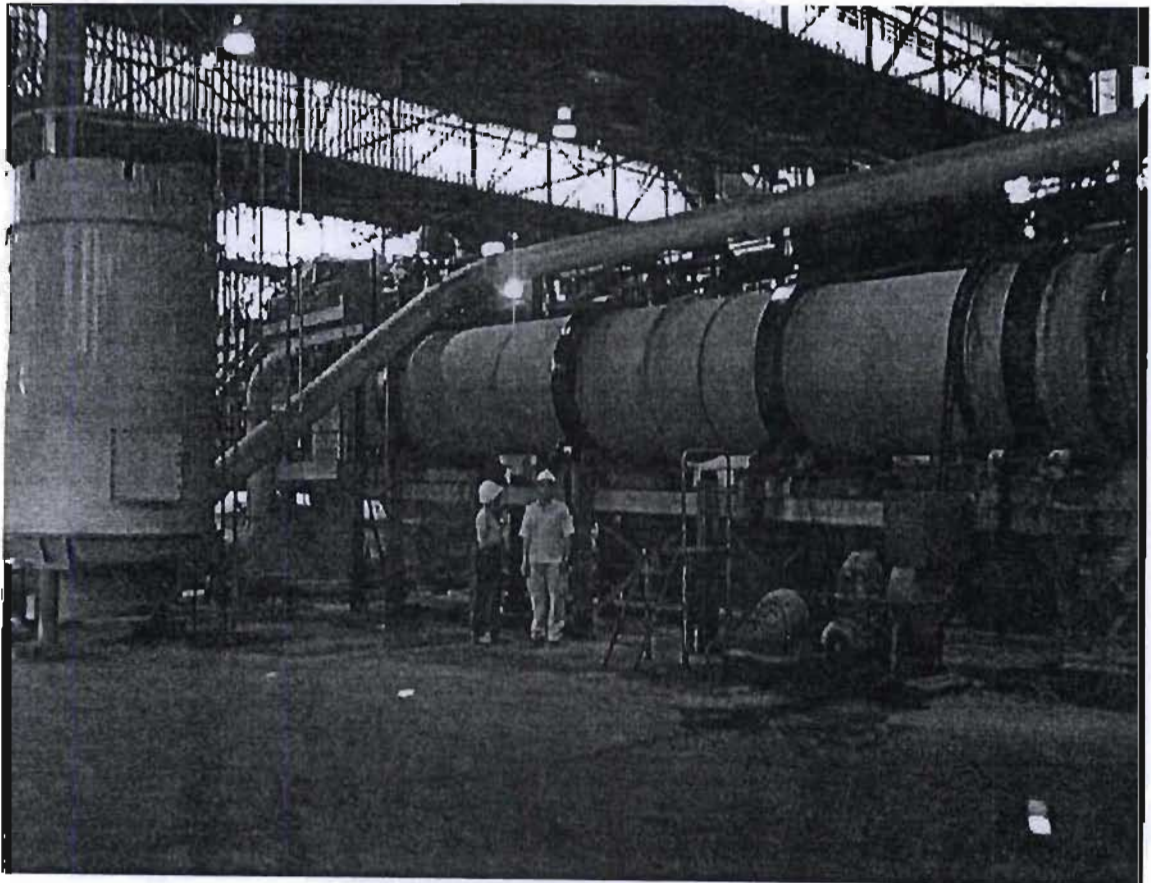


**Figure 2-1: Picture of the dryer**



Figure 2-2: Picture of the sugar coming into the dryer

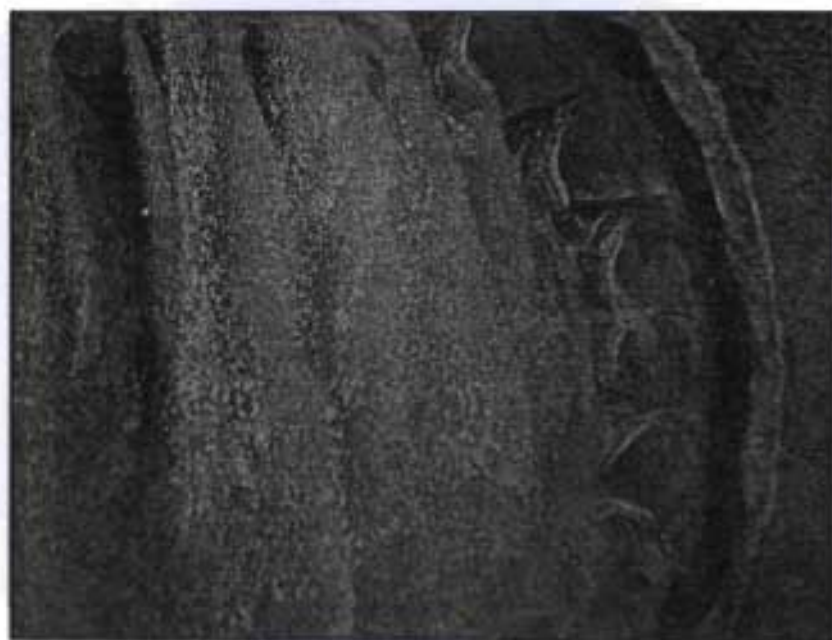


Figure 2-3: Picture of the sugar crystals at the end of the dryer

## CHAPTER 3

### DATA COLLECTION

#### 3.1 ON - LINE DATA COLLECTION

---

##### 3.1.1 Air flow

The pressure drop across the ducting varies with the square of the flow in turbulent flow, so measuring the differential pressure gives a signal that can be related to the flow rate, as follows:

$$f_A = k \times \sqrt{\frac{\Delta P}{T_{absolute}}} \quad (3.1)$$

##### 3.1.2 Sugar flow

The sugar flow is not directly measurable on the plant. Estimates were made from oscillations in the outlet sugar temperature record.

The sugar temperature sensor was placed in the container that collects the sugar at the exit of the sugar dryer. Every time that this weight of the container reaches 350 kg, it empties. This creates a periodic rise and fall of the sensor temperature. From this, the sugar flow rate can be calculated.

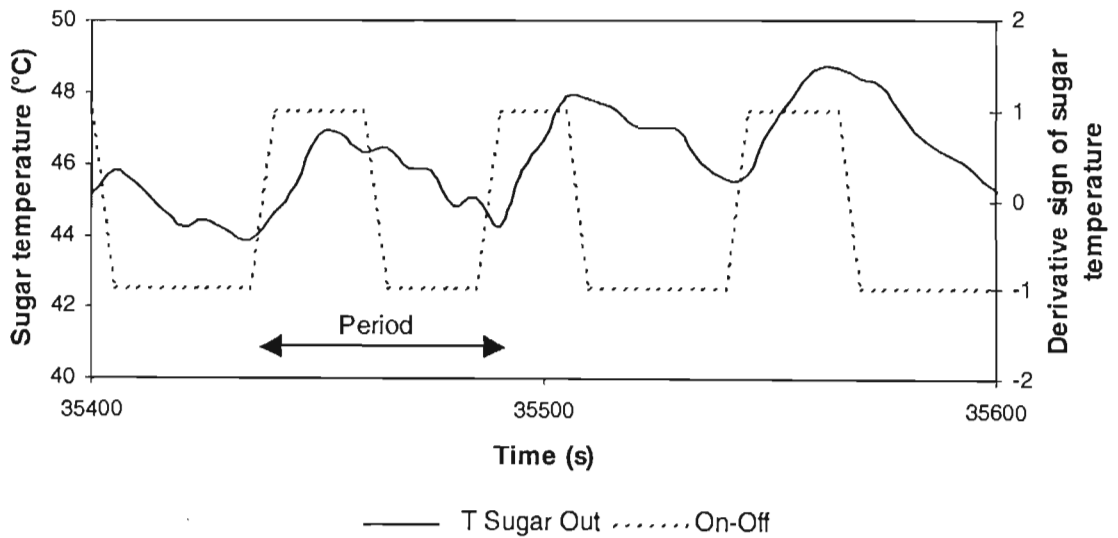


**Figure 3-1: Determination of sugar flow**



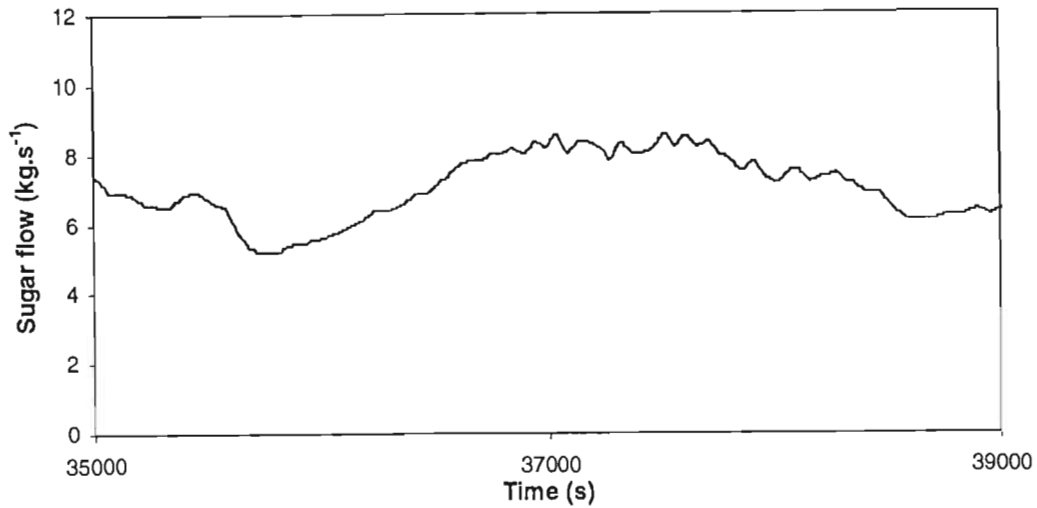


**Figure 3-2: Sugar flow**

### 3.1.3 Moisture in the air at the entrance

The dry bulb and wet bulb temperature sensors had been placed close to the sugar dryer to give a relevant indication of the moisture in the feed air.  $W_{A0}$  is calculated by an equation in common use in Tongaat-Hulett Sugar Ltd:

$$W_{A0} = 0,0000010286T_{wet}^3 - 0,00004466T_{wet}^2 + 0,001504T_{wet} - 0,0056 - 0,00042(T_{dry} - T_{wet})$$

Due to poor calibration of the temperature sensor (Pt100), the wet bulb temperature sensor gave a higher signal than the dry bulb temperature sensor. Thus with the help of the South African Weather Bureau, the data for the days studied were compared with the data from three meteorological stations around Darnall: Durban, Mtunzini and Mandini for the temperature and the relative humidity.

## 3.2 DATA TREATMENT

---

### 3.2.1 Relation between $H_A$ and $W_A$

The enthalpy of humid air can be estimated from its water content and temperature as follows:

$$H_A = [W_A C_{p_{vap}} + (1 - W_A) C_{p_A}] (T_{Air} - T^\circ) + W_A L_H \quad (3.3)$$

where  $T^\circ$  is a reference datum temperature.

### 3.2.2 Balances

At the steady state, the energy balance and mass balance around the dryer are given by:

$$f_A H_{A0} + f_S H_{S0} = f_A H_{An} + f_S H_{Sn} \quad (3.4)$$

$$f_A W_{A0} + f_S W_{S0} = f_A W_{An} + f_S W_{Sn} \quad (3.5)$$

assuming that the airflow and the sugar flow remain constant along the dryer.

From (3.4),  $H_{An}$  can be found, and using (3.3),  $W_{An}$  can be obtained. Then:

$$\Delta W_S = \frac{f_A}{f_S} (W_{An} - W_{A0}) \quad (3.6)$$

Following this, a reverse calculation is done to find the sugar moisture at equilibrium with the moisture at the exit in the air. These inverse calculations are based on the equations from Tait *et al.* (1994).

From  $W_{An}$ , the moisture mole fraction  $y_A$  is calculated:

$$y_A = \frac{29 W_{An}}{18 + 11 W_{An}} \quad (3.7)$$

The vapour pressure [Pa] of pure water at temperature  $T$  [°C] is given from Tait *et al.* (1994).

by:

$$p(T) = 1367,6 - 132,54T + 9,635T^2 - 0,115T^3 + 0,00132T^4 \quad (3.8)$$

The sugar is at temperature  $T_s$  but the moisture on the surface of the crystals does not exert a partial pressure  $p(T_s)$  for two reasons:

- (i) The elevation of boiling point due to the dissolved solids clearly impacts on the vapour-pressure/temperature relationship, and this may be compensated for (following Tait *et al.*, 1994) by scaling the vapour pressure of the water at the operating temperature using the ratio of the pure vapour pressures expected at 100°C to that at pure water at the actual boiling point of the solution. (See (3.9))
- (ii) As the solution becomes more saturated, there is simply less and less water present, and a *Henry's Law* effect is expected in which the vapour pressure will drop in proportion to the “concentration” of water present. Firstly, note the variables:

$W_s$ : kg water in film per kg of dry sugar crystal

$S_F$ : kg sucrose dissolved in film per kg of dry sugar crystal

In the present approach to define an isotherm it is assumed that the crystallization from the film onto the crystal surface is a slow process, so  $S_F$  is taken as a constant, and different amounts of water associated with it are considered. There will be a particular  $W_s$  which the given  $S_F$  just saturates ( $W_{SAT}$ ). As further water evaporates, lower values of  $W_s$  arise representing various degrees of supersaturation for the fixed  $S_F$ . Following Tait *et al.* (1994), from this a further scaled reduction in the exerted water vapour pressure in the ratio of  $W_s/W_{SAT}$  is inferred.

Applying the product of the ratios suggested by (i) and (ii) above, the following expression is obtained for the water vapour pressure exerted by the crystal film at a given temperature  $T$ :

$$p_s(T) = p(T) \cdot \frac{p(100)}{p(T_{bp})} \cdot \frac{W_s(S_F)}{W_{SAT}(S_F)} \quad (3.9)$$

Following Tait *et al.* (1994), the boiling point at 1atm can be predicted by:

$$T_{bp} = 100 + 2 \frac{100 \cdot S_F}{W_s(S_F) \cdot pur} \quad (3.10)$$

Let

$$\beta = \frac{100 \cdot S_F}{W_s(S_F) \cdot pur} \quad (3.11)$$

So

$$p_s(T) = p(T) \cdot \frac{p(100)}{\beta \cdot p(100 + 2\beta)} \cdot \frac{100}{pur} \cdot \frac{S_F}{W_{SAT}(S_F)} \quad (3.12)$$

Now it is noted that the partial pressure of water in the air surrounding the drying crystal is:

$$p_A = y_A p(100) \quad (3.13)$$

where  $p(100)$  is simply used to represent the atmospheric pressure. An equilibrium should be reached (no further drying) when:

$$p_A = p_s \quad (3.14)$$

Looking for this equilibrium at a given sugar temperature  $T_s$  there is:

$$y_A = p(T_s) \cdot \frac{1}{\beta \cdot p(100 + 2\beta)} \cdot \frac{100}{pur} \cdot \frac{S_F}{W_{SAT}(S_F)} \quad (3.15)$$

$$\beta \cdot p(100 + 2\beta) = \frac{100 p(T_s)}{y_A pur} \left( \frac{S_F}{W_{SAT}(S_F)} \right)_{T_s}$$

It is possible to evaluate the right-hand-side (RHS) of this equation for a given  $y_A$ ,  $T_s$ , and  $pur$  as follows: the solubility of pure sucrose at temperature  $T_s$  is given by:

$$SOL = 64,407 + 0,07251 T_s + 0,0020569 T_s^2 - 9,035 \cdot 10^{-6} T_s^3 \quad (3.16)$$

The solubility coefficient (to correct for impurities in the film) is given by:

$$SC = 1,0 - 0,088 \frac{I}{W_s} \quad (3.17)$$

For a given  $S_F$  associated with this amount of water ( $W_s$ ), this correction for impurities is used to calculate the supersaturation as:

$$SS = \frac{S_F}{W_S(S_F)} \frac{100 - SOL}{SOL \cdot SC} \quad (3.18)$$

Noting that

$$\frac{I}{W_S} = \left( \frac{100}{pur} - 1 \right) \frac{S_F}{W_S(S_F)} \quad (3.19)$$

it follows that,

$$SC = 1 - \alpha \left( \frac{S_F}{W_S(S_F)} \right) \quad \text{with} \quad \alpha = 0,088 \left( \frac{100}{pur} - 1 \right) \quad (3.20)$$

For a solution which is just super-saturated to the point at which crystallisation begins ( $SS=1+K_0$  with  $K_0 = 0,0046$  according to Tait *et al*, 1994). It follows that:

$$\left( \frac{S_F}{W_S(S_F)} \right)_{SAT} = \frac{(1+K_0) \cancel{SOL}}{\underbrace{(100 - SOL)}_{SOL} + (1+K_0)\alpha} \quad \text{with} \quad SOL = SOL(T_s), \alpha = \alpha(pur) \quad (3.21)$$

Thus, for a given  $y_w$ ,  $T_s$  and  $pur$  the right-hand-side (RHS) of equation (3.15) can be evaluated. The left-hand-side (LHS) can be inverted to obtain the appropriate value of  $\beta$  by plotting  $\beta$  vs RHS, and fitting a curve to this plot to obtain:

$$\beta = -2 \cdot 10^{-12} (\text{RHS})^2 + 8 \cdot 10^{-6} (\text{RHS}) + 0,0962 \quad (3.22)$$

allowing evaluation of  $\frac{S_F}{W_S(S_F)}$  from equation (3.11).

Finally, the equilibrium moisture content of the drying sugar is obtained, for the *given*  $y_A$ ,  $T_s$ , and  $pur$  by

$$W_{S \text{ equilibrium}} = \frac{(S_F)_{FEED}}{\left( \frac{S_F}{W_S(S_F)} \right)} \quad (3.23)$$

The case for  $\frac{W_S(S_F)}{W_{SAT}(S_F)} > 1$  is similar, except that this ratio does not appear in equation (3.9)

(ie. it is replaced by 1). This results instead of equation (3.22) in

$$\beta = \text{MAX}(0, -4 \cdot 10^{-10} (\text{RHS})^2 + 2 \cdot 10^{-4} (\text{RHS}) - 17.171) \quad (3.24)$$

Which of these to use is not known *a priori*, so a test is necessary:

$$\begin{aligned} &\text{If } \frac{\text{pur}}{100} \{\beta\}_{\text{FROM (3.22)}} > \left( \frac{S_F}{W_S(S_F)} \right)_{\text{SAT}} \\ &\text{then } \left( \frac{S_F}{W_S(S_F)} \right) = \frac{\text{pur}}{100} \{\beta\}_{\text{FROM (3.22)}} \\ &\text{else } \left( \frac{S_F}{W_S(S_F)} \right) = \frac{\text{pur}}{100} \{\beta\}_{\text{FROM (3.24)}} \end{aligned} \quad (3.25)$$

The feed moisture content  $W_{S0}$  is approximately  $0.01 \text{ kg.kg}^{-1}$ . The initial  $S_F$  is estimated as close to saturation. It is noted that if the drying proceeds to equilibrium:

$$W_{S0} = W_{Sn \text{ equilibrium}} + \Delta W_S \quad (3.26)$$

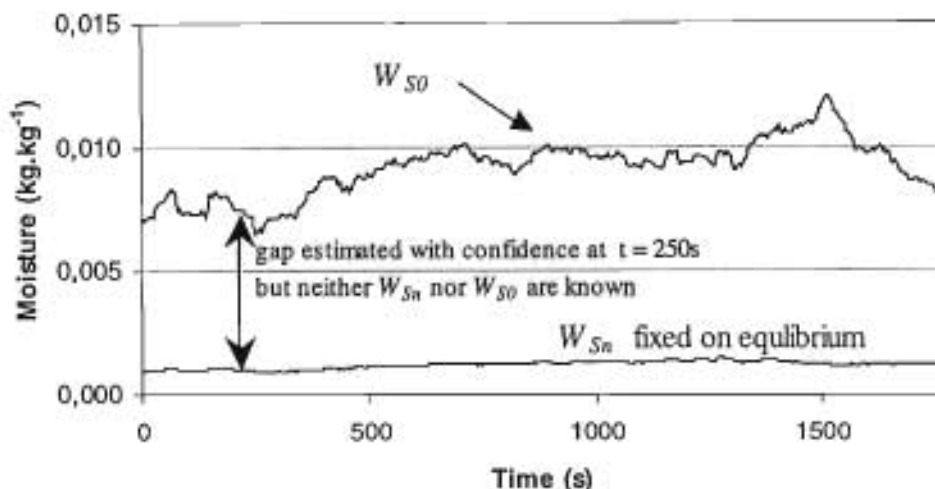


**Figure 3-1: Profiles of sugar moisture content when  $W_{Sn}$  is fixed at equilibrium**

The results from the procedure up to equation (3.26) are shown in Fig. 3-3. To verify, the calculations are done forward to eventually compare the  $y_A$ . The purpose of the above exercise is as follows: what is known with measurable accuracy is  $\Delta W_S$  (from the mass and energy balance (3.4) and (3.5)). However, the feed sugar moisture content is not continuously monitored. Thus a limiting case of equilibrium at the dryer exit has been considered to determine if this implies a consistent feed moisture in (3.26). Subsequently it has become

clearer in the actual dryer modelling that equilibrium is not generally matched, due to the slow progress of the sugar in the dryer providing enough time for crystallization from the sugar moisture. Thus the current strategy is based on a “more constant  $W_{S0}$ ”. This is not a serious limitation for estimation of the transfer coefficients, since these are predominantly related to  $\Delta W_S$  away from equilibrium.

### 3.2.3 Transformation to obtain suitable $W_{S0}$

Bear in mind, that there is some confidence in the estimate of  $\Delta W_S$ . If  $W_{Sn}$  is fixed at the equilibrium result of section (3.2.2), an estimation of  $W_{S0}$  is obtained from :

$$W_{S0} = W_{Sn} + \Delta W_S \quad (3.27)$$

This produces an unlikely plot where  $W_{S0}$  frequently falls below 0,1% moisture, and it is expected that  $W_{S0}$  should be a little above this. The explanation is that the transfer is rate-limited, and that equilibrium has not been achieved. A method is required to “ lift ” such  $W_{Sn}$  values above equilibrium to restore a more constant  $W_{S0}$  . Eq. (3.26) can be expected to hold at the lowest sugar rates measured –  $f_s = 7 \text{ kg.s}^{-1}$ . This implies that the feed the sugar has about 1,0% moisture ( $W_{S0} = 0,010 \text{ kg.kg}^{-1}$ ). Setting  $W_{S0 \text{ fixed}} = 0,010$ , an error is observed:

$$Error = W_{S0 \text{ fixed}} - W_{S0} \quad (3.28)$$

with  $W_{S0}$  obtained as in (3.26). This error was fitted as:

$$Error = 0,000044 f_s^2 - 0,000556 f_s + 0,001711 \quad (3.29)$$

Now this “smooth” error was used to lift  $W_{Sn}$  above equilibrium, thus resulting in a more constant  $W_{S0}$ :

$$\text{If } f_s \geq f_{s \text{ min}}, \quad W_{Sn} = W_{Snequilibrium} + Error \quad (3.30)$$

and obviously:

$$W_{S0 \text{ corrected}} = W_{Sn} + \Delta W_S \quad (3.31)$$

Finally, the new estimates of  $W_{S0}$  and  $W_{Sn}$  are subjected to the following double filter ( $0 < \chi < 1$ ,  $0 < \gamma < 1$ ) to distribute the process variations more or less equally, at the same time maintaining the exact calculated gap  $\Delta W_S$  throughout, which varies in time as the mass and energy balance

varies. Since most of the time there is no equilibrium,  $\Delta W_S$  is the key result implying the heat and mass transfer coefficients at any instant.

$$W_{Sn} = \gamma \text{Max} \left[ W_{S0 \text{ average}} - (Sm\Delta W_S + \chi(\Delta W_S - Sm\Delta W_S)), 0 \right] \quad (3.32)$$

$$\begin{aligned} W_{S0} = & W_{S0 \text{ average}} + \gamma \text{Max} \left[ Sm\Delta W_S + \chi(\Delta W_S - Sm\Delta W_S) - W_{S0 \text{ average}}, 0 \right] \\ & + (1 - \chi)(\Delta W_S - Sm\Delta W_S) \\ & + (1 - \gamma)(Sm\Delta W_S + \chi(\Delta W_S - Sm\Delta W_S) + W_{S0 \text{ average}}) \end{aligned} \quad (3.33)$$

$W_{S0 \text{ average}}$  is the average of  $W_{S0}$  on the whole set of data. The value is set at 0,010 kg.kg<sup>-1</sup>.  $Sm\Delta W_S$  is an average value of the  $\Delta W_S$ . Fig. 3-4 illustrates the result of the whole procedure of reconciliation.

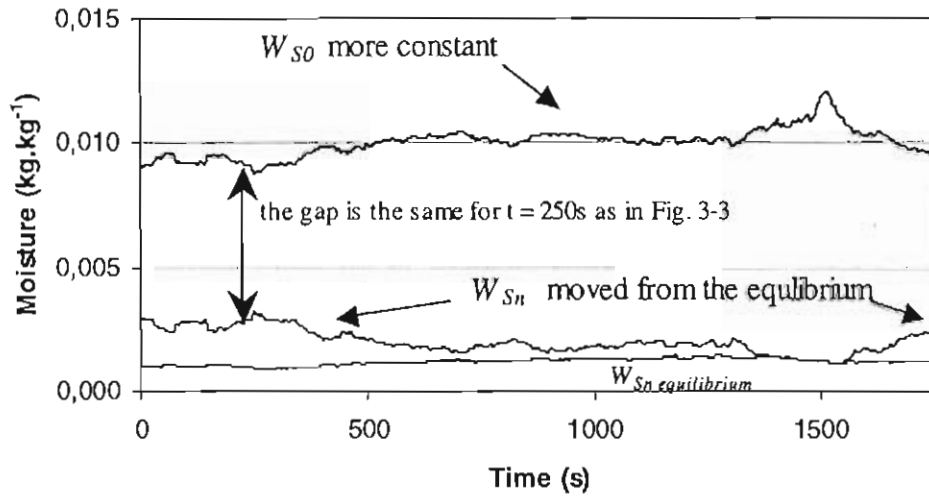


**Figure 3-1: Profiles of reconciled sugar moisture content**

### 3.2.4 Final reconciled data set

From all of these calculations, it is possible to establish a consistent data set for the model.

The data coming into the model are :  $W_{S0}$ ,  $W_{A0}$ ,  $T_{S0}$ ,  $T_{A0}$ ,  $S_{F0}$ ,  $f_S$ ,  $f_A$ .

The data coming out are :  $W_{Sn}$ ,  $W_{An}$ ,  $T_{Sn}$ ,  $T_{An}$ ,  $S_{Fn}$ .

The following graphs represent for each trial:

- The air and sugar temperature versus time
- The air and sugar moisture versus time
- The air to sugar ratio and sugar flow versus time

Data were collected on four different days. One day is split into two parts because the set of data was too long.



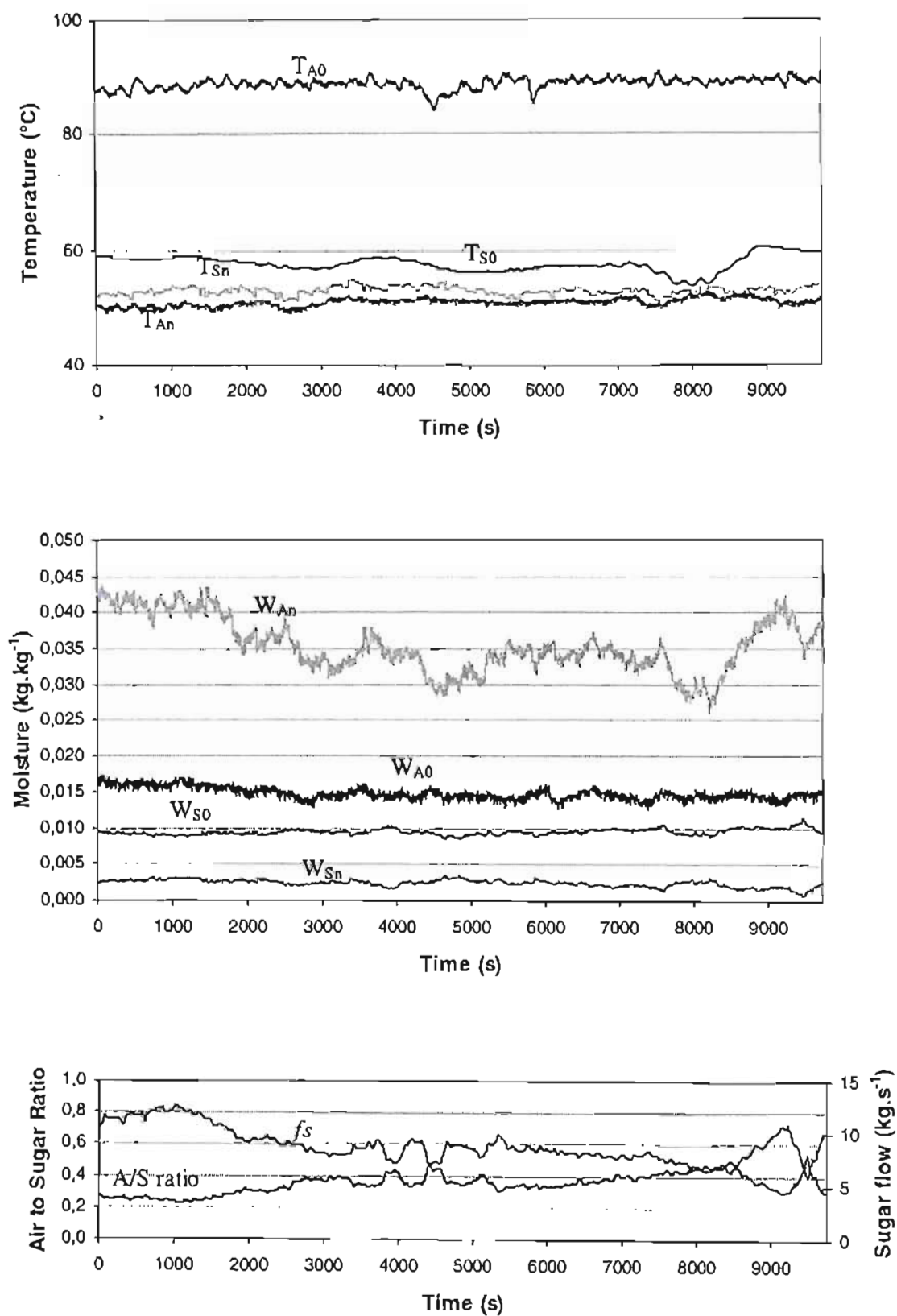


Figure 3-1: Data set from the 29 August 2000

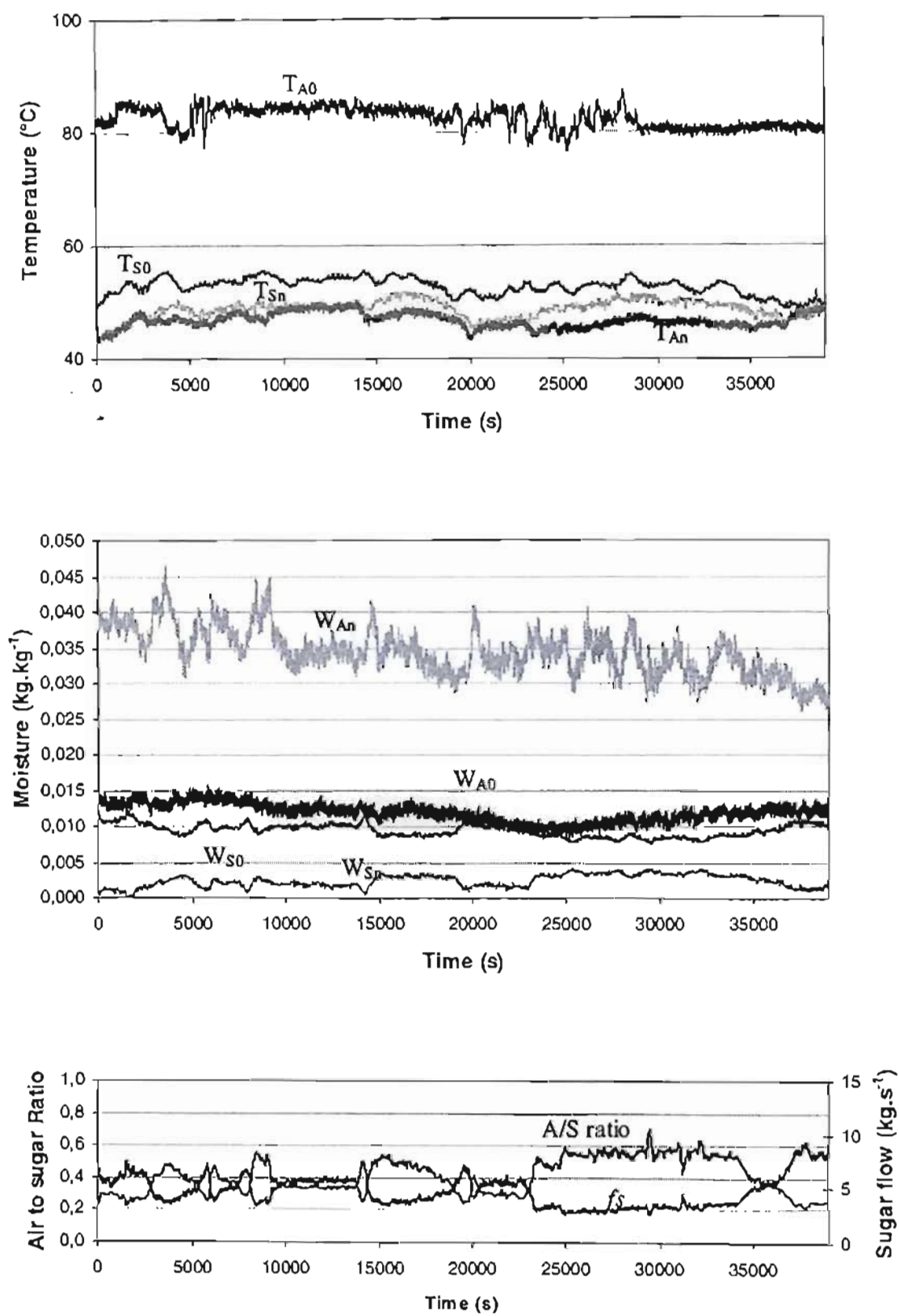


Figure 3-2: Data set from the 16 October 2000

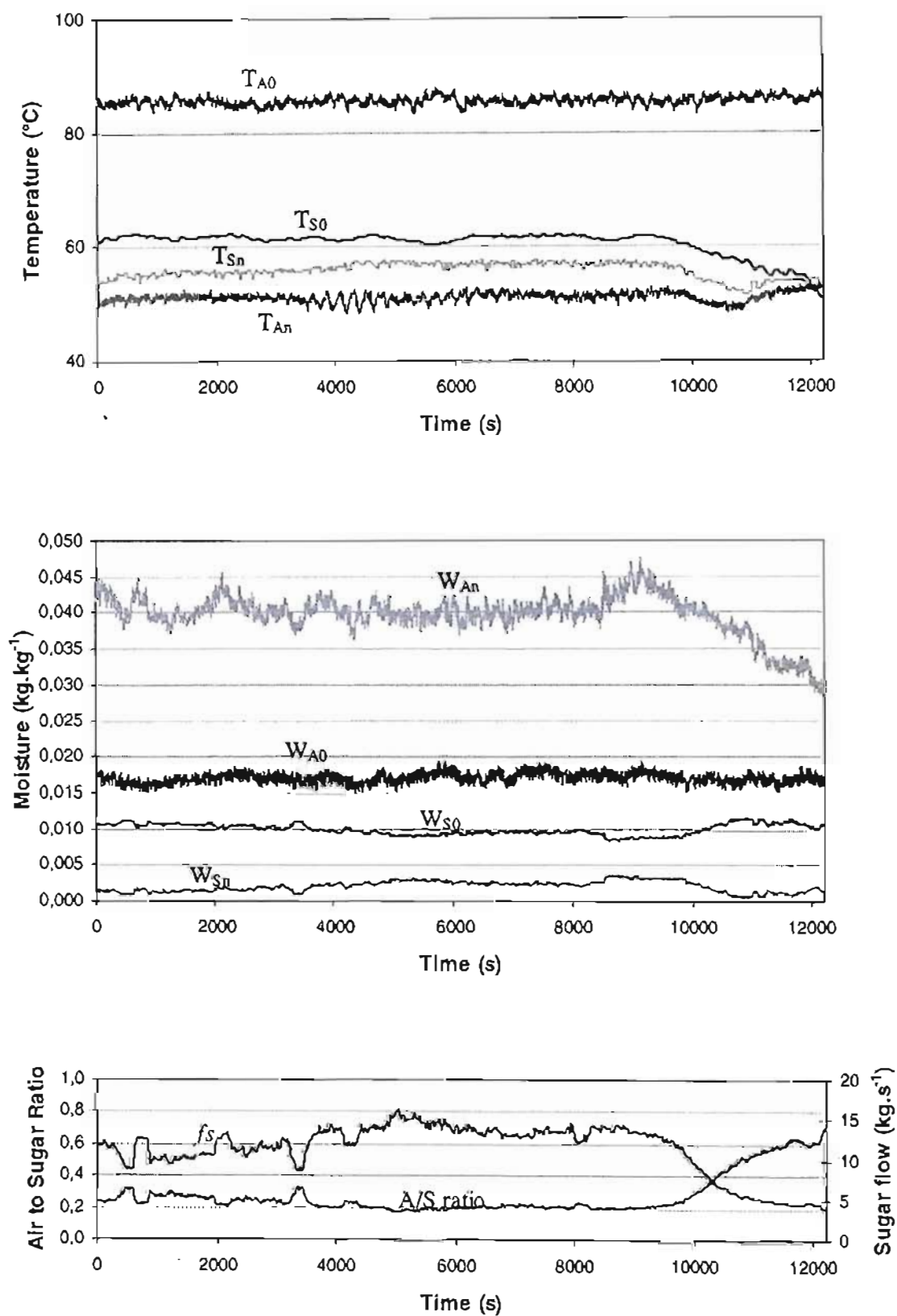


Figure 3-3: Data set from the 18 October 2000 (part I)

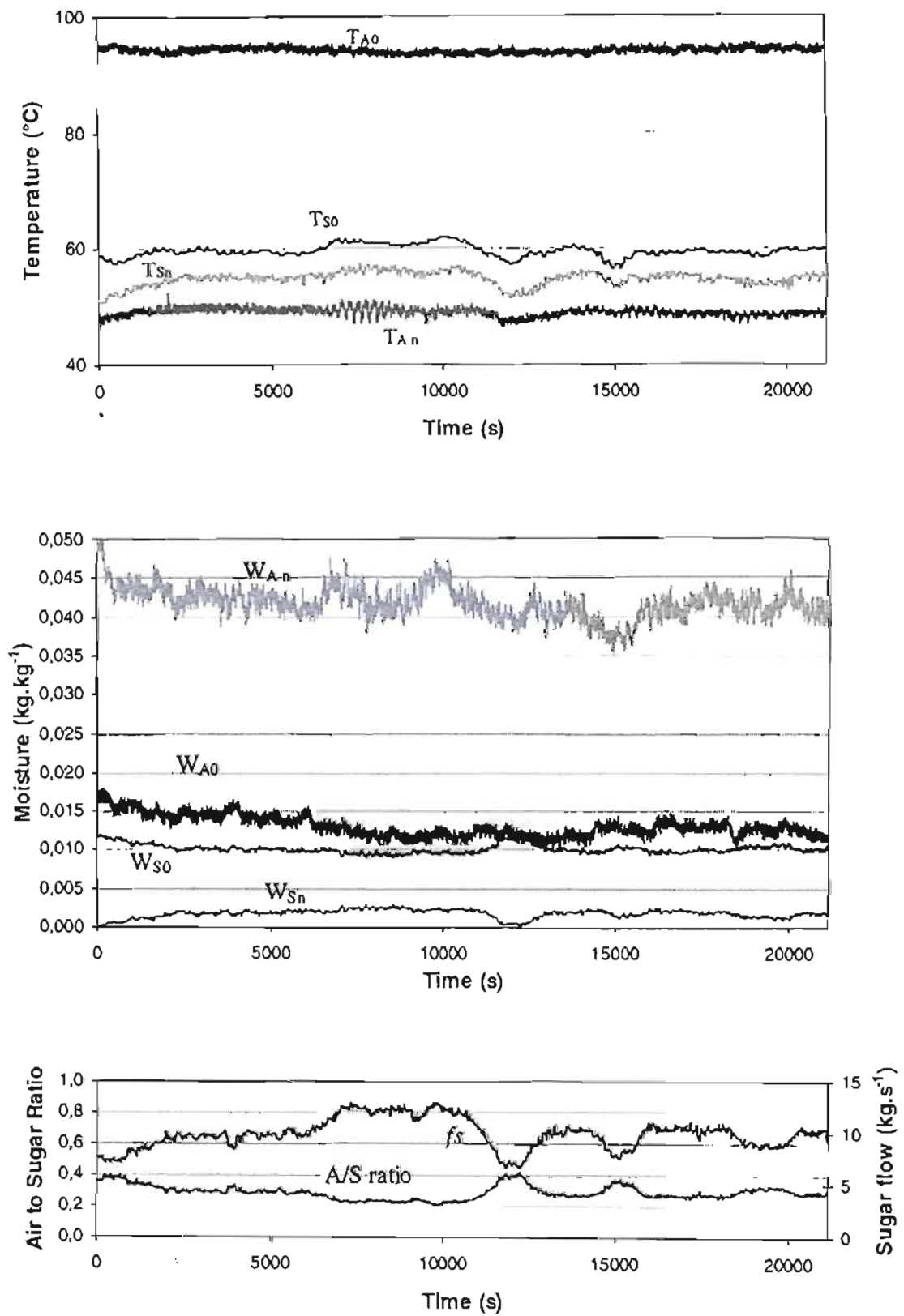


Figure 3-4: Data set from the 18 October 2000 (part II)

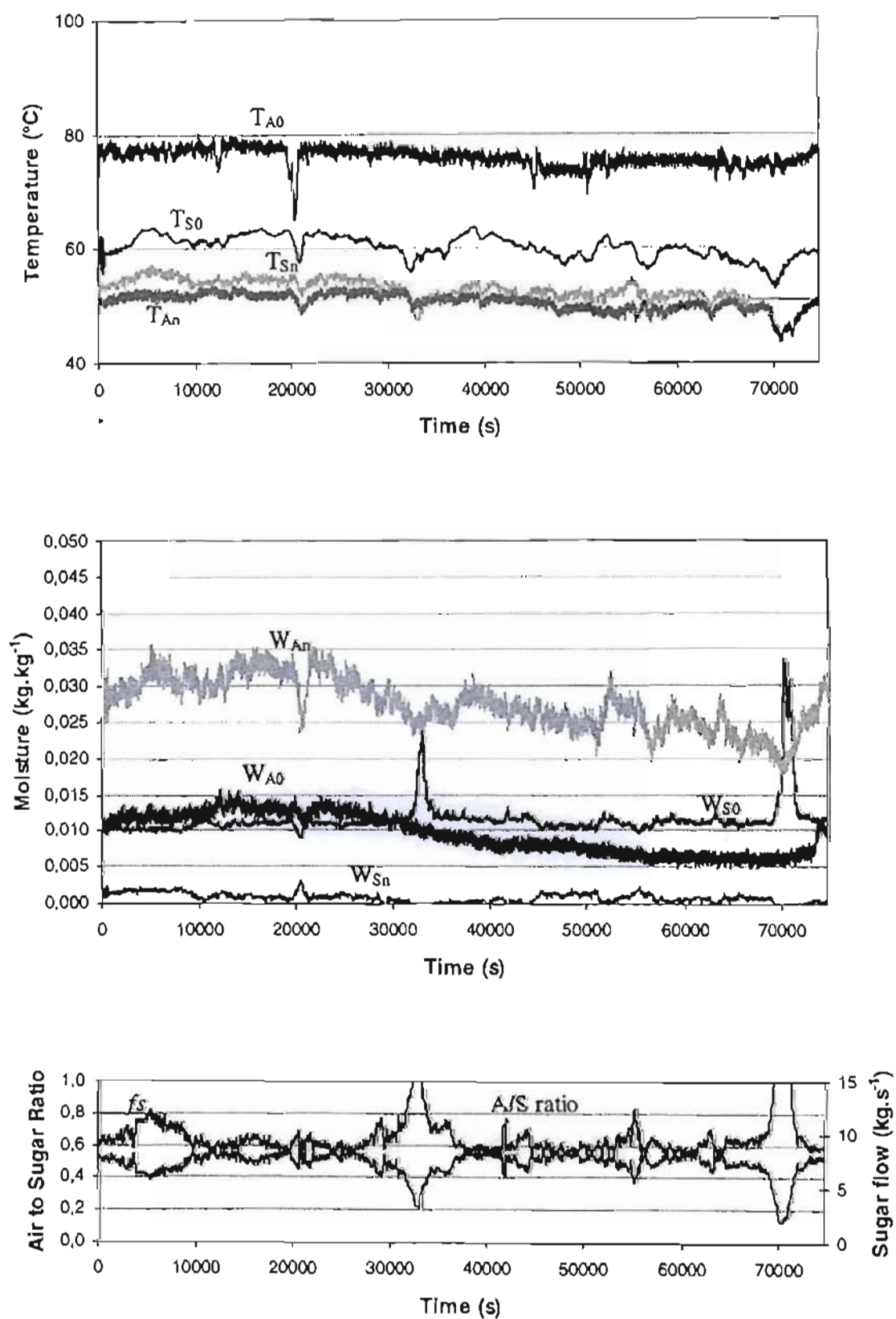


Figure 3-5: Data from the 13 December 2000

### 3.2.5 Discussion

#### 3.2.5.1 Temperature

The temperatures are direct measurements from the plant. No reconciliation treatment was carried out on them. The average values are:

**Table 3-1: Average temperature values from the trials**

Average Value (°C)	Trial 29/08/00	Trial 16/10/00	Trial 18/10/00 (I)	Trial 18/10/00 (II)	Trial 13/12/00
$T_{Ao}$	81.3	82.4	85.4	94.0	75.9
$T_{So}$	57.6	52.7	60.5	59.5	60.2
$T_{An}$	50.9	46.8	51.1	48.8	50.5
$T_{Sn}$	52.9	48.8	55.8	54.6	52.0

The behaviour of the air and sugar temperatures at the exit of the sugar dryer is interesting. The two curves are quite parallel. They join each other when the sugar flow is low and there is otherwise a temperature gap of a few degrees Celsius when the sugar flow is higher. Clearly when the sugar flow is low, an equilibrium is reached before the end of the dryer between the air and the sugar. Besides it is worth noticing that most of the time the sugar outlet temperature is higher than the air temperature. Firstly, it was thought that the calibration of the sensor might have failed but the agreement between these two temperatures at low sugar rates confirmed the similar behaviour of the sensor. In the drying process, energy is required to evaporate the water from the film around the crystal. The hot air provides this energy. The following two temperature profiles (Fig. 3-10) could explain why the sugar temperature is higher than the air temperature.

The sugar temperature is raised by the heated air at the start of drying. So the air temperature drops. The sugar temperature decreases more slowly so a gap of temperature can occur between the sugar and the air. This gap appears if the sugar flow rate is high. Sugar and air have not spent enough time in the dryer to reach a thermal equilibrium. Even if there is an apparent moisture equilibrium, the sugar temperature is always a little bit higher. A possible explanation is that a gradient of temperature occurs across the crystal, with the surface being slightly cooler. Once it lands in the exit hopper, where temperature is measured, there is no further surface evaporation, so a more uniform higher temperature is conducted through the hopper

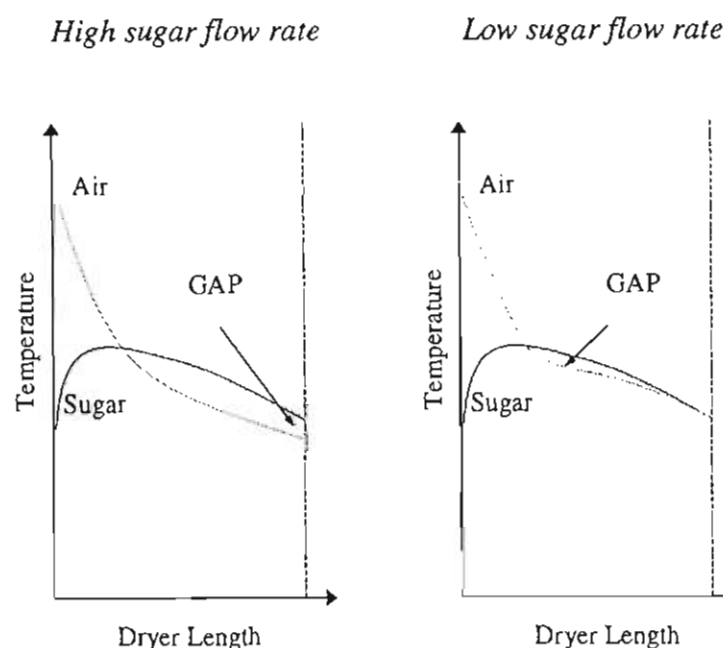


**Figure 3-1: Hypothetical temperature profiles along the dryer**

This behaviour in the temperatures profiles was also observed by Ben-Yoseph *et al.* (2000). They suggested that the heat generated by the crystallisation occurring inside the dryer was large enough to raise the crystal temperature.

### 3.2.5.2 Moisture

Only the moisture of the feed air is independently available (wet and dry bulb temperature). The other moisture contents are obtained from the data reconciliation.

**Table 3-1: Average moisture values from the trials**

Average Value (kg.kg <sup>-1</sup> )	Trial 29/08/00	Trial 16/10/00	Trial 18/10/00 (I)	Trial 18/10/00 (II)	Trial 13/12/00
$W_{A0}$	0.015	0.012	0.017	0.013	0.010
$W_{S0}$	0.010	0.010	0.010	0.010	0.012
$W_{An}$	0.035	0.034	0.040	0.041	0.028
$W_{Sn}$	0.002	0.002	0.002	0.002	0.001

$W_{sn}$  varies between 0 and 0,003. In some trials [16/10/00, 18/10/00 (II), 13/12/00],  $W_{sn}$  reaches as low as zero. This is similar to what Savaresi *et al.*(2001) found in their work. This phenomenon, occasionally occurring when the sugar rate is low, appears to be an “over-dried” mode.



## CHAPTER 4

### MODEL

#### 4.1 MODEL OF THE DRYER

##### 4.1.1 Theory

The model is based on the usual equations for convective heat transfer and mass transfer between the liquid around the sugar crystal and the stream of air. However, as the water is evaporated and the sugar cools, the liquid film becomes supersaturated and sucrose may crystallize, leaving the film with a lower purity. The rate of this crystallization is determined according to Love (2001) and Tait *et al.* (1994) who used equations developed by Broadfoot *et al.* (1980). For convenience, the relevant nomenclature is repeated in Table 4-1.

**Table 4-1: Relevant nomenclature for dryer model**

$\alpha$	Interfacial area ( $\text{m}^2 \cdot \text{m}^{-3}$ )	$k_s$	Mass transfer coefficient ( $\text{kg} \cdot \text{m}^{-2} \cdot \text{s}^{-1} \cdot \text{Pa}^{-1}$ )
$A$	Sugar dryer section ( $\text{m}^2$ )	$L_H$	Latent heat of vaporisation of water ( $\text{kJ} \cdot \text{kg}^{-1}$ )
$C_{pA}$	Heat capacity for air ( $\text{kJ} \cdot \text{kg}^{-1} \cdot ^\circ\text{C}^{-1}$ )	$p_A$	Partial pressure of air (Pa)
$C_{pS}$	Heat capacity for sugar ( $\text{kJ} \cdot \text{kg}^{-1} \cdot ^\circ\text{C}^{-1}$ )	$p_S$	Partial pressure of sugar (Pa)
$C_{p\text{vap}}$	Heat capacity for vapor ( $\text{kJ} \cdot \text{kg}^{-1} \cdot ^\circ\text{C}^{-1}$ )	$S_F$	Sucrose in film dissolved per dry sugar crystal ( $\text{kg} \cdot \text{kg}^{-1}$ )
$D_A$	Diffusivity coefficient for air ( $\text{m} \cdot \text{s}^{-1}$ )		
$D_S$	Diffusivity coefficient for sugar ( $\text{m} \cdot \text{s}^{-1}$ )	$t$	Time (s)
$f_A$	Air flow ( $\text{kg} \cdot \text{s}^{-1}$ )	$W_A$	Moisture in the air ( $\text{kg} \cdot \text{kg}^{-1}$ )
$f_S$	Sugar flow ( $\text{kg} \cdot \text{s}^{-1}$ )	$W_S$	Moisture in the sugar ( $\text{kg} \cdot \text{kg}^{-1}$ )
$G$	Crystallisation growth rate ( $\text{m} \cdot \text{s}^{-1}$ )	$\lambda_{\text{H}_2\text{O}}$	Latent heat of water ( $\text{kJ} \cdot \text{kg}^{-1}$ )
$h_S$	Sugar hold up volume fraction ( $\text{kg} \cdot \text{kg}^{-1}$ )	$\rho_A$	Air density ( $\text{kg} \cdot \text{m}^{-3}$ )
$h_s$	Heat transfer coefficient ( $\text{kW} \cdot \text{m}^{-2} \cdot \text{K}^{-1}$ )	$\rho_S$	Sugar density ( $\text{kg} \cdot \text{m}^{-3}$ )

The equations for dryer modelling are:

Water mass balance in the sugar, i.e. mass moisture in the sugar per unit mass of sugar:

$$\frac{\partial W_s}{\partial t} = -k_s \cdot \frac{a}{\rho_s} \cdot (p_s - p_A) + \frac{f_s}{A h_s \rho_s} \cdot \frac{\partial W_s}{\partial x} + D_s \cdot \frac{\partial^2 W_s}{\partial x^2} \quad (4.1)$$

Water mass balance in the air, i.e. mass moisture in the air per unit of mass air:

$$\frac{\partial W_A}{\partial t} = +k_g \times \frac{a}{\rho_A} \times \frac{h_s}{(1-h_s)} \times (p_s - p_A) + \frac{f_A}{A(1-h_s)\rho_A} \times \frac{\partial W_A}{\partial x} + D_A \times \frac{\partial^2 W_A}{\partial x^2} \quad (4.2)$$

Heat balance in the sugar:

$$\frac{\partial T_s}{\partial t} = -k_g \times \frac{a \lambda_{H_2O}}{\rho_s C p_s} \times (p_s - p_A) + h_i \times \frac{a}{\rho_s C p_s} \times (T_A - T_s) + \frac{f_s C p_s}{A h_s \rho_s C p_s} \times \frac{\partial T_s}{\partial x} + D_s \times \frac{\partial^2 T_s}{\partial x^2} \quad (4.3)$$

Heat balance in the air:

$$\begin{aligned} \frac{\partial T_A}{\partial t} = & +k_g \times \frac{a L H}{\rho_A C p_A} \times \frac{h_s}{(1-h_s)} \times (p_s - p_A) - h_i \times \frac{a}{\rho_A C p_A} \times \frac{h_s}{(1-h_s)} \times (T_A - T_s) \\ & + \frac{f_A C p_A}{A \rho_A C p_A} \times \frac{1}{(1-h_s)} \times \frac{\partial T_A}{\partial x} + D_A \times \frac{\partial^2 T_A}{\partial x^2} \end{aligned} \quad (4.4)$$

Concentration of sugar in the film, i.e. mass dissolved sugar per unit mass of dry sugar:

$$\frac{\partial S_F}{\partial t} = -G a + \frac{f_s}{A h_s \rho_s} \times \frac{\partial S_F}{\partial x} + D_s \times \frac{\partial^2 S_F}{\partial x^2} \quad (4.5)$$

These five equations have two unknowns:  $h_i$  and  $k_g$ , respectively the heat transfer coefficient and the mass transfer coefficient.

#### 4.1.2 The model

The dryer is simulated using a multi-compartment model which is solved over a time sequence using the computer language MATLAB<sup>®</sup>. The dryer is divided into ten compartments (all of the same size). Certain assumptions are made:

- The air and sugar temperature at the compartment exit represent their respective temperatures throughout the compartment.
- The air and sugar flow are supposed constant in the compartment.
- The heat loss through the cylindrical shell is neglected. Although the estimated loss could be as high as 10%, the drying is treated as an adiabatic process (See Appendix A).

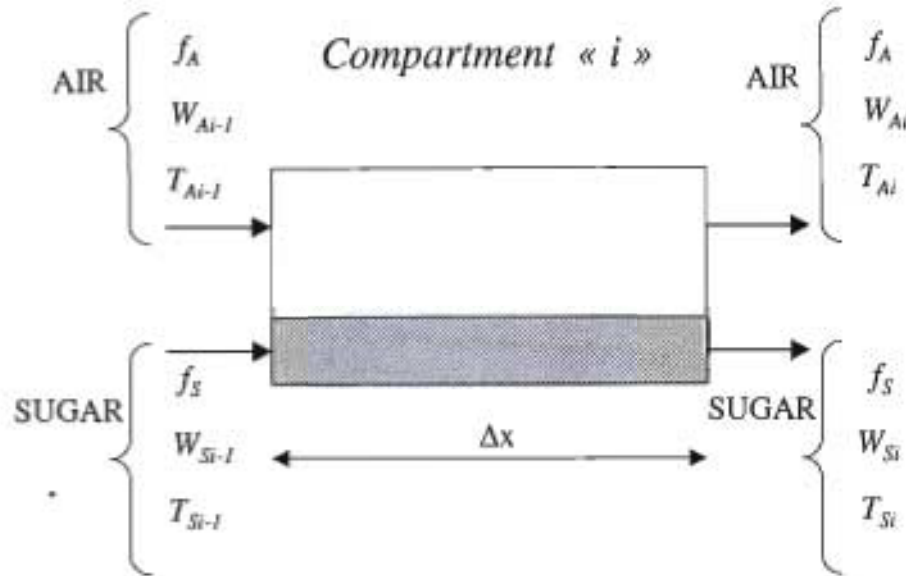


Figure 4-1: Illustration of a general compartment

#### 4.1.2.1 Partial pressure drying force from moisture content

To simplify the calculations, the partial pressure of the air moisture  $p_A$  and the partial pressure of the sugar moisture  $p_S$  should be related to the respective moisture contents on each step. Two parameters are created to give a value to  $p_A$  and  $p_S$ , respectively  $\alpha$  and  $\beta$ :

$$p_A = \xi W_A \quad (4.6)$$

$$p_S = \psi W_S \quad (4.7)$$

$p_A$  is evaluated as in section 3.2.2 from Tait *et al.* (1994). Rearranging,

$$p_A = 101325 \frac{W_A}{\frac{W_A}{18} + \frac{1}{29}} \quad (4.8)$$

$p_S$ , the partial pressure expected by the super saturated film, is estimated as in section 3.2.2 from Tait *et al.* (1994) by:

$$p_S = \frac{p(T_S) p(100)}{p(T_{bp})} \cdot \frac{W_s}{W_{sat}} \quad (4.9)$$

The boiling point temperature is calculated from the following formula suggested by Tait *et al.* (1994):

$$T_{Bp} = 100 + 2 \cdot \frac{\%Dry}{100 - \%Dry} \quad (4.10)$$

where:

$$\%Dry = 100 \cdot \frac{S_F + I}{S_F + I + W_s} \quad (4.11)$$

$p(T_s)$ ,  $p(100)$ ,  $p(T_{Bp})$  are calculated from the equation (3.8).

$\xi$  and  $\psi$  need to be re-evaluated in every compartment after each iteration.

#### 4.1.2.2 Sugar hold up volume fraction $h_s$

$h_s$  is a parameter defined as

$$h_s = \frac{\text{Volume of Sugar}}{\text{Volume of Air} + \text{Volume of Sugar}} \quad (4.12)$$

On average the sugar flow rate is around  $10 \text{ kg.s}^{-1}$ , and the residence time 5 minutes. A 5 minute residence time corresponds to a hold-up of 3 tons of sugar within the dryer. This has a volume of  $2 \text{ m}^3$ . The volume of the dryer is around  $30 \text{ m}^3$ .

So,  $h_s$  is set at 0,0625.

#### 4.1.2.3 Crystallization

To complete the model equations, the crystallisation rate  $G$  in equation (4.5) is required. It is assumed that even if the sugar has left the crystallisation pan, and has gone through the centrifugation step, this crystallisation will continue, allowing the moisture partial pressure to increase.  $S_F$  is a parameter defined as the mass of dissolved sucrose in the moisture film per unit mass of sugar.

The calculation of the growth rate is done following Love (2001).

$$G = K_1 (SS - (1 + K_0)) \exp \left( K_2 - K_3 \frac{I}{W_s} \right) \quad (4.13)$$

The parameters have been set according to the results of Love (2001)

- $K_0 = 0,005$
- $K_1 = 0,000\ 000\ 87$
- $K_2 = -\frac{E_a}{8,314 \cdot 10^{-3}} \left( \frac{1}{273,16 + T_s} - \frac{1}{333,16} \right)$
- $K_3 = 1,75$

Love (2001) defines  $E_a$  as:

$$E_a = 62,86 - 0,84(T_s - 60) \quad (4.15)$$

#### 4.1.2.4 Air flow

With a view to including both co current and counter current, and more complex arrangements, a facility is provided to specify inflows and outflows of air at every compartment.

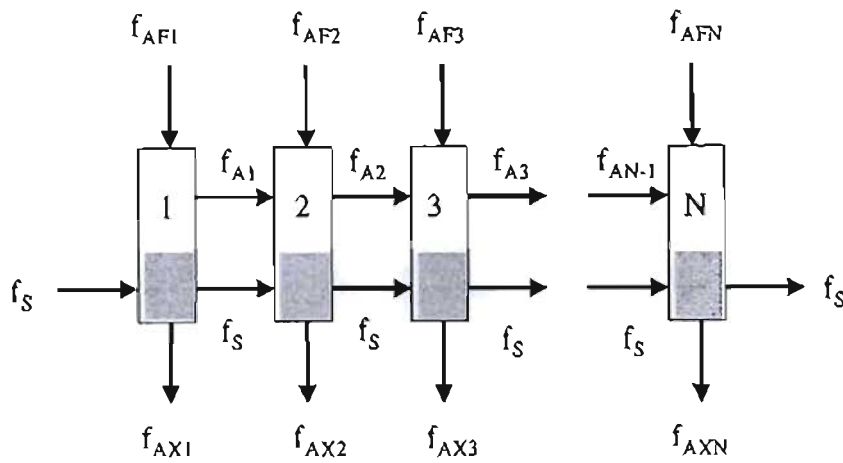


**Figure 4-1: Illustration of the airflow design in the sugar dryer**

$f_{AFi}$  is for the external air flow coming into each compartment. So the air flow supplied at the entrance with the sugar is  $f_{AF1}$ .  $f_{AXi}$  represents the airflow going out of the sugar dryer at the compartment  $i$ . So the main airflow going out in the modelled case is  $f_{AXN}$ .

Air mass balances for the sugar dryer are thus represented:

$$\begin{cases} f_{A1} = 0 + f_{AF1} - f_{AX1} \\ f_{A2} = f_{A1} + f_{AF2} - f_{AX2} \\ f_{A3} = f_{A2} + f_{AF3} - f_{AX3} \\ \vdots \\ 0 = f_{AN-1} + f_{AFN} - f_{AXN} \end{cases}$$

This can be re-arranged to give:

$$\begin{pmatrix} f_{A1} \\ f_{A2} \\ f_{A3} \\ \vdots \\ f_{AXN} \end{pmatrix} = \begin{bmatrix} 0 & 0 & 0 & \cdots & 0 \\ 1 & 0 & 0 & \cdots & 0 \\ 0 & 1 & 0 & \cdots & 0 \\ \vdots & \vdots & 1 & \ddots & \vdots \\ 0 & 0 & 0 & 1 & 0 \end{bmatrix} \begin{pmatrix} f_{A1} \\ f_{A2} \\ f_{A3} \\ \vdots \\ f_{AXN} \end{pmatrix} + \begin{bmatrix} 1 & -1 & 0 & 0 & 0 & \cdots & \cdots & 0 \\ 0 & 0 & 1 & -1 & 0 & \cdots & \cdots & 0 \\ 0 & 0 & 0 & 0 & 1 & -1 & \cdots & 0 \\ \vdots & \vdots & \vdots & \vdots & \vdots & \vdots & \ddots & \vdots \\ 0 & 0 & 0 & 0 & 0 & \cdots & 0 & 1 \end{bmatrix} \begin{pmatrix} f_{AF1} \\ f_{AX1} \\ f_{AF2} \\ f_{AX2} \\ f_{AF3} \\ f_{AX3} \\ \vdots \\ \vdots \\ f_{AFN} \end{pmatrix}$$

Thus,

$$\begin{pmatrix} f_{A1} \\ f_{A2} \\ f_{A3} \\ \vdots \\ f_{AXN} \end{pmatrix} = \begin{bmatrix} 1 & 0 & 0 & \cdots & 0 \\ -1 & 1 & 0 & \cdots & 0 \\ 0 & -1 & 1 & \cdots & 0 \\ \vdots & \vdots & -1 & \ddots & \vdots \\ 0 & 0 & 0 & -1 & 1 \end{bmatrix}^{-1} \begin{bmatrix} 1 & -1 & 0 & 0 & 0 & \cdots & \cdots & 0 \\ 0 & 0 & 1 & -1 & 0 & \cdots & \cdots & 0 \\ 0 & 0 & 0 & 0 & 1 & -1 & \cdots & 0 \\ \vdots & \vdots & \vdots & \vdots & \vdots & \vdots & \ddots & \vdots \\ 0 & 0 & 0 & 0 & 0 & \cdots & 0 & 1 \end{bmatrix} \begin{pmatrix} f_{AF1} \\ f_{AX1} \\ f_{AF2} \\ f_{AX2} \\ f_{AF3} \\ f_{AX3} \\ \vdots \\ \vdots \\ f_{AFN} \end{pmatrix}$$

In the case of this study, the extra air feeds and off-takes are not used.

#### 4.1.2.5 Discretisation of spatial derivatives

The whole model is constituted by different equations, mostly non linear. As the model is written in the MATLAB<sup>®</sup> language, it is easier to transform all the equations into a discrete form following these principles:

$$\frac{\partial^2 C}{\partial x^2} = \frac{C_{x+\Delta x} - 2C_x + C_{x-\Delta x}}{\Delta x^2} = \frac{C_{i+1} - 2C_i + C_{i-1}}{\Delta x^2} \quad (4.16)$$

$$\frac{\partial C}{\partial x} = \frac{C_x - C_{x-\Delta x}}{\Delta x} = \frac{C_i - C_{i-1}}{\Delta x} \quad (4.17)$$

All of the discretised equation coefficients can be regrouped in one matrix called the  $[CM]$  matrix. See appendix B.

The model can be represented by the single system of equations:

$$\frac{d\bar{X}}{dt} = A\bar{X} + B\bar{U} \quad (4.18)$$

$$\bar{X} = \begin{pmatrix} W_{S1} \\ \vdots \\ W_{Sn} \\ W_{A1} \\ \vdots \\ W_{An} \\ T_{S1} \\ \vdots \\ T_{Sn} \\ T_{A1} \\ \vdots \\ T_{An} \\ S_{F1} \\ \vdots \\ S_{Fn} \end{pmatrix}$$

with

The  $[A]$  and  $[B]$  matrix are built from elements of the  $[CM]$  matrix.

$\bar{U}$  is a vector that contains all of the exogenous inputs (feed: flow and conditions).

## 4.2 AXIAL DISPERSION

### 4.2.1 Theory

In this section, a theoretical description of the axial dispersion is developed for comparison with modelled dispersion in section 4.2.2. An instantaneous unit mass point source expanding from  $x = 0$  at  $t = 0$ , with Fick's diffusion

$$flux = -D_a \frac{\partial C}{\partial x} \quad (4.19)$$

can be shown (Seinfeld, 1975) to have the 1-dimensional "puff" distribution:

$$C(x, t) = \frac{1}{\sigma\sqrt{2\pi}} \exp\left\{\frac{-x^2}{2\sigma^2}\right\} \quad \text{with} \quad \sigma = \sqrt{2D_a t} \quad (4.20)$$

It is easily shown that the total mass of this distribution is:

$$M = \int_{-\infty}^{+\infty} C(x, t) dx = 1 \quad (4.21)$$

Displacing the "puff" at velocity  $v$  will clearly result in:

$$C(x, t) = \frac{1}{\sigma\sqrt{2\pi}} \exp\left\{\frac{-(x - vt)^2}{2\sigma^2}\right\} \quad (4.22)$$

If the distribution is integrated along a duct, the integral results from a concentration step at the duct entrance from 1 to 0 at  $t = 0$ . The following curve in Fig. 4-3 is obtained:

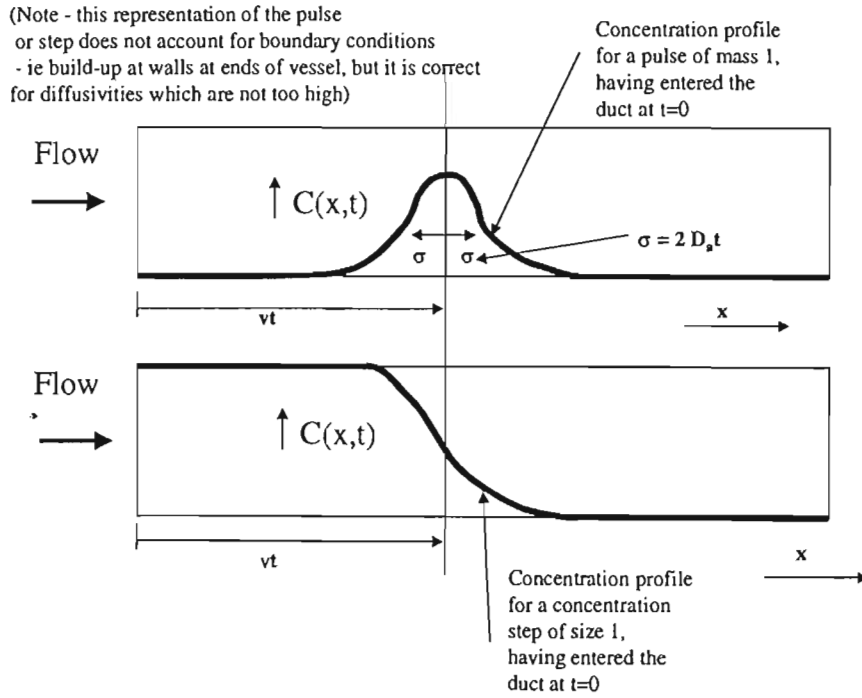


**Figure 4-1: Axial dispersion in a duct**

The formula for the incoming step ( $t=0$ ), from  $C(0,0)=0$  to  $C(0,0_+)=1$ , is found by integrating as follows:

$$C(x,t) = 1 - \int_{-\infty}^x \frac{1}{\sigma\sqrt{2\pi}} \exp\left\{-\frac{(x' - vt)^2}{2\sigma^2}\right\} dx' \quad (4.23)$$

Let  $y = \left(\frac{x' - vt}{\sigma\sqrt{2}}\right)$ , so  $dy = \left(\frac{1}{\sigma\sqrt{2}}\right) dx'$

And  $C(x,t) = 1 - \frac{1}{\sigma\sqrt{2\pi}} \int_{-\infty}^{\left(\frac{x-vt}{\sigma\sqrt{2}}\right)} e^{-y^2} (\sigma\sqrt{2}) dy$

$$= 1 - \frac{1}{\sqrt{\pi}} \int_{-\infty}^{\left(\frac{x-vt}{\sigma\sqrt{2}}\right)} e^{-y^2} dy$$

Now,  $\frac{2}{\sqrt{\pi}} \int_0^P e^{-y^2} dy = \text{erf}(P)$  and  $\text{erf}(\infty) = 1$

$$\frac{2}{\sqrt{\pi}} \int_P^\infty e^{-y^2} dy = \text{erfc}(P) \text{ and } \text{erfc}(\infty) = 0$$

So, for  $x \leq vt$ ,



$$C(x, t) = 1 - \frac{1}{2} \operatorname{erfc} \left( \frac{vt - x}{\sigma\sqrt{2}} \right) = \frac{1}{2} \left\{ 1 + \operatorname{erf} \left( \frac{vt - x}{\sigma\sqrt{2}} \right) \right\} \quad (4.24)$$

And,  $x \geq vt$ ,

$$C(x, t) = \frac{1}{2} \left\{ 1 - \operatorname{erf} \left( \frac{x - vt}{\sigma\sqrt{2}} \right) \right\} = \frac{1}{2} \operatorname{erfc} \left( \frac{x - vt}{\sigma\sqrt{2}} \right) \quad (4.25)$$

#### 4.2.2 Comparison of theoretical and modelled axial dispersion

The first step when the model was created in MATLAB<sup>®</sup> was to ensure that the axial dispersion was well predicted. Several runs were done with the following profiles:

- The heat and mass transfer coefficients were set to zero.
- Air and sugar steps were considered separately.
- An increase of temperature occurs during the modelled period time: step of 50°C.

It was chosen to work with this temperature for convenience, but it was equally possible to deal with the moisture in the sugar or the air.

The modelled data captured as a result were analysed to be sure that the axial dispersion modelled matched the theory. The theory was represented as follows:

$$\text{If } x \leq f_i \cdot t, \quad T = T_{\min} + (T_{\max} - T_{\min}) \cdot 0.5 \cdot \left( 1 + \operatorname{erf} \left( \frac{f_i \cdot t - x}{\sigma\sqrt{2}} \right) \right) \quad (4.26)$$

$$\text{If } x \geq f_i \cdot t, \quad T = T_{\min} + (T_{\max} - T_{\min}) \cdot 0.5 \cdot \left( 1 - \operatorname{erf} \left( \frac{x - f_i \cdot t}{\sigma\sqrt{2}} \right) \right) \quad (4.27)$$

$f_i$  can be either the sugar flow or the air flow.

##### 4.2.2.1 Improved convection

Early tests suggested that the convection and diffusion aspects of the model should be separated, to reduce “numerical diffusion”. Indeed, if the discretisation of the model is shown on a grid analysis (Fig. 4-4):

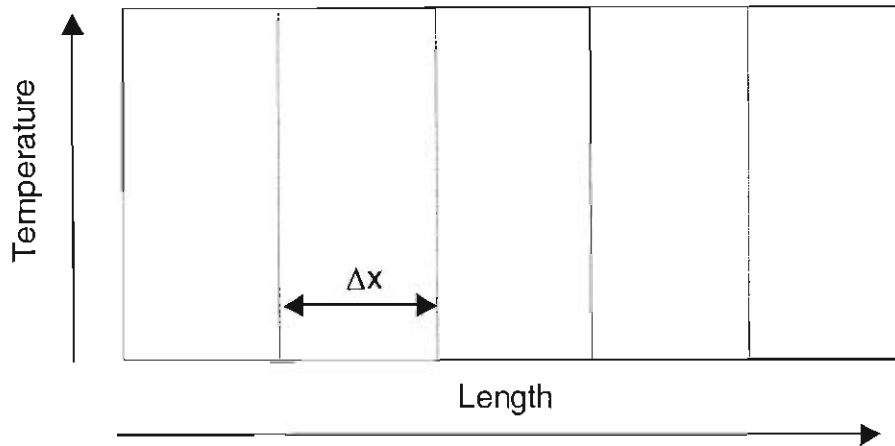


**Figure 4-1: Grid analysis for the discrete model**

On the y-axis the temperatures are on a scale that can represent the temperature inside the dryer. The x-axis represents the length along the dryer but predictions are only done at multiples of  $\Delta x$ . The “movement” inside the dryer is not smooth as in reality but a succession of small jumps. When a change in temperature occurs, the temperature step moves along the dryer as in Fig. 4-5:

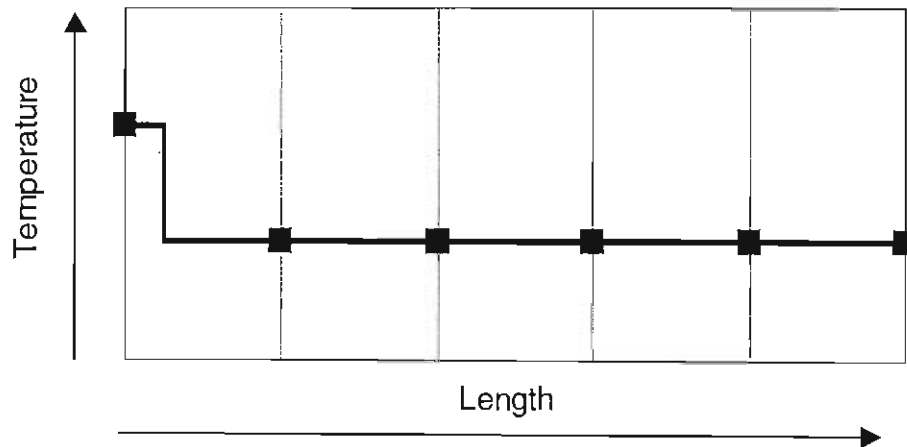


**Figure 4-2: Increase of temperature**

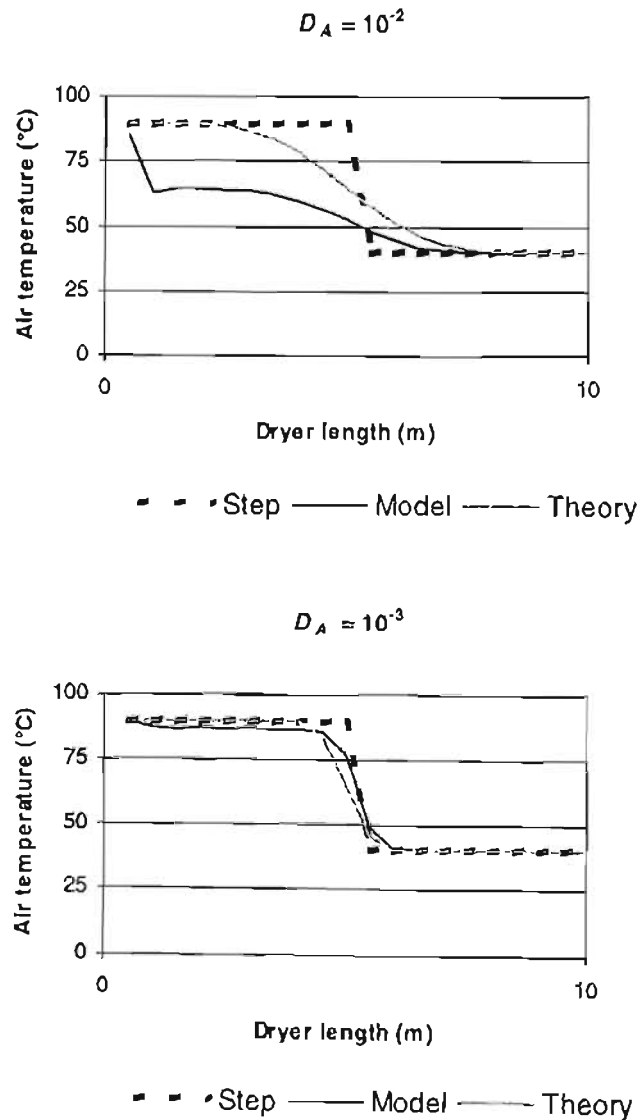
This situation cannot be represented in the grid analysis. The movement must agree with the predefined crossing points to maintain accuracy. So a new  $[CC]$  matrix was built similar to the  $[CM]$  matrix containing only the convective coefficients. The integration process of (4.18) was split into two steps. Firstly, an integration of the Euler type is done for the convective aspect of the model only. This needs two new matrices  $[AC]$  and  $[BC]$ .

$$\bar{X}_{i+1} = \bar{X}_i + dt \cdot (AC \cdot \bar{X}_i + BC \cdot \bar{U}_i) \quad (4.28)$$

Then the integration represented (4.18) can be done, using the new  $\bar{X}$ . A “stop-start” convection mode was used such that the total distance travelled was represented by the nearest whole  $\Delta x$  step. This “operator splitting” gave only a small ripple on the model output.

4.2.2.2 Results

In order to validate the model, the theoretical diffusion profile has been developed for comparison with the numerical solution of diffusion by the model. One example of the test is shown in the following figure. A step of  $+50^{\circ}\text{C}$  was chosen to increase the air temperature from  $40^{\circ}\text{C}$  to  $90^{\circ}\text{C}$ . These graphs show the front of the step-change moving forward through the dryer. Initially, the temperature inside the dryer is  $40^{\circ}\text{C}$ , and this rises to  $90^{\circ}\text{C}$  as the step passes through. Different values for  $D_A$  were tried from  $10^{-2}$  to  $10^{-7} \text{ m}^2.\text{s}^{-1}$ , the results are shown in Fig. 4-6. Similar results are observed with  $D_S$ . (Note, for the model of the actual process,  $D_A = D_S = 10^{-6} \text{ m}^2.\text{s}^{-1}$  was used).



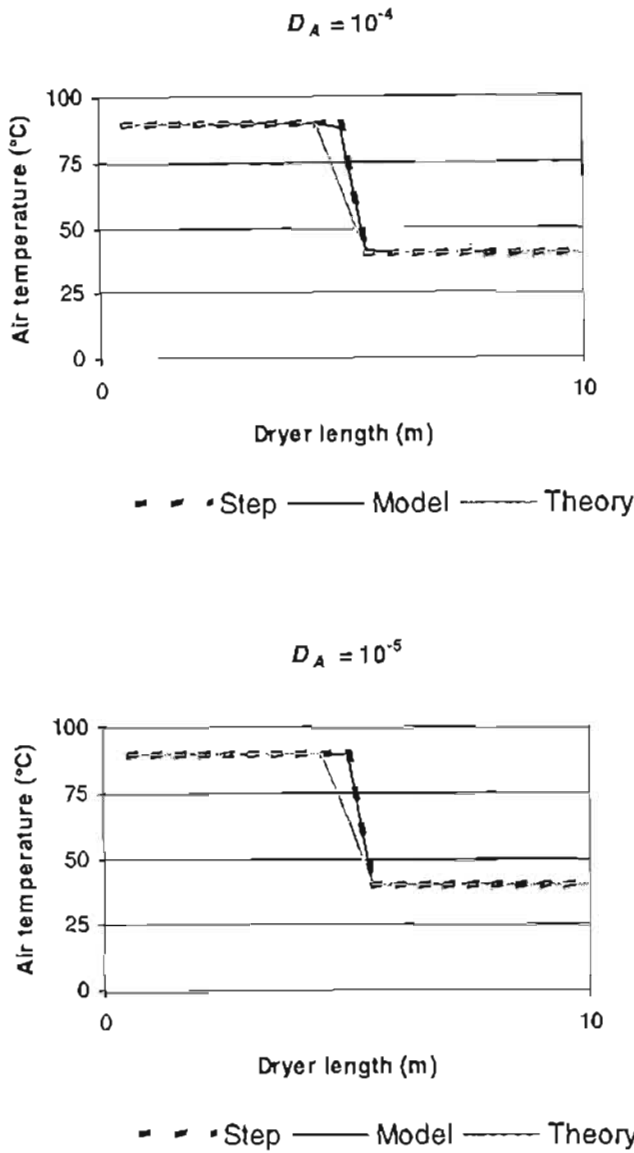


Figure 4-1: Graphs representing axial dispersion

As the value of  $D_A$  decreases, the model plot tends to join the theoretical plot. The theoretical axial dispersion prediction at low axial diffusivity,  $D_A < 10^{-5} \text{ m}^2.\text{s}^{-1}$ , gives acceptable agreement. The modelled air temperature along the dryer follows the forced temperature step. When  $D_A \geq 10^{-5} \text{ m}^2.\text{s}^{-1}$ , significant deviations are observed - especially for high values of axial diffusivity, the prediction tends to diverge. Similar results were obtained with the sugar for the temperature and the moisture content.

### 4.3 MOISTURE CONTENT ISOTHERM

Sugar crystals left for a while in contact with air will achieve a state of equilibrium. The moisture content in the film surrounding the sugar crystal is in equilibrium with the moisture content in the air. The model equations should be able to recreate this phenomenon.

Two situations are relevant. Firstly, the sugar crystal is considered at a temperature  $T_0$ , where it is in equilibrium with the surrounding environment. This situation can represent an initial equilibrium state. Secondly, the sugar crystal is moved to a temperature  $T_1$  that is higher than  $T_0$ . The water contained in the film is going to leave it to reach a new equilibrium. As the crystallisation has a slight effect, it is neglected in the following analysis.

The sorption isotherm of white sugar for different temperatures from Schindler and Juncker (1993) has been used as reference. (Fig. 4-7)

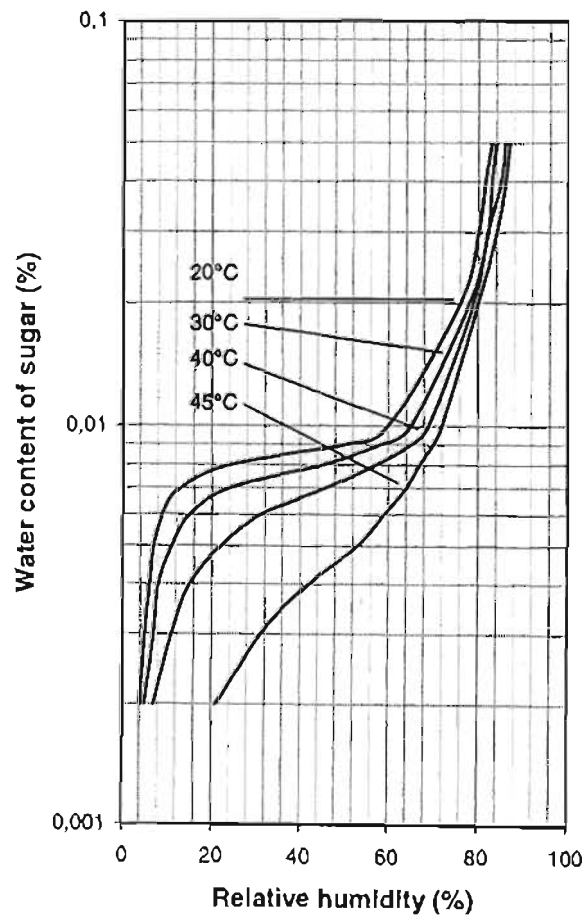


**Figure 4-1: Sorption isotherms of white sugar for different temperatures (Schindler and Juncker, 1993)**

The model equations proposed by Tait *et al.*(1994) are solved inversely in an EXCEL spreadsheet to simulate an equivalent isotherm.

Before entering the sugar dryer, parameters are fixed to calculate the mass percent of water in the sugar feed.

Before entering the sugar dryer:

$$M_{Total} = M_{Crystal} + (M_{Sucrose} + M_{Water} + M_{Impurity})_{in\ the\ film} \quad (4.29)$$

Where  $M_{Sucrose}$  refers to the dissolved sucrose in the film. The parameters fixed are:  $M_{Crystal}$ ,  $M_{Sucrose}$ ,  $T_{S0}$ , and  $pur$ .

$$pur = 100 \cdot \frac{M_{Sucrose}}{M_{Sucrose} + M_{Impurity}} \quad (4.30)$$

From (4.30),  $M_{Impurity}$  is calculated.

It is assumed that the water in the film at the feed ( $M_{Waterf}$ ) is supersaturated to the point of crystallisation. From (3.16), (3.20), and 4.1.2.3,

$$M_{Waterf} = M_{Sucrose} \frac{100 - SOL + (1 + K_0) \cdot \alpha \cdot SOL}{(1 + K_0) \cdot SOL} \quad (4.31)$$

The mass percentage of water in the sugar can be calculated:

$$\%Water = 100 \cdot \frac{M_{Waterf}}{M_{Waterf} + M_{Crystal} + M_{Sucrose} + M_{Impurity}} \quad (4.32)$$

Inside the dryer in the present isotherm analysis, it is assumed that there is no crystallisation. The water content of sugar is fixed at different points lower than  $\%Water$  to determine the isotherm. The calculation process is then similar to the one in paragraph 4.1.2.1 to find  $p_S$ . The equilibrium is reached when  $p_S = p_A$ . From there the relative humidity is found.

With the Tait *et al.* (1994) equations used to determine the vapour pressure of the crystal film, it was resolved to run the main simulation model to equilibrium to check whether it was able to simulate the Schindler and Juncker (1993) isotherm. The inherent difficulty of this is that it is very dependent on the original amount of dissolved sucrose in the crystal film, as supplied to the dryer. Ultimately this sucrose, or the portion left after partial crystallisation during the drying, determines the reduction of the film vapour pressure, and thus determines the equilibrium air moisture content. Finally, this initial film sucrose content was “tuned” to match a single point ( $W_S = 0,008$  and  $RH = 45\%$  with the  $30^\circ\text{C}$  sorption isotherm), giving the complete isotherm in Fig. 4-8.

In a normal dynamic situation there will be a change of moisture content with time until an equilibrium is reached, and that final equilibrium moisture will, on the basis of the theory used, have no dependence on the mass of dry sugar. It is rather dependent on the mass of dissolved sucrose. So the attempts to “tune”  $S_{Fn}$  were merely a means to “second-guess” the typical conditions under which the isotherm might have been generated.

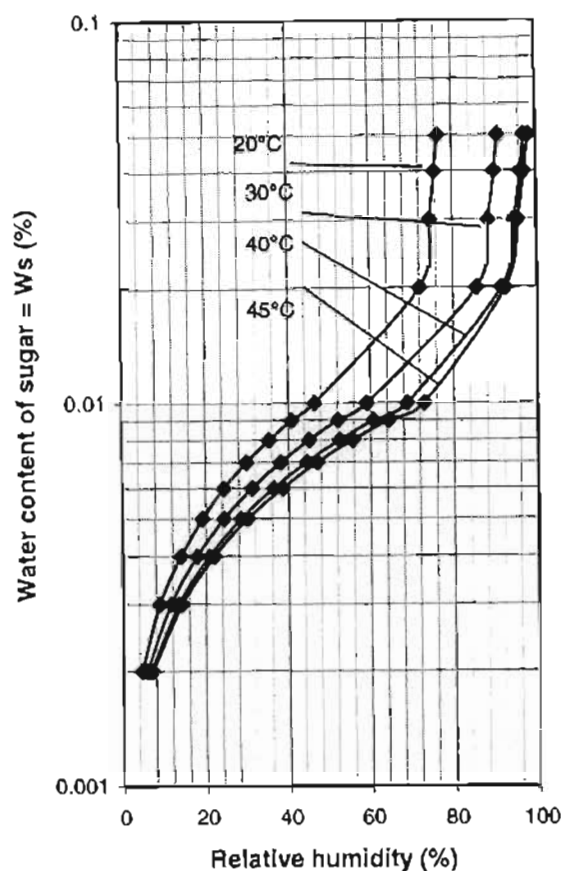


Figure 4-2: Sorption isotherm results from the model

Resemblance/Difference:

- The graphs are located in the correct range of values
- The shape is similar: when the water content of sugar tends to go up, the relative humidity increases in a hyperbolic way. The gap between 0,01 and 0,02 for  $W_s$  is observed.
- The slope of the curves is not so pronounced for the low range of  $W_s$ , especially for high temperatures.

The difficulty in fitting exactly the Schindler and Juncker (1993) isotherm remains in that the model depends on too many parameters that are not exploited here. Besides, the sorption isotherms from the literature are for white sugar, while the model is arranged for raw sugar.

The Tait *et al.* (1994) equations could be solved to give similar behaviour to the Schindler and Juncker (1993) isotherm for equilibrium sugar moisture content. However, the match was found to be strongly dependent on the initial dissolved sucrose in the water film, for which a single value was eventually chosen to fit the entire isotherm. The double equilibrium of zero net crystallisation and zero net evaporation was not achieved, and even if it were, it would be independent of the amount of dry sugar present.

## 4.4 THE HEAT AND MASS TRANSFER COEFFICIENTS

### 4.4.1 Results

Using the reconciled data, the model written in the MATLAB<sup>®</sup> language has been run over the associated time sequences. The results are shown in Fig. 4-9 for the 29/08/2000, Fig. 4-10 for the 16/10/2000, Fig. 4-11 for the 18/10/2000 (part I), Fig. 4-12 for the 18/10/2000 (part II), Fig. 4-13 for the 13/12/2000.

After a few runs of the program, trying to fit the model to the plant data, it appeared that the heat and mass transfer coefficient varied together. For each trial, a best tuning was found. The results are in Table 4-1.

**Table 4-1: Heat and mass transfer coefficient values to match data for each trial**

	Heat transfer coefficient (kW.m <sup>-2</sup> .K <sup>-1</sup> )	Mass transfer coefficient (kg water.m <sup>-2</sup> .s <sup>-1</sup> .Pa <sup>-1</sup> )
Trial 29/08/2000	0,013	1,3×10 <sup>-9</sup>
Trial 16/10/2000	0,011	1,1×10 <sup>-9</sup>
Trial 18/10/2000 (part I)	0,015	1,5×10 <sup>-9</sup>
Trial 18/10/2000 (part II)	0,015	1,5×10 <sup>-9</sup>
Trial 13/12/2000	0,014	1,4×10 <sup>-9</sup>

An average value is determined for the model.

$$h_t = 0,0136 \text{ kW.m}^{-2}.\text{K}^{-1}$$

$$k_g = 1,36 \times 10^{-9} \text{ kg water.m}^{-2}.\text{s.Pa}^{-1}$$

The ranges of values for the transfer coefficients from the literature are 0,3 to 0,0019 kW.m<sup>-1</sup>.K<sup>-1</sup> for the heat transfer coefficient and 2,7×10<sup>-9</sup> to 72×10<sup>-9</sup> kg.m<sup>-2</sup>.s<sup>-1</sup>.Pa<sup>-1</sup> for the mass transfer coefficient (Table 1-1). The estimated values found from the reconciled data are within the literature heat transfer range, and just below the literature mass transfer range. The sugar quality in terms of origin and location might explain this difference. The indicated average values are used in subsequent modelling.



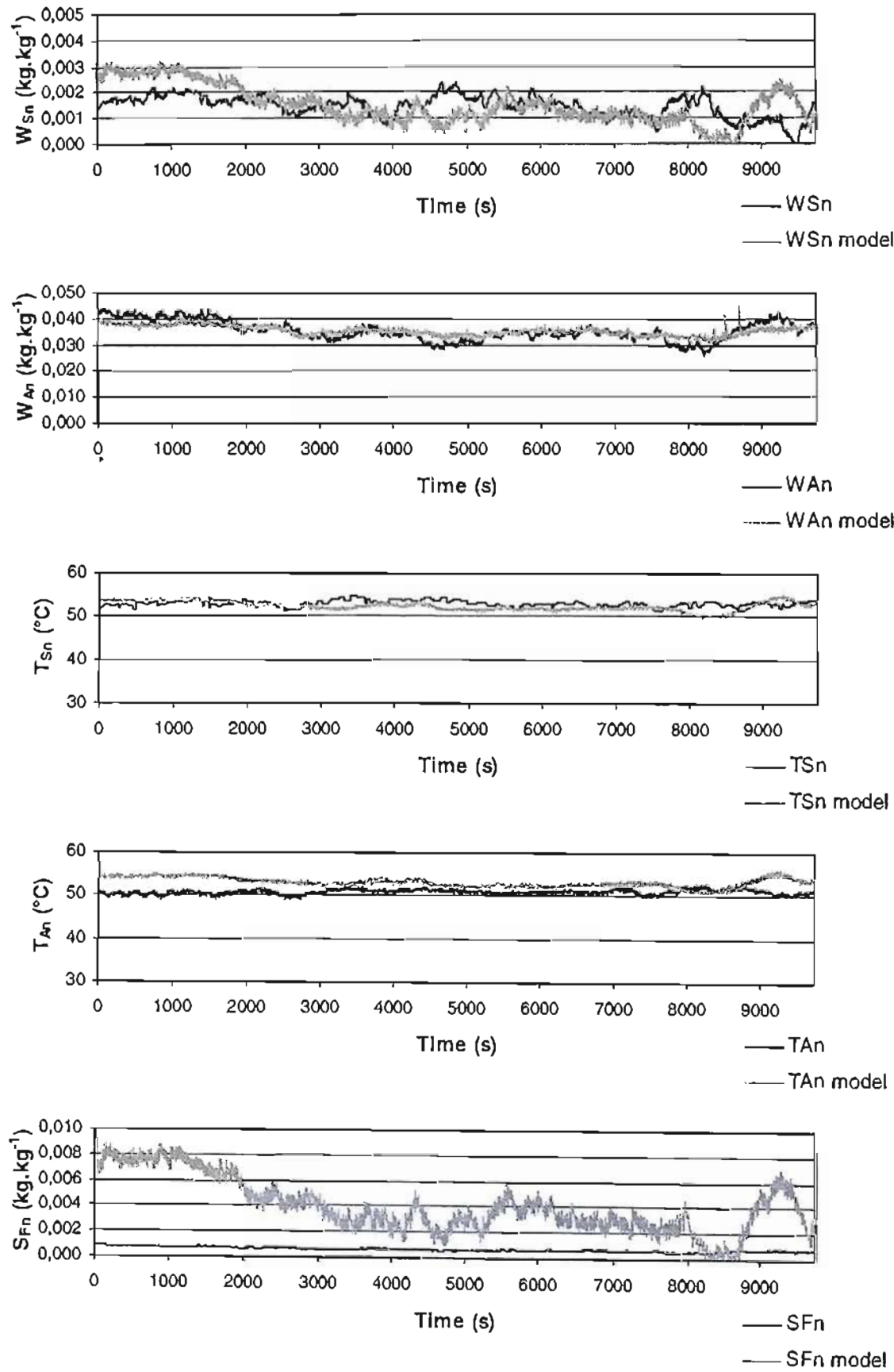


Figure 4-1: Comparison between data plant and data model for 29 August 2000

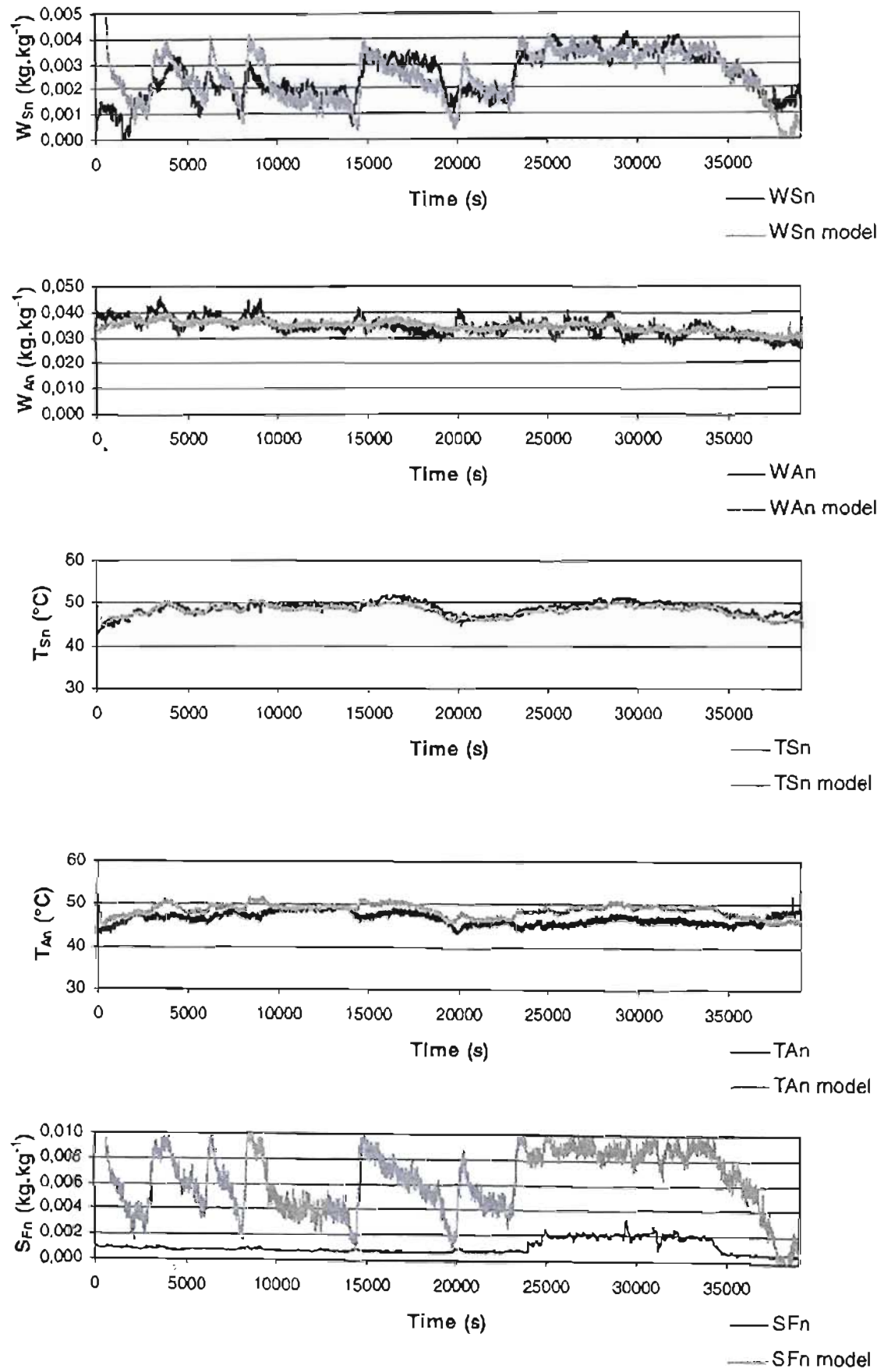


Figure 4-2: Comparison between data plant and data model for 16 October 2000

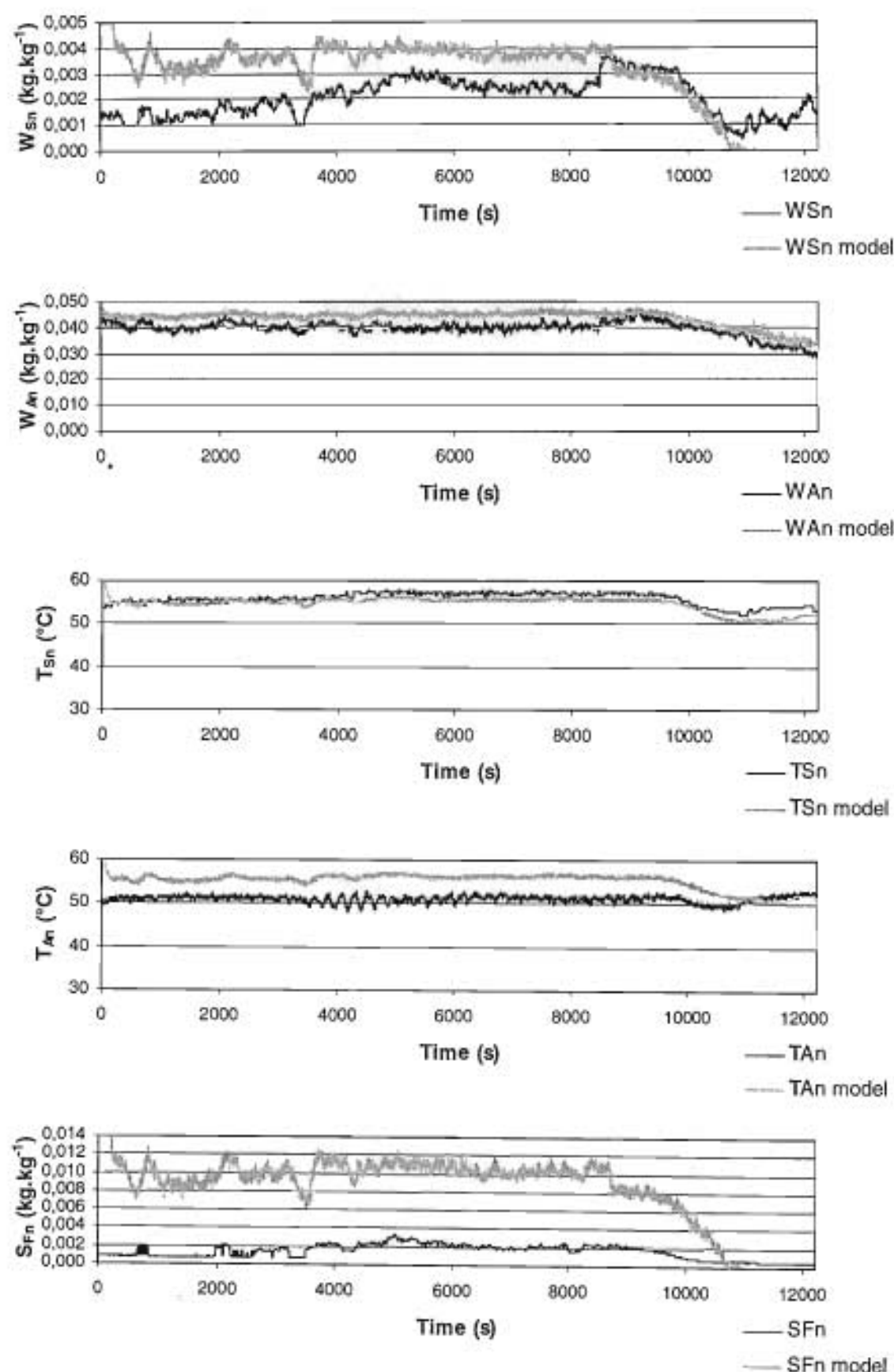


Figure 4-3: Comparison between data plant and data model for 18 October 2000 (I)

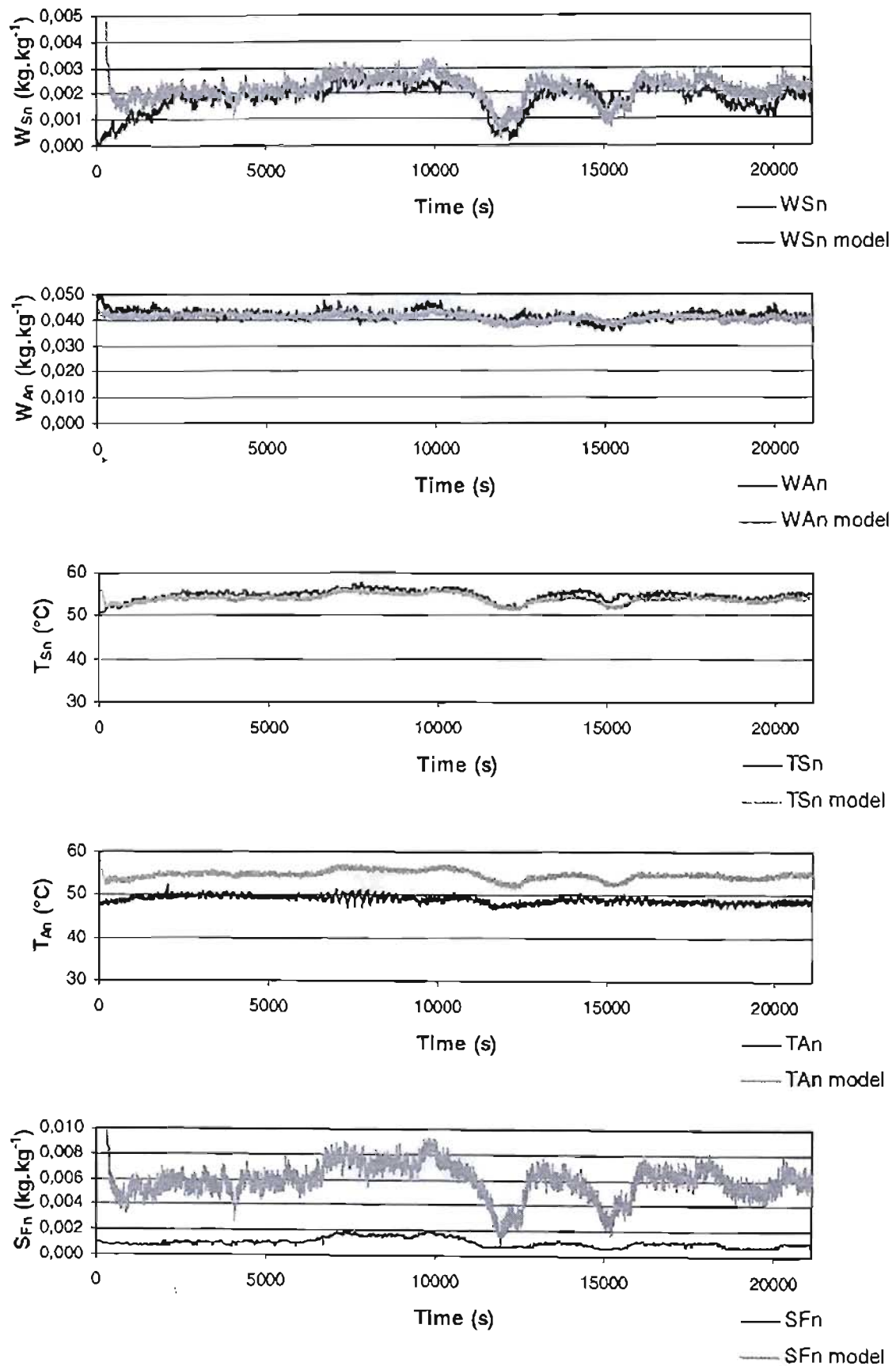


Figure 4-4: Comparison between data plant and data model for 18 October 2000 (II)

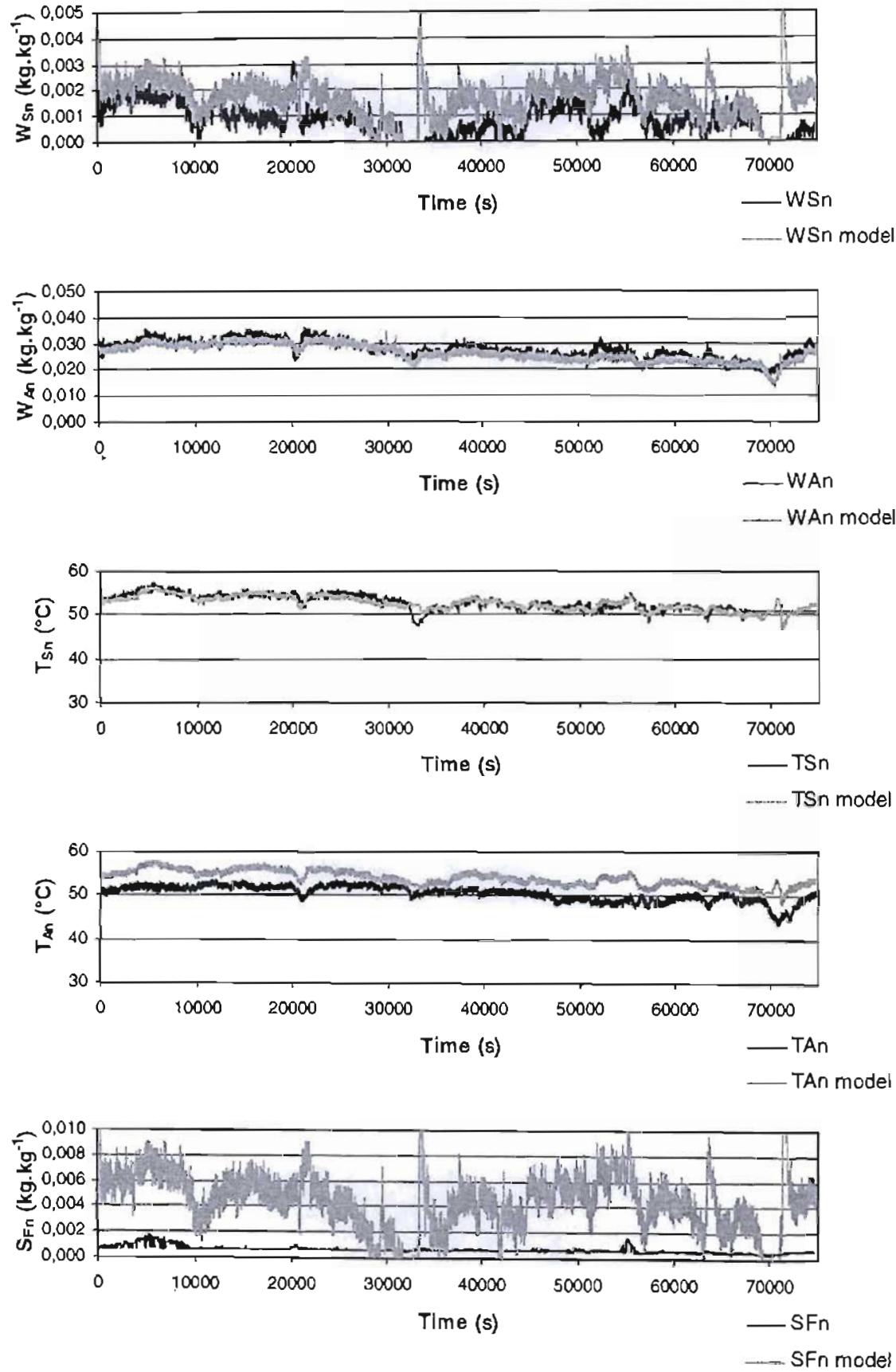


Figure 4-5: Comparison between data plant and data model for 13 December 2000

### 4.4.2 Discussion

#### 4.4.2.1 Moisture content

The model response concerning the exit sugar moisture is acceptable in most of the trials. The model manages to remain around the plant value with particularly good matches in Fig. 4-10 and Fig. 4-12. The changes in  $W_{Sn}$  are simulated very nicely. The model is able to simulate the “over-dried” mode described by Savarei *et al.*(2001). The close tracking of  $W_{Sn}$  in most cases is largely the result of the reduced pressure differential driving the mass transfer as the equilibrium is approached. Recall that the reconciled data in section 3.2 was arranged to achieve equilibrium when the plant was operating at its lowest sugar rates. This was the only way of fixing the absolute levels of  $W_{Sn}$  and  $W_{So}$  (though the gap  $\Delta W_S$  was more accurately known). Thus the dryer model is simply using the same available sugar moisture until it meets mass transfer resistance near the dryer exit. Figures 3-3 / 4-9, 3-4 / 4-10, 3-5 / 4-11, 3-6 / 4-12 and 3-7 / 4-13 need to be compared in these given pairs. This is the same evidence, as in 3-5 / 4-11, that lower sugar rates  $f_s$  often result in better comparisons of measured and modelled  $W_{Sn}$ . This is clearly because the equilibrium determines the final transferable amount of moisture. Conversely, it is in the periods of higher sugar rates where matches are achieved, that it is hoped there is support for the fitted mass transfer coefficients in Table 4-1.

The air moisture from the model gives a very smooth curve. It follows the plant data quite correctly being able to simulate the changes. The response is better than for the sugar moisture.

#### 4.4.2.2 Temperature

Again, because of the process of data reconciliation, the predicted and measured temperature of the sugar ( $T_{Sn}$ ) and the air ( $T_{An}$ ) follow each other well, with the  $T_{Sn}$  measurement and prediction being particularly close. The fact that the modelled exit air temperature  $T_{An}$  is usually 2-3 °C higher than the reconciled measurement is related to the modelled  $W_{Sn}$  being slightly higher than the measured  $W_{Sn}$  in similar periods, arising as in section 4.4.2.1. In the reconciled measurement, the latent heat required to evaporate this residual moisture would bring  $T_{An}$  down to its reconciled measurement.

#### 4.4.2.3 Dissolved sucrose $S_{Fn}$

It is noted that the  $S_{Fn}$  arising from the model, differs somewhat. This is because the reconciled data were based on a steady-state mass and energy balance, and thus could not recognize the continuing crystallization of sucrose from the film onto the crystal. The initial sucrose content for reconciliation was merely set at saturation, and not supersaturation. It is noted that  $W_{Sn}$  and  $S_{Fn}$  generally move together in Fig. 4-9 to 4-13, showing that a particular concentration is being

maintained in the crystal film, and this no doubt is the concentration at which the vapour pressure is significantly reduced, restricting the mass transfer. In Fig. 4-11, this prevents  $W_{Sn}$  from matching the measurements, but this is not the case in Fig. 4-12.

## CHAPTER 5

### ADAPTIVE CONTROL

#### 5.1 DYNAMIC MATRIX CONTROL THEORY

---

##### 5.1.1 Definition

Dynamic Matrix Control is a form of Model Predictive Control (MPC) which uses a step-response convolution model for prediction of the effect of possible control actions. Since the early work of Cutler and Ramaker, (1979) and Garcia and Morshedi (1984), these controllers, particularly DMC, have proved their worth in many industrial applications.

##### 5.1.2 Theory

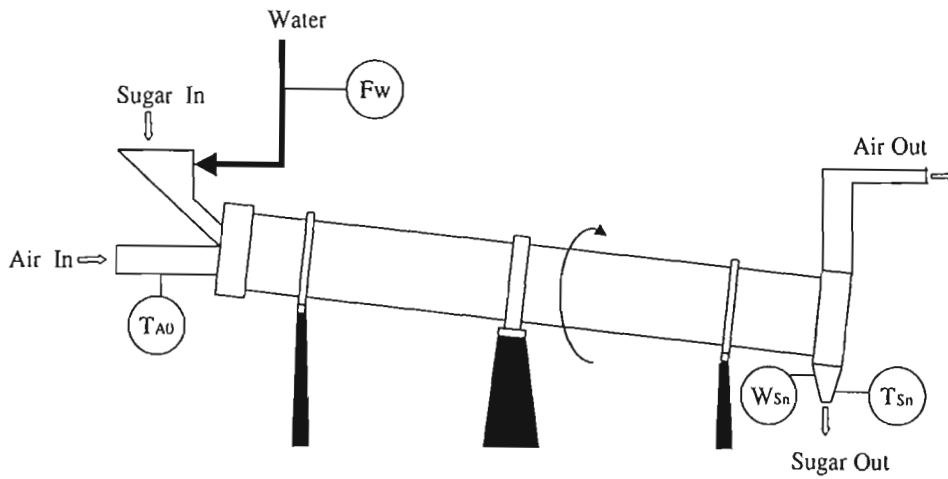


**Figure 5-1: Rotary dryer with exit moisture and temperature determined by air temperature and water addition**

Consider a 2-input, 2-output system, for example a rotary sugar dryer (Fig. 5-1) in which air temperature ( $T_{A0}$ ) and the flow of water added ( $F_w$ ) cause variations in the sugar exit temperature ( $T_{Sn}$ ) and its moisture content ( $W_{Sn}$ ). If the system is steady and a step is made in  $T_{A0}$ , two separate responses for  $T_{Sn}$  and  $W_{Sn}$  are expected. Likewise, distinct responses for  $T_{Sn}$  and  $W_{Sn}$  for a step in  $F_w$  would be expected. This is shown graphically in Fig. 5-2, for unit



positive steps in  $T_{A0}$  and  $F_w$ . Note that only changes in  $T_{Sn}$  and  $W_{Sn}$  from their original steady values are considered.

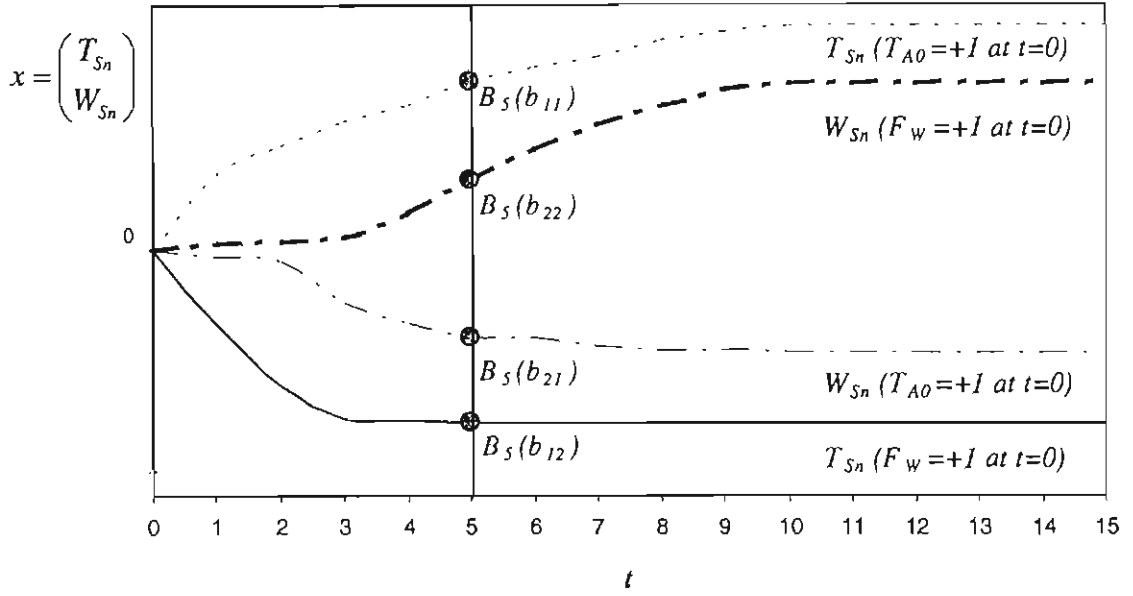


Figure 5-2: Step responses for a 2-input 2-output system

For the input vector  $m(T_{A0}, F_w)$ , now consider not just one step but a series of control vector moves  $\Delta m_1, \Delta m_2, \dots, \Delta m_M$ , over a sequence of  $M$  time steps. If the system is linear, the resultant sequence in  $x(T_{Sn}, W_{Sn})$  over  $P$  intervals can be built by shifting, scaling and superposing the above step responses:

$$\begin{pmatrix} x_1 \\ x_2 \\ x_3 \\ \vdots \\ x_M \\ x_{M+1} \\ \vdots \\ x_P \end{pmatrix} = \begin{bmatrix} B_1 & 0 & 0 & 0 & 0 & \cdots & 0 \\ B_2 & B_1 & 0 & 0 & 0 & \cdots & 0 \\ B_3 & B_2 & B_1 & 0 & 0 & \cdots & 0 \\ \vdots & \vdots & \vdots & \vdots & \vdots & \vdots & \vdots \\ B_M & B_{M-1} & \cdots & B_1 & 0 & \cdots & 0 \\ B_M & B_M & B_{M-1} & \cdots & B_1 & \cdots & 0 \\ \vdots & \vdots & \vdots & \vdots & \vdots & \vdots & \vdots \\ B_M & B_M & B_M & B_M & B_{M-1} & \cdots & B_1 \end{bmatrix} \begin{pmatrix} \Delta m_1 \\ \Delta m_2 \\ \Delta m_3 \\ \vdots \\ \Delta m_M \\ \Delta m_{M+1} \\ \vdots \\ \Delta m_P \end{pmatrix} \quad \begin{array}{l} \text{(Steady-state response} \\ \text{achieved } M \text{ time intervals} \\ \text{ahead with } M < P) \end{array} \quad (5.1)$$

This represents the convolution model for future outputs as  $x = B\Delta m$ , where the “matrix of matrices”  $B$  is generally known as the “Dynamic Matrix”. Now defining the  $P \times M$  matrices:

$$B_{OL} = \begin{bmatrix} B_M & B_M & B_{M-1} & B_{M-2} & B_{M-3} & \cdots & B_3 & B_2 \\ B_M & B_M & B_M & B_M & B_M & \cdots & \cdots & B_3 \\ B_M & B_M & B_M & B_M & B_M & \cdots & \cdots & \vdots \\ B_M & B_M & B_M & B_M & B_M & \cdots & \cdots & \vdots \\ \vdots & \vdots & \vdots & \vdots & \vdots & & \vdots & B_{M-1} \\ B_M & B_M & B_M & B_M & B_M & \cdots & B_M & B_M \\ \vdots & \vdots & \vdots & \vdots & \vdots & & \vdots & \vdots \\ B_M & B_M & B_M & B_M & B_M & \cdots & B_M & B_M \end{bmatrix}$$

$$B_0 = \begin{bmatrix} B_M & B_{M-1} & B_{M-2} & B_{M-3} & \cdots & B_2 & B_1 \\ B_M & B_{M-1} & B_{M-2} & B_{M-3} & \cdots & B_2 & B_1 \\ B_M & B_{M-1} & B_{M-2} & B_{M-3} & \cdots & B_2 & B_1 \\ B_M & B_{M-1} & B_{M-2} & B_{M-3} & \cdots & B_2 & B_1 \\ \vdots & \vdots & \vdots & \vdots & & \vdots & \vdots \\ B_M & B_{M-1} & B_{M-2} & B_{M-3} & \cdots & B_2 & B_1 \end{bmatrix}$$

and the present measurements ( $P$ ) and past inputs ( $M$ ):

$$x_{OMEAS} = \begin{pmatrix} x_{OMEAS} \\ x_{OMEAS} \\ x_{OMEAS} \\ x_{OMEAS} \\ \vdots \\ x_{OMEAS} \end{pmatrix} \quad \text{and} \quad \Delta m_{PAST} = \begin{pmatrix} \Delta m_{-M+1} \\ \Delta m_{-M+2} \\ \Delta m_{-M+3} \\ \Delta m_{-M+4} \\ \vdots \\ \Delta m_0 \end{pmatrix}$$

then the “open-loop” response, corrected for present model offset  $x_{OMEAS} - B_0 \Delta m_{PAST}$ , is

$$x_{OL} = x_{OMEAS} + [B_{OL} - B_0] \Delta m_{PAST} \quad (5.2)$$

Notice that  $B_{OL} \Delta m_{PAST}$  gives the contribution of past control input steps (moves) to the future output, whereas  $B_0 \Delta m_{PAST}$  merely predicts what the *present* output should be according to the past moves. The “closed loop” response up to the  $P$ -step horizon is obtained by including the contribution of the future control moves  $\Delta m$ :

$$x_{CL} = x_{OL} + B \Delta m \quad (5.3)$$

On each time-step it is possible to compute the future open-loop response  $x_{OL}$  based on past inputs and the present output. Thus the control problem to achieve the desired trajectory  $x_{CL}$  amounts to finding suitable  $\Delta m$  as in Fig. 5-3.

A constrained multivariable Linear Dynamic Matrix Controller (LDMC), based on the linear programming solution of Chang and Seborg (1983), and the formulation of Morshedi *et al.* (1985), has been developed as follows.

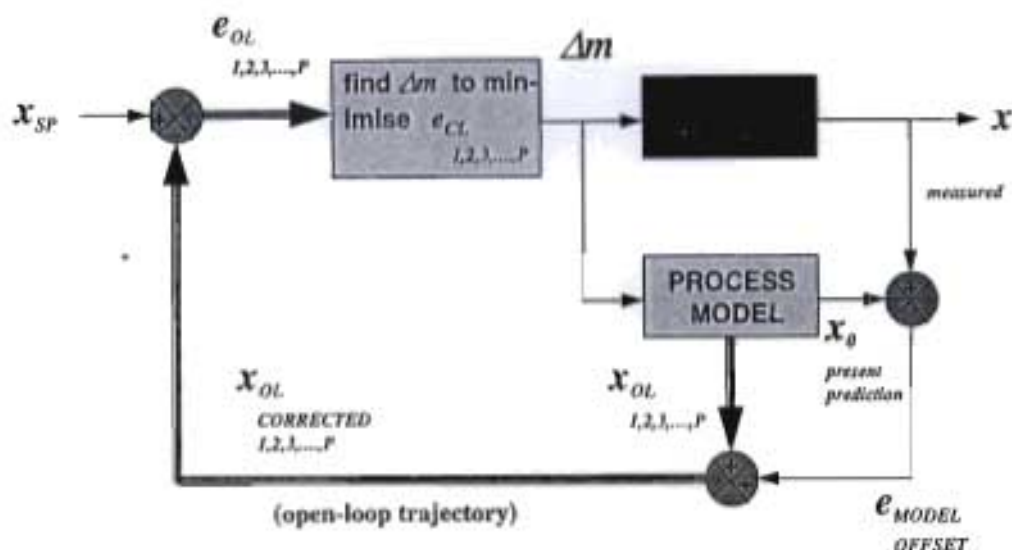


Figure 5-3: Model Predictive Control configuration

Define  $x_{SP}$  to contain a sequence of set-points for the outputs up to the time horizon  $P$  steps ahead, so that the open loop error may be calculated in advance as  $e_{OL} = x_{OL} - x_{SP}$ . Then the closed-loop error for a control move sequence  $\Delta m$  will be, using equation (5.3):

$$e_{CL} = x_{CL} - x_{SP} = e_{OL} + B\Delta m \quad (5.4)$$

Generally only a limited sequence of  $N$  moves ( $\Delta m^*$ ) are optimised ( $N \ll P$ ). This is equivalent to setting  $\Delta m_k = 0$  for  $k > N$ , or alternately replacing  $B$  with the non-square  $P \times N$  matrix:

$$A = \begin{bmatrix} B_1 & & & & 0 \\ B_2 & B_1 & & & \\ \vdots & \vdots & \ddots & & \\ B_N & B_{N-1} & & \ddots & B_1 \\ \vdots & \vdots & & & \vdots \\ B_M & B_M & & & B_{M-N+1} \\ \vdots & \vdots & & & \\ B_M & B_M & \dots & \dots & B_M \end{bmatrix}$$

Then

$$e_{CL} = e_{OL} + A\Delta m^* \quad (5.5)$$

Now a quadratic objective function  $J$  is defined dependent only on the strategy  $\Delta m^*$  with  $W$  and

$$A \text{ matrices that are usually diagonal } W = \begin{bmatrix} w_1 & & 0 \\ & \ddots & \\ 0 & & w_M \end{bmatrix} \text{ and } \Lambda = \begin{bmatrix} \lambda_1 & & 0 \\ & \ddots & \\ 0 & & \lambda_M \end{bmatrix}.$$

$$\begin{aligned} J(\Delta m^*) &= (e_{CL})^T W (e_{CL}) + (\Delta m^*)^T \Lambda (\Delta m^*) \\ &= (e_{OL} + A \Delta m^*)^T W (x_{OL} - x_{SP} + A \Delta m^*) + (\Delta m^*)^T \Lambda (\Delta m^*) \end{aligned} \quad (5.6)$$

By minimising  $J$  with respect to  $\Delta m^*$ , it is possible to find an optimal sequence of control moves,  $\Delta m^*$ , which achieve minimum square deviation from the set-point trajectory up to the time horizon  $P$ , for minimum square control move effort. It is the weights in the matrices  $W$  and  $\Lambda$ , generally diagonal, which determine the extents to which deviations of either parameter are discouraged. Higher “gains” will generally be associated with higher values in  $W$  than  $\Lambda$ . The values in  $\Lambda$  cause “move suppression”. It is easily shown that differentiation of  $J$  with respect to the elements of  $\Delta m^*$ , and setting the result to the zero vector, yields the *unbounded quadratic optimum* control move strategy

$$\Delta m_{UQO} = - [A^T W A + \Lambda]^{-1} A^T W e_{OL} \quad (5.7)$$

The sequence of actual control settings is clearly obtained by adding the successive moves:

$$m_{OPT} = L \Delta m_{UQO} + m_{INT} \quad (5.8)$$

$$L = \begin{bmatrix} I & 0 & 0 & 0 & 0 & \dots & 0 \\ I & I & 0 & 0 & 0 & \dots & 0 \\ I & I & I & 0 & 0 & \dots & 0 \\ I & I & I & I & 0 & \dots & 0 \\ \vdots & \vdots & \vdots & \vdots & \vdots & & \vdots \\ I & I & I & I & I & \dots & I \end{bmatrix}$$

A global method which will seek the minimum of  $J$  within defined constraints for both the inputs  $m$  and the outputs  $x$  requires *Quadratic Programming*, and is quite computation-intensive. In a less demanding approximation, Linear Dynamic Matrix Control (LDMC), Morshedi *et al* (1985) seek that combination of control moves which will get us as close as possible to  $\Delta m_{vgo}$ , yet keep us within the constraints. This re-definition of the problem then allows us to use *Linear Programming* to handle the constraints. Although it does not guarantee us the *quadratic optimum*, it is expected to be close (and identical within the constraints).

Ultimately, the solution for the optimal  $\Delta m$  found, whether constrained or otherwise, contains optimal values for the limited sequence of steps  $\Delta m_1, \Delta m_2, \dots, \Delta m_N$ , but it is only the first step  $\Delta m_1$  which is actually implemented, before the entire optimisation process is repeated on the next time-step. The effect of optimising more than one step is that the first step can be more severe (overshooting), with subsequent steps correcting the steady-state response.

## 5.2 APPLICATION TO EXIT MOISTURE CONTROL

For the dryer considered in this study, the control model is single-input, single-output, where only the inlet air temperature is varied to achieve the desired exit moisture. An adaptive DMC technique is proposed. The model simulates the drying process in real time with the same flow and temperature used on the plant, using the collected data.

The model is used to generate updated step responses in real time as follows. For a  $P$ -step horizon,  $P$  separate solutions are continuously being updated on each step. These solutions have exactly the same time-varying inputs as the actual process model, except that the manipulated variable ( $T_A$ ) is given a small fixed offset from the actual input (in this case,  $+1^\circ\text{C}$  is adequate). As each control step is executed, one of the solutions (in sequence) is reset to the present modelled output. Between this time and the next “resetting” of this particular solution, its output trajectory will progressively deviate from the model output trajectory, on account of the  $+1^\circ\text{C}$  offset in input. This difference will clearly be a good representation of a local step response, and at any time, each of the  $P$  solutions gives a different point on this step response (Fig. 5-4).

Note that the model parameters change as the operating point moves, ensuring a continuous updating of the step response.

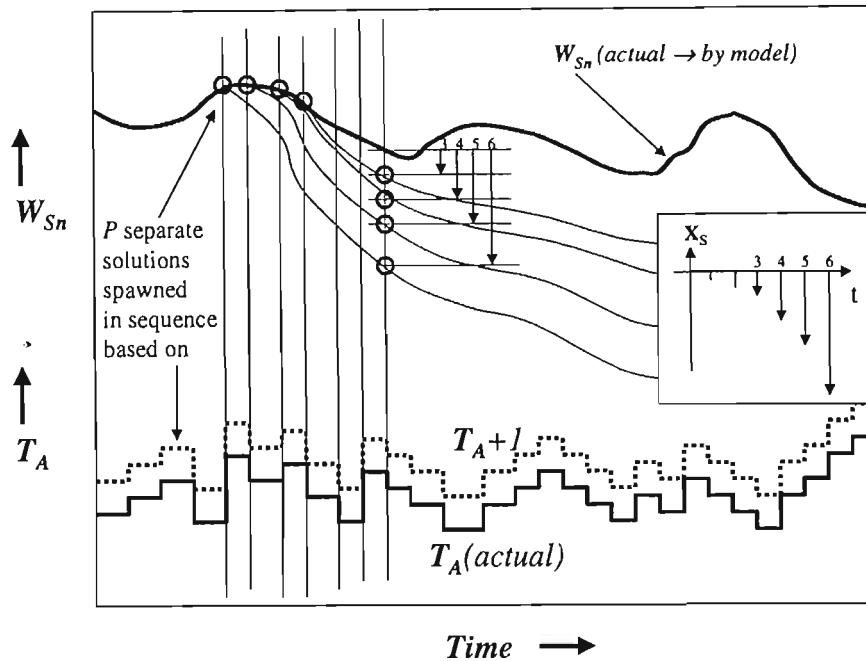


**Figure 5-1: Continuously updated step response from parallel solutions of real-time model**

The difficulty in this control strategy is that the variable measured is the exit moisture sugar content. It is not easy to have this measurement on-line because it involves complicated analysis and it is expensive. One solution would be, as Temple and van Boxtel (2000) suggest, to have access to the exit moisture sugar content through another measurement. The outlet air temperature looks like a good candidate because it is reliable and easy to measure. The idea would be to do step in the sugar moisture and to analyse the response at the exit in the air temperature. From there a function would be created that would transform air temperature into sugar moisture content.

### 5.3 THE STRUCTURE OF THE PROGRAM

The program written in MATLAB<sup>®</sup> language is shown in Appendix E. The program is divided into three main parts. Plant data are read from a separate file.

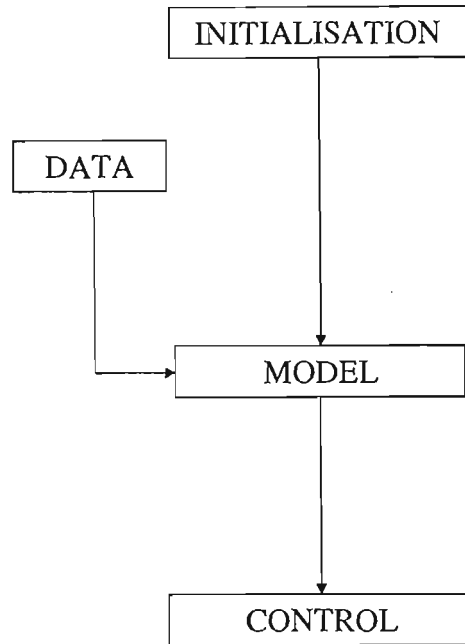


**Figure 5-1: Program diagram**

#### 5.3.1 Initialisation

Initialisation is done at the beginning of the program prior to the main time-step cycle. This part of the program is divided into smaller ones where the initialisation is done for:

- The control
- The sugar and air properties. They are also shown in Appendix B.
- The matrices and the vector, especially for the calculation of  $\alpha$ ,  $\beta$  and  $G$ .
- The plotting information

#### 5.3.2 Model

##### 5.2.3.1 Present operating conditions

The data are read from another file. Every five seconds, the values of *time*,  $W_{SO}$ ,  $W_{AO}$ ,  $T_{SO}$ ,  $T_{AO}$ ,  $S_{FO}$ ,  $f_S$ ,  $f_A$ ,  $W_{Sn}$ ,  $W_{An}$ ,  $T_{Sn}$ ,  $T_{An}$ ,  $S_{Fn}$  are obtained from a single file record.

##### 5.2.3.2 Heat and mass transfer coefficients

These values are set from the comparison between the reconciled data and the model.

### 5.2.3.3 Determination of the vector flow $f_A$

This represents in the MATLAB language what is developed in section 4.1.2.4.

### 5.2.3.4 Initialisation of $X$ and $U$

This initialisation is set at the first iteration. It is assumed that the situation inside the dryer is same along the dryer at  $t = 0$ .

### 5.2.3.5 Control computations

The small perturbation on the inlet air temperature  $+1^\circ\text{C}$  gives a small offset – see section 5.2.

### 5.2.3.6 Axial Convection

The axial convection developed here represents the theory developed in § 4.2.2.1. The idea of moving in one step to avoid numerical dispersion is implemented. Besides, a test has been added “dx/dt too small for sugar flow” and “dx/dt too small for air flow” if the movement is greater than one division.

### 5.2.3.7 Tuning of A and B matrices

To build the  $[CM]$  matrix described in § 4.1.2.5 and shown in Appendix B, the vectors  $\alpha$ ,  $\beta$  and  $G$  need to be calculated. The matrices  $[A]$ ,  $[AC]$ ,  $[B]$  and  $[BC]$  are then built.

### 5.2.3.8 Integration

Following the discrete model, the single system of equations (4.18) becomes:

$$\bar{X}_{i+1} = e^{A\Delta t} \bar{X}_i + [e^{A\Delta t} - I] A^{-1} B \bar{U}_i \quad (5.9)$$

The matrix exponential is defined as:

$$e^{A\Delta t} = L^{-1} \left\{ [sI - A]^{-1} \right\} \quad (5.10)$$

where  $L$  is the Laplace's transform and  $I$  is the identity matrix.

$A_s = e^{A\Delta t}$  and  $B_s = [e^{A\Delta t} - I] A^{-1} B$  are defined for the computation.

For the convection, the integration is done with an Euler model using the matrix  $[AC]$  and  $[BC]$ . Then the integration is done with  $[A_s]$  and  $[B_s]$ .

## 5.3.3 Control

### 5.3.3.1 Dynamic matrix control

The theory is translated into the MATLAB® language. To facilitate the reading of the program, the Table 5-1 translates the symbols used in the theory to their equivalents in the program. It is possible to vary the set point to different values to see how the controller behaves.



**Table 5-1: Translator from theory to program**

Theory	MATLAB® language
$\Delta m$	DM
$\Delta m_{UGO}$	dmopt
$\Delta m_{PAST}$	dmpast
$e_{OL}$	eol
$B_{OL}$	DMol
$B_0$	DM0
W	WW
$\Lambda$	Lam

### 5.3.4 Plotting

All of the information concerning the temperatures, the moistures and the flows during the time period are kept in a results.dat file that can be opened with EXCEL. From the MATLAB®, three kinds of graphs are plotted. An example is shown in Appendix D.

- The temperature and moisture content profile along the dryer at t
- The comparison between the data from the plant and the data from the model
- The control response

## 5.4 RESULTS AND DISCUSSION

---

### 5.4.1 Off-line

The controller was tuned with the following values:

$$W = 2000000$$

$$\Lambda = 1$$

W is the penalty weight on squared set-point deviation  $W_{Sn}$ .

$\Lambda$  is the penalty weight on the control move  $\Delta T_{AO}$ .

Bigger values for W would tend make the controller unstable.

The results are shown in Fig. 5-6 and Fig. 5-7 for fixed plant conditions (i.e. no other disturbances). The set point was given different values to see how the controller responded.

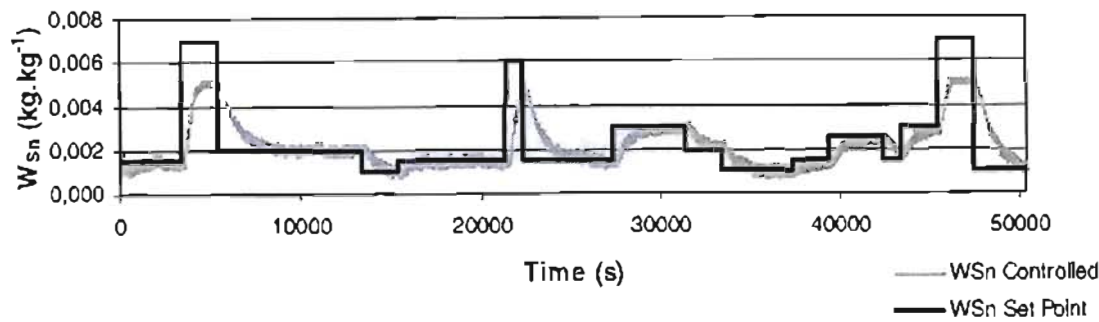


Figure 5-1: Response from the controller for  $W_{sn}$

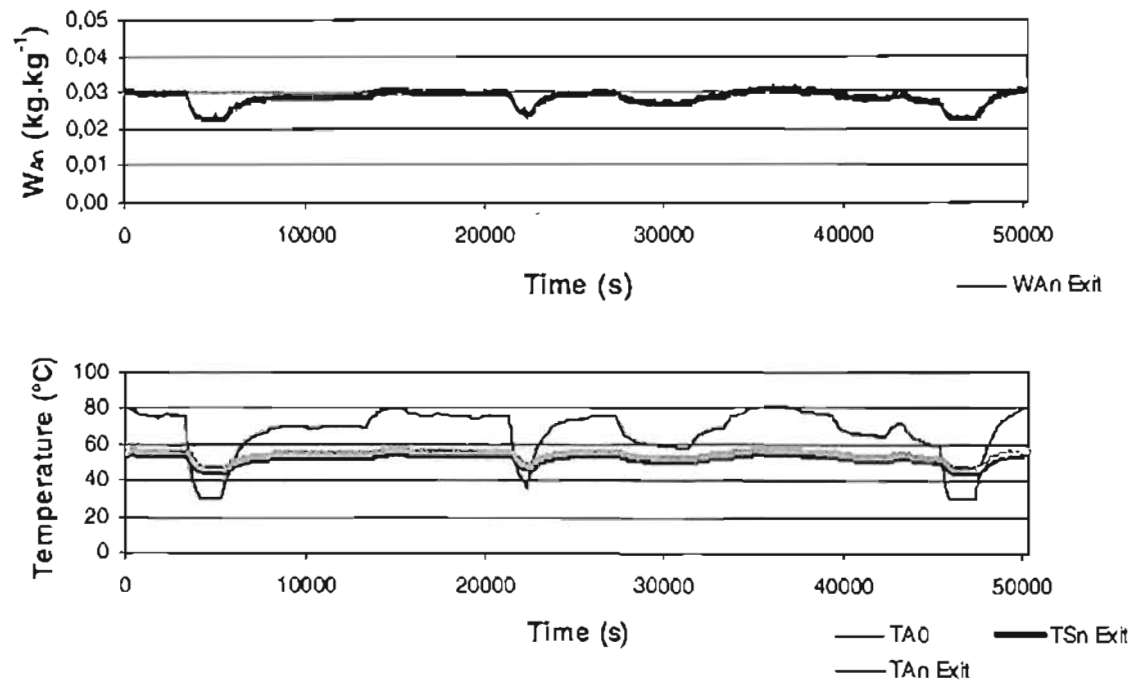


Figure 5-2: Controller effect on  $W_{An}$ ,  $T_{A0}$ ,  $T_{Sn}$ ,  $T_{An}$

The effect is very significant on the inlet air temperature. When the set point is increased, the air temperature drops: indeed, less heat is needed to evaporate water from the moist sugar. Consequently, the outlet air and sugar temperature drop but less.

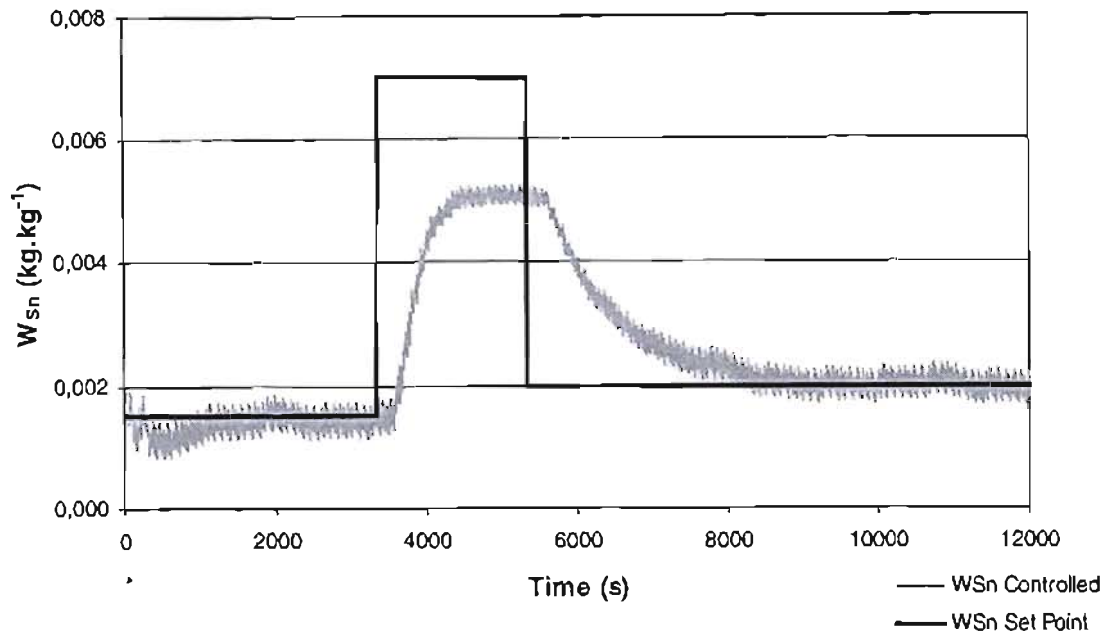


Figure 5-3: Zoom on the controller response

Zooming in on the beginning of Fig. 5-6, it appears in Fig. 5-8 that the response time is about 300s for an increase in the setpoint of the exit sugar moisture (the average residential time is 300s). The high moisture content required in the indicated step could not be achieved because the air inlet temperature was bounded by a lower constraint of 30°C. The negative step in the set-point of  $W_{Sn}$  consistently has a longer response time, taking about 1300s to reach 95% of the new value.

5.4.2 As on-line

The results are shown in Fig. 5-9 and Fig. 5-10. The controller seems to have some difficulties in following the set point when the natural process variations are fed through on the other variables, providing disturbance loading.

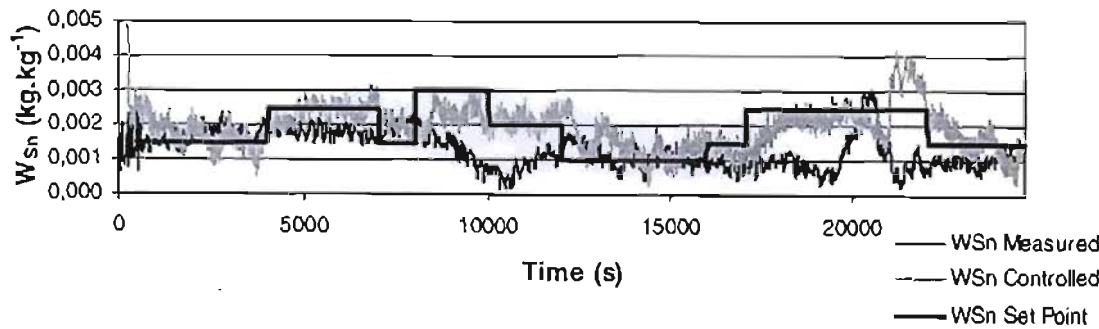


Figure 5-1: Closed-loop response for  $W_{Sn}$  with plant data

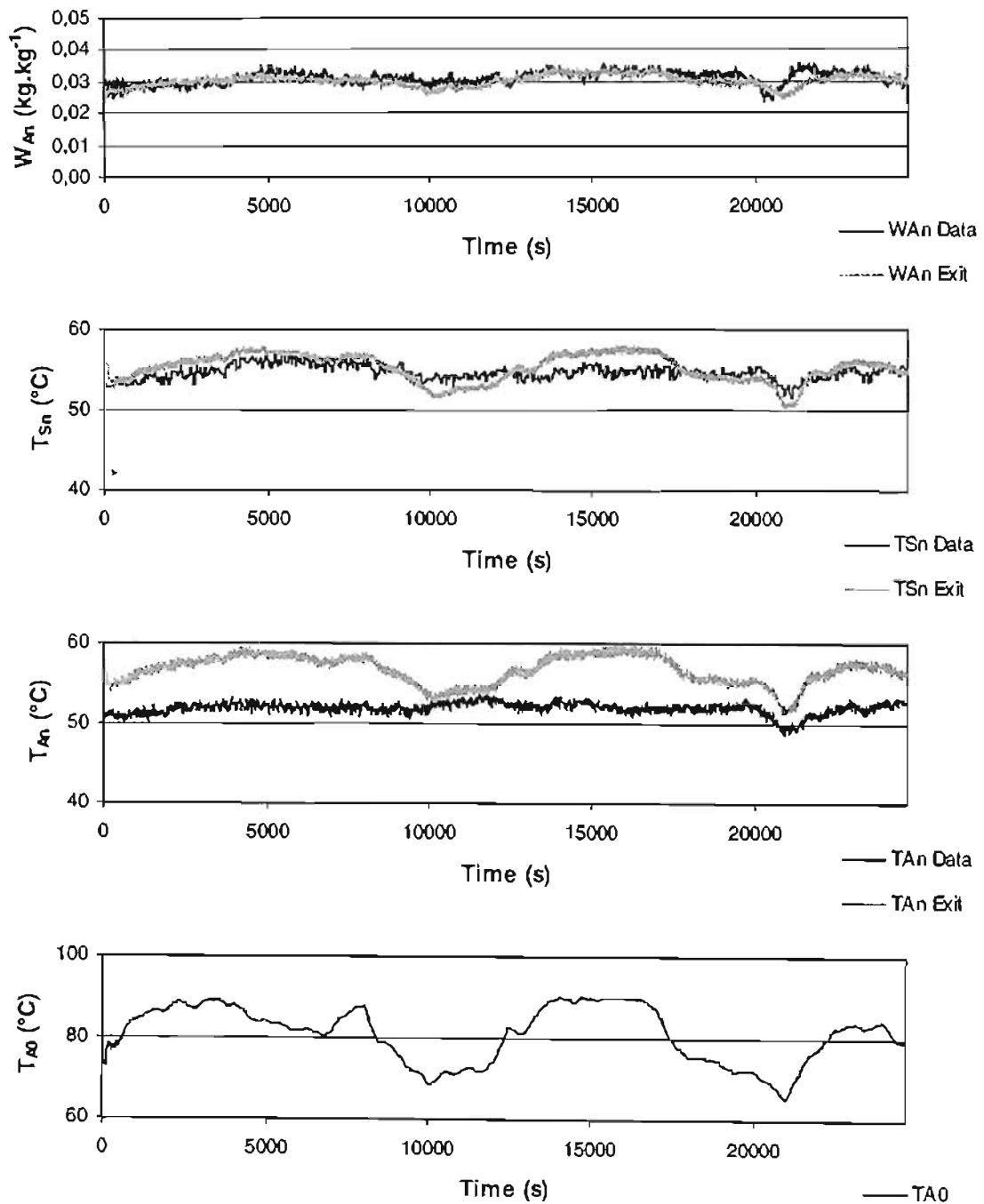


Figure 5-2: Controller effect on  $W_{An}$ ,  $T_{A0}$ ,  $T_{Sn}$ ,  $T_{An}$  compared with the data

Note that the “data” values in Fig. 5-10 refer to the original outputs recorded in the plant data, whereas the “exit” values refer to the changed outputs arising from the new variation of  $T_{A0}$ .

5.4.3 Effect of  $W$  the penalty weight on squared deviation  $W_{Sn}$  from set-point

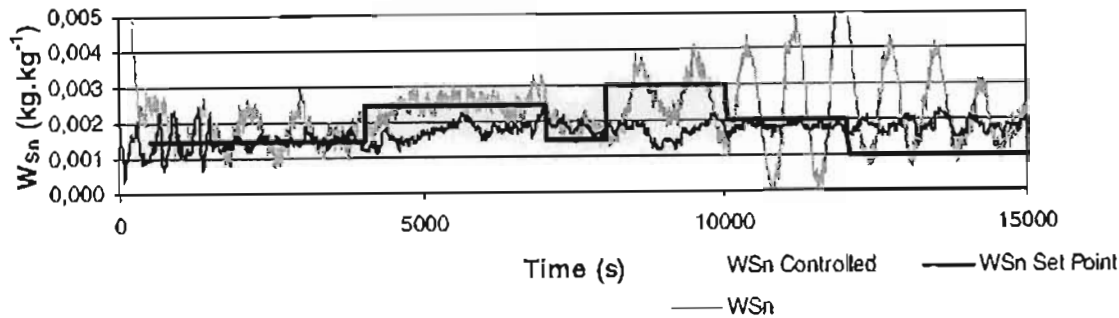


Figure 5-1: Closed-loop response for  $W_{Sn}$  with plant data and  $W = 6000000$

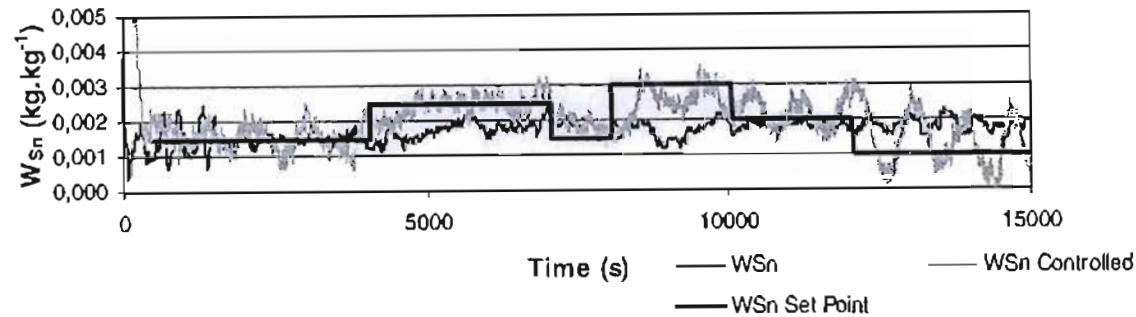


Figure 5-2: Closed-loop response for  $W_{Sn}$  with plant data and  $W = 4000000$

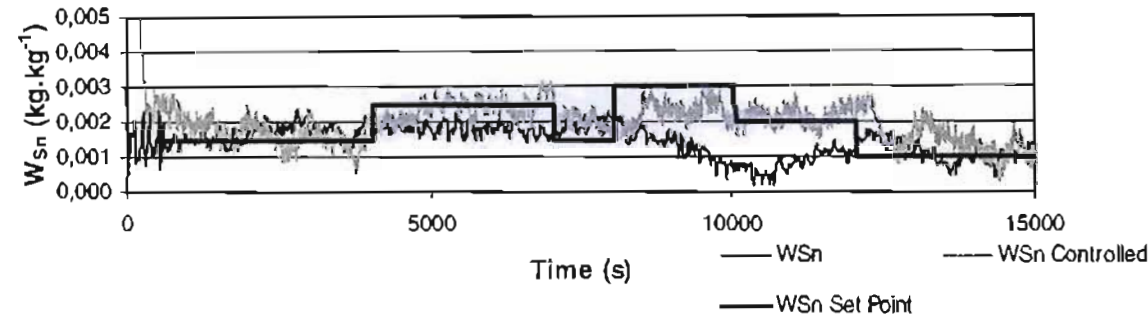


Figure 5-3: Closed-loop response for  $W_{Sn}$  with plant data and  $W = 2000000$

Different values of the penalty weight on squared set-point deviation were tried to see how it affects the controller. As the penalty weight is increased, the closed-loop becomes oscillatory and less stable, eventually becoming a limit cycle with bang-bang control action.

5.4.4 Advantages

The DMC technique has a considerable advantage for the control of the dryer, because the algorithm explicitly handles dead-time, which will result from the near plug-flow of sugar

assumed. This is a good indicator that automatic control is required, as operators find it difficult to make corrections with these long responses.

The controller is seen to react to noise on the process measurement sequences, but still gives acceptable control.

# CHAPTER 6

## CONCLUSIONS

### 6.1 CONCLUSIONS

---

The drying process in the sugar industry is not the best understood. This is probably because the mechanism is not simple: it involves several fields from chemical engineering science. More than a simple process of evaporation, sugar drying includes convective heat and mass transfer, equilibrium, and the kinetics of crystallisation.

Data were collected from the Darnall sugar mill belonging to Tongaat-Hulett Sugar Ltd. The co-current rotary sugar dryer was of the concave louvre type. As it was not possible to have access to the whole set of process variables, only the temperatures and the air flow were recorded. A technique was developed to reconcile the data. It was based on a strong confidence in the calculated difference between the sugar moisture content at the entrance and at the exit of the dryer. Assuming that the exit sugar moisture content was at equilibrium at low sugar rates, a plausible reconciled data set was found.

The model built to simulate this sugar dryer was directly inspired by Tait *et al.* (1994). Heat and mass balances for the moisture of both sugar and air, and the tracking of the dissolved sucrose in a residual “film” along the dryer, with simultaneous crystallisation from the film, were the main features of the model. To avoid any numerical diffusion, an effective convection scheme was developed, based on the integration of the total sugar and air movement.

The model was set up to be able to recreate the sorption isotherm determined by Schindler and Juncker (1993). The Tait *et al.* (1994) equations could be solved to give similar behaviour to this isotherm for equilibrium sugar moisture content. However, the match was found to be strongly dependent on the initial dissolved sucrose in the water film, for which a single value was eventually chosen to fit the entire isotherm. The double equilibrium of zero net crystallisation and zero net evaporation was not achieved, and even if it were, it would be independent of the amount of dry sugar present.

The tuning to match the collected data was done by varying the heat and mass transfer coefficients. It was found that better results were achieved when the sugar rate was low, especially for the exit sugar moisture content, though the best periods to determine the transfer coefficients would in fact have been under conditions far from equilibrium (high sugar rates).

The ranges of values for the transfer coefficients from the literature are 0,3 to 0,0019 kW.m<sup>-1</sup>.K<sup>-1</sup> for the heat transfer coefficient and 2,7×10<sup>-9</sup> to 72×10<sup>-9</sup> kg.m<sup>-2</sup>.s<sup>-1</sup>.Pa<sup>-1</sup> for the mass transfer coefficient (Table 1-1). The estimated values found from the reconciled plant data were within the literature heat transfer range ( $h_i = 0,0136$  kW.m<sup>-2</sup>.K<sup>-1</sup>), and just below the literature mass transfer range ( $k_g = 1,36 \times 10^{-9}$  kg water.m<sup>-2</sup>.s.Pa). The sugar quality in terms of origin and location might explain this difference.

An application of adaptive control theory was done on the sugar dryer employing unconstrained Dynamic Matrix Control (DMC). The aim was to control the exit sugar moisture content by manipulating the inlet air temperature. A MATLAB<sup>®</sup> program was written to simulate closed-loop control with otherwise steady process conditions, and then using actual process variations recorded on the plant. It gave acceptable performance, handling the system dead-time without difficulties.

The DMC technique has a considerable advantage for the control of the dryer, because the algorithm explicitly handles dead-time, resulting from the near plug-flow of sugar. This is a good indication that automatic control is required, as operators find it difficult to make corrections with these long time-responses. The controller was seen to react to noise on the process measurement sequences, but still gave acceptable control.

Implementation of closed-loop control will rely on a feedback measurement for the exit moisture content. Methods have been proposed in this work for estimation of this parameter using temperature and flow measurements.



## REFERENCES

- Bazin, C., Hodouin, D., Duschene, C., Thibault, J., Trusiak, A.R. (1998). Reconciliation of mass and energy data measurements: application to a rotary dryer. *Canadian Metallurgical Quarterly*, Vol. 37, N° 3-4, 333-342.
- Ben-Yoseph, E., Hartel, R. W., Howling, D. (2000). Three-dimensional model of phase transition of thin sucrose films during drying. *Journal of Food Engineering* 44, 13-22.
- Broadfoot, R. (1980). Modelling and Optimum design of Continuous Sugar Pans. *PhD thesis, University of Queensland, Australia*.
- de Bruijn, J.M., Marijnissen, A.A.W. (1996). Moisture content of sugar crystals and influence of storage conditions. *Conference on Sugar Processing Research*. News Orleans.
- Chang, T.S. and Seborg, D.E. (1983). A linear programming approach for multivariable feedback control with inequality constraints. *Int. J. Control*, 37, 583-597.
- Clarke, D.W., Mohtadi, C., Tuffs, P.S. (1987). Generalized Predictive Control – Part I. The basic Algorithm. *Automatica*, Vol. 23, N° 2, 137-148.
- Clarke, G. (2000). High and Dry. *The chemical engineer*, May, 38.
- Coulson, J.M. and Richardson, J.F. (1965). Chemical Engineering: Volume One: Fluid Flow, Heat Transfer and Mass Transfer, *Revised Second Edition*, Pergamon, Oxford, 220.
- Cutler, C.R. and Ramaker, B.L. (1979). Dynamic Matrix Control – A computer control algorithm. *AIChE National Meeting*, Houston, Texas.
- García, C.E. and Morshedi, A.M. (1984). Quadratic Programming Solution of Dynamic Matrix Control (QDMC). *Proc. Am. Control Conf., San Diego, California*.
- García, C.E., Prett, D.M., Morari, M. (1989). Model Predictive Control: Theory and Practice – a survey. *Automatica*, Vol. 25, N° 3, 335-348.

- Lipták, B. (1998). Optimizing dryer performance through better control. *Chemical Engineering, February, 110-114.*
- Lipták, B. (1998). Optimizing dryer performance through better control. *Chemical Engineering, March, 110-114.*
- Love, J.D. (2001). Dynamic Modelling and Optimal Control of Sugar Crystallization in a Multi – Compartment Continuous Vacuum Pan. *PhD thesis, University of Natal, Durban.*
- Morshedi, A.M., Cutler, C.R., Skrovanek, T.A. (1985). Optimal Solution of Dynamic Matrix Control with Linear Programming Techniques (LDMC). *Proc. Am. Control Conf., Boston, Massachusetts, 199-208.*
- Mulholland, M. and Prosser, J.A. (1997). Linear Dynamic Matrix Control of a Distillation Column. *SA Inst. Chem. Eng. 8<sup>th</sup> Nat. Meeting, Cape Town, April 16-18.*
- Peacock, S.D. (1995). Selected physical properties of sugar factory process streams. *Sugar Milling Research Institute, Technical report, N° 1714.*
- Pérez-Correa, J. R., Cubillos, F., Zavala, E., Shene, C., Álvarz, P. I. (1998). Dynamic simulation and control of direct rotary dryers. *Food Control, Vol. 9, N° 4.*
- Rastikian, K., Capart, R., Benchimol, J. (1999). Modelling of sugar drying in a countercurrent cascading rotary dryer from stationary profiles of temperature and moisture. *Journal of Food Engineering 41 (1999) 193-201.*
- Rodgers, T., Lewis, C. (1963). The drying of white sugar and its effect on bulk handling. *15<sup>th</sup> Technical Conference, British Sugar Corporation, Ltd. (part IV)*
- Savaresi, S. M., Bitmead, R. R., Peirce, R. (2001). On modelling and control of a rotary sugar dryer. *Control Engineering Practice 9 (2001) 249-266.*
- Shardlow, P.J., Wright, P.G., Watson, L.J. (1996). Sugar dryer modelling and control. *Proceeding of Australian Society of Sugar Cane Technologists, 368-375.*
- Shindler, H. Juncker, B. (1993). *Zuckerindustrie 118, 103-106.*

- Shinskey, F.B. (1996). Process Control Systems. *Mc-Graw-Hill, New-York, Fourth Edition*.
- Tait, P.J., Schinkel, A.L., Grieg, C.R. (1994). The development and application of a generalised model for sugar drying. *9<sup>th</sup> Internat. Drying Symposium., August, 1994*.
- Thompson, P. (1998). Drying, cooling and bulk storage of sugar. *International Sugar Journal, Vol. 100, N° 1193, 223-230*.
- Trelea, I.C., Courtois, F., Trystram, G. (1996). Dynamics analysis and control strategy for a mixed flow corn dryer. *J. Proc. Cont., Vol. 7, N° 1, 57-64*.
- Temple, S.J. van Boxtel, A.J.B. (2000). Control of fluid bed tea dryers: controller design and tuning. *Computers and Electronics in Agriculture, 26, 159-170*.
- Van der Poel, P. W., Schiweck, H. and Schwartz, T. (1998). *Sugar technology. Beet and Sugar Cane Manufacture. 867-880*.
- Wright, P.G., White, E.T. (1974). A Mathematical Model of Vacuum Pan Crystallisation. *Proc. Int. Soc. Sugar Cane Technol., 15<sup>th</sup> Congress, 1546-1560*.

## APPENDIX A    HEAT LOSS

The heat provided by the air is used by the sugar to evaporate the moisture from the sugar. In the following calculation, following a personal communication with Prof. M. Mulholland, we determine whether a significant portion of the supplied heat might be lost to the surroundings, rather than being entirely used in the drying process as assumed in the model.

Coulson and Richardson (1965) provide the following relations for the convective heat transfer coefficient acting on the surface of heated pipes in the air:

*STREAMLINE*

$$h = 0,28 \left( \frac{\Delta T}{d} \right)^{\frac{1}{4}}$$

*TURBULENT*

$$h = 0,29 (\Delta T)^{\frac{1}{4}}$$

with  $h$  = heat transfer coefficient in [ $\text{lb-cal.ft}^{-2}.\text{h}^{-1}.\text{°C}^{-1}$ ]

$\Delta T$  = temperature difference in [ $\text{°C}$ ]

$d$  = pipe diameter in [ft]

Converting to SI Units:

*STREAMLINE*

$$h = 1,18 \left( \frac{\Delta T}{d} \right)^{\frac{1}{4}}$$

*TURBULENT*

$$h = 1,22 (\Delta T)^{\frac{1}{4}}$$

with  $h$  = heat transfer coefficient in [ $\text{W.m}^{-2}.\text{°C}^{-1}$ ]

$\Delta T$  = temperature difference in [ $\text{°C}$ ]

$d$  = pipe diameter in [m]

Taking an average dryer temperature of 60 °C, and an ambient temperature of 20 °C, we could then expect a maximum convective heat loss from our 1,75 m diameter by 12,5 m long dryer as follows:

*STREAMLINE*

$$\begin{aligned} Q &= 1,18 \left( \frac{40}{1,75} \right)^{\frac{1}{4}} \times 40 \times \pi \times 1,75 \times 12,5 \\ &= 7092 \text{ W} = 7,092 \text{ kW} \rightarrow \end{aligned}$$

*TURBULENT*

$$\begin{aligned} Q &= 1,22 (40)^{\frac{1}{4}} \times 40 \times \pi \times 1,75 \times 12,5 \\ &= 8434 \text{ W} = 8,434 \text{ kW} \rightarrow \end{aligned}$$

Now considering the radiation loss (Coulson and Richardson (1965), pp223-224), we have

### *RADIATION*

$$Q = e \sigma (T^4 - T_{ambient}^4) \times \pi \times 1,75 \times 12,5$$

where

$e$  is the emissivity (assume 0,9)

$\sigma$  is the Stefan-Boltzmann constant =  $1,01 \times 10^{-8} \text{ lb-cal.ft}^{-2} \cdot \text{h}^{-1} \cdot \text{K}^{-4}$   
 $= 5,73 \times 10^{-8} \text{ W.m}^{-2} \cdot \text{K}^{-4}$

so

$$Q = 0,9 \times 5,73 \times 10^{-8} \times \left( (40 + 273,15)^4 - (20 + 273,15)^4 \right) \times \pi \times 1,75 \times 12,5$$

$$= 7907 \text{ W} = 7,907 \text{ kW} \rightarrow$$

So we consider in this dryer a heat loss to the surroundings of approximately 16 kW through convection and radiation. For a sugar flow of 30 tons per hour, losing 1% by mass of moisture, the latent heat required is approximately 188 kW. Clearly this heat loss of nearly 10% of the evaporation heat would affect the various balances which have been performed in the calculations. Nevertheless, it has been considered that the effect would not greatly alter the results presented, and thus the calculations have not been repeated with this heat loss taken into account.

# APPENDIX B CM MATRIX

Table B-1 : Overview of CM matrix

	$\frac{\partial W_s}{\partial t}$	$\frac{\partial W_A}{\partial t}$	$\frac{\partial (c_{ps}T_s)}{\partial t}$	$\frac{\partial (c_{pa}T_A)}{\partial t}$	$\frac{\partial S_f}{\partial t}$
$W_{Si-1}$	$\frac{D_s}{(\Delta x)^2} + \frac{f_s}{2A h_s \rho_s \Delta x}$				
$W_{Si}$	$-2 \frac{D_s}{(\Delta x)^2} - \frac{k_s a \beta_i}{\rho_s}$	$\frac{k_s a h_s \beta_i}{\rho_s h_A}$	$-\frac{k_s a \lambda \beta_i}{\rho_s}$		
$W_{Si+1}$	$\frac{D_s}{(\Delta x)^2} - \frac{f_s}{2A h_s \rho_s \Delta x}$				
$W_{Ai-1}$		$\frac{D_A}{(\Delta x)^2} + \frac{f_{Ai-1}}{2A h_A \rho_A \Delta x}$			
$W_{Ai}$	$\frac{k_s a \alpha_i}{\rho_s}$	$-2 \frac{D_A}{(\Delta x)^2} - \frac{k_s a h_s \alpha_i}{\rho_A h_A} - \frac{f_{Ax1}}{A h_A \rho_A \Delta x}$	$\frac{k_s a \lambda \alpha_i}{\rho_s}$		
$W_{Ai+1}$		$\frac{D_A}{(\Delta x)^2} - \frac{f_{Ai+1}}{2A h_A \rho_A \Delta x}$			
$c_{ps}T_{Si-1}$			$\frac{D_s}{(\Delta x)^2} + \frac{f_s}{2A h_s \rho_s \Delta x}$		
$c_{ps}T_{Si}$			$-2 \frac{D_s}{(\Delta x)^2} - \frac{h_s a}{\rho_s c_{ps}}$	$\frac{h_s a h_s}{\rho_A c_{ps} h_A}$	
$c_{ps}T_{Si+1}$			$\frac{D_s}{(\Delta x)^2} - \frac{f_s}{2A h_s \rho_s \Delta x}$		
$c_{pa}T_{Ai-1}$				$\frac{D_A}{(\Delta x)^2} + \frac{f_{Ai-1}}{2A h_A \rho_A \Delta x}$	
$c_{pa}T_{Ai}$			$\frac{h_s a}{\rho_s c_{pa}}$	$-2 \frac{D_A}{(\Delta x)^2} - \frac{h_s a h_s}{\rho_A c_{pa} h_A} - \frac{f_{Ax1}}{A h_A \rho_A \Delta x}$	
$c_{pa}T_{Ai+1}$				$\frac{D_A}{(\Delta x)^2} - \frac{f_{Ai+1}}{2A h_A \rho_A \Delta x}$	
$S_{Fi-1}$					$\frac{D_s}{(\Delta x)^2} + \frac{f_s}{2A h_s \rho_s \Delta x}$
$S_{Fi}$					$-2 \frac{D_s}{(\Delta x)^2}$
$S_{Fi+1}$					$\frac{D_s}{(\Delta x)^2} - \frac{f_s}{2A h_s \rho_s \Delta x}$
FORCE		$\frac{f_{AF1} W_{AF1}}{A h_A \rho_A \Delta x}$	$\frac{f_{AF1} W_{AF1}}{A h_A \rho_A \Delta x}$	$\frac{f_{AF1} c_{pa} T_{AF1}}{A h_A \rho_A \Delta x}$	$G_i a$

## APPENDIX C    PARAMETER VALUES

### C1    GENERAL

Different parameters are used to model the sugar dryer. Some of these are physical, and were found in the technical description of the dryer, or obtained from the Darnall sugar mill. The physical properties of sugar are taken from Peacock (1995), Tait *et al.* (1994), Love (2001).

#### C11    Dryer design

**Table C-1 : Dryer design values**

Parameter		Unit
$A$	2.4	m <sup>2</sup>
$L$	12.5	m

#### C12    Sugar crystal properties

**Table C-1 : Sugar crystal properties**

Parameter		Unit
$C_{ps}$	1.25	kJ.kg <sup>-1</sup> .K <sup>-1</sup>
$D_s$	10 <sup>-6</sup>	m <sup>2</sup> .s <sup>-1</sup>
$\rho_s$	1500	kg.m <sup>-3</sup>
<i>Length of crystal edge</i>	57.10 <sup>-5</sup>	m

The model uses not the crystal size but a parameter  $a$  that represent the surface offered to the environment over the volume. It is assumed that the crystal model for the sugar crystal is cubic so,

$$a = \frac{6 \cdot (57 \cdot 10^{-5})^2}{(57 \cdot 10^{-5})^3} \quad (C.1)$$

C13 Air properties

Table C-1 : Air properties

Parameter		Unit
$C_{pA}$	1.045	$\text{kJ.kg}^{-1}.\text{K}^{-1}$
$D_A$	$10^{-6}$	$\text{m}^2.\text{s}^{-1}$
$\rho_A$	0.9	$\text{kg.m}^{-3}$



# APPENDIX D GRAPHS

## D1 GRAPHS FROM THE MATLAB® PROGRAM

The data used in this appendix come from the 18 October 2000 (part II).

### D11 Temperature and moisture content profiles along the dryer

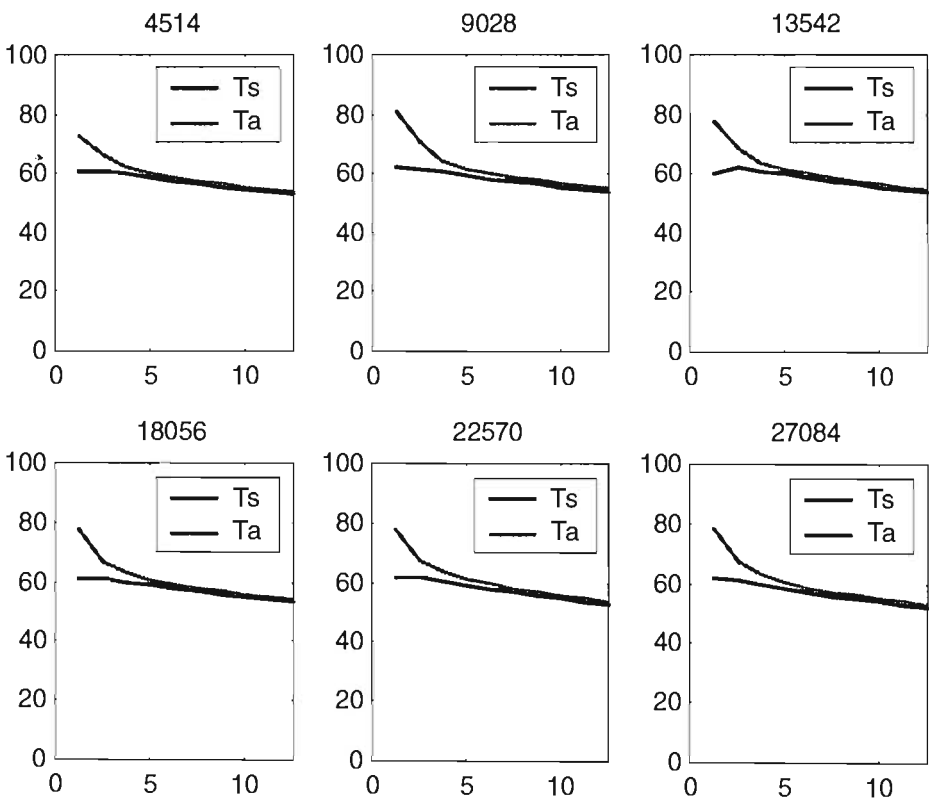


Figure D-1 : Temperature profile along the dryer at different times

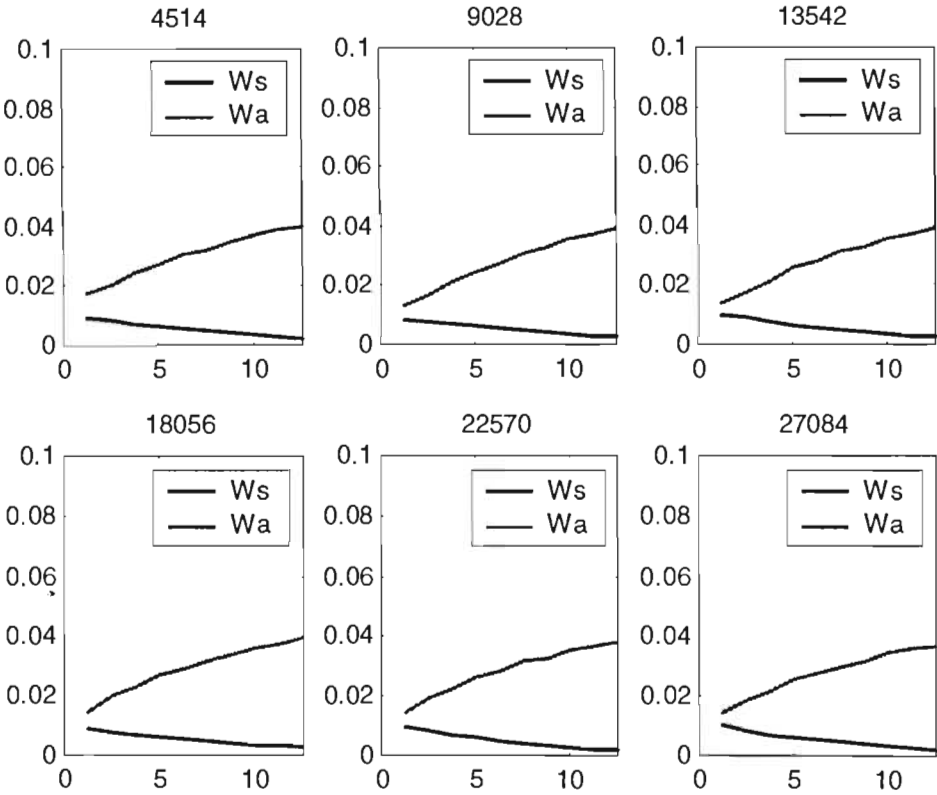


Figure D-2 : Moisture content profile along the dryer at different times

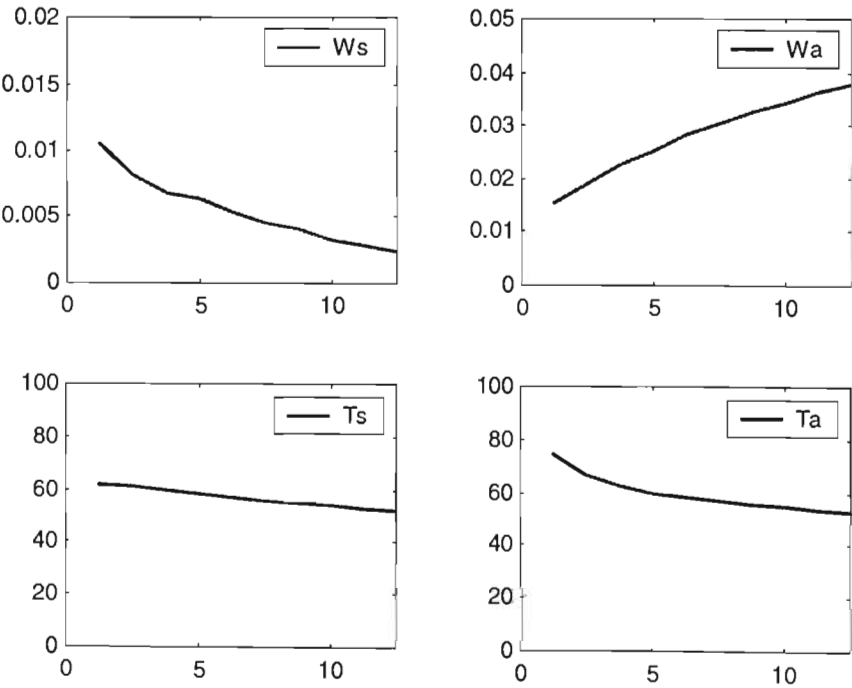


Figure D-3 : Temperatures and moisture contents profiles along the dryer for  $t = \text{tend}$

D12 Comparison between the data from the plant and the data from the model

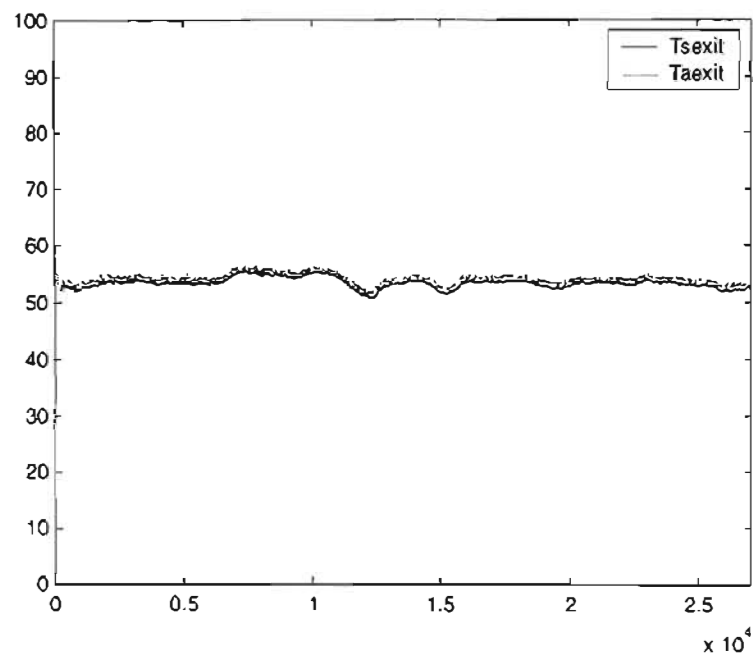


Figure D-1 : Air and sugar temperature from the model

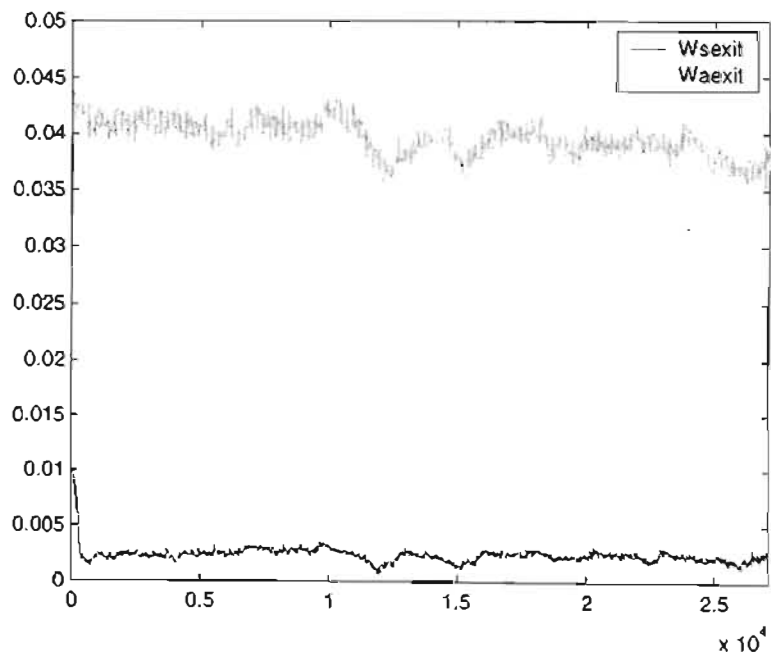
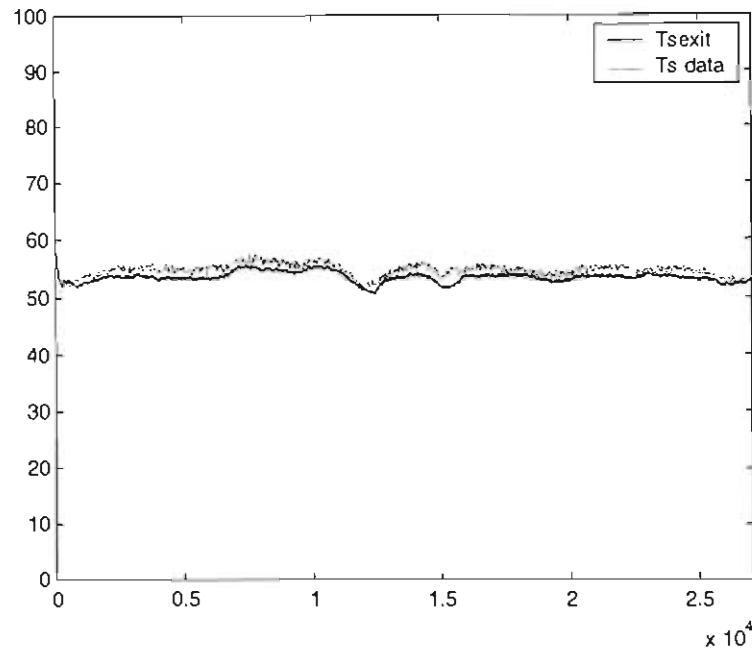
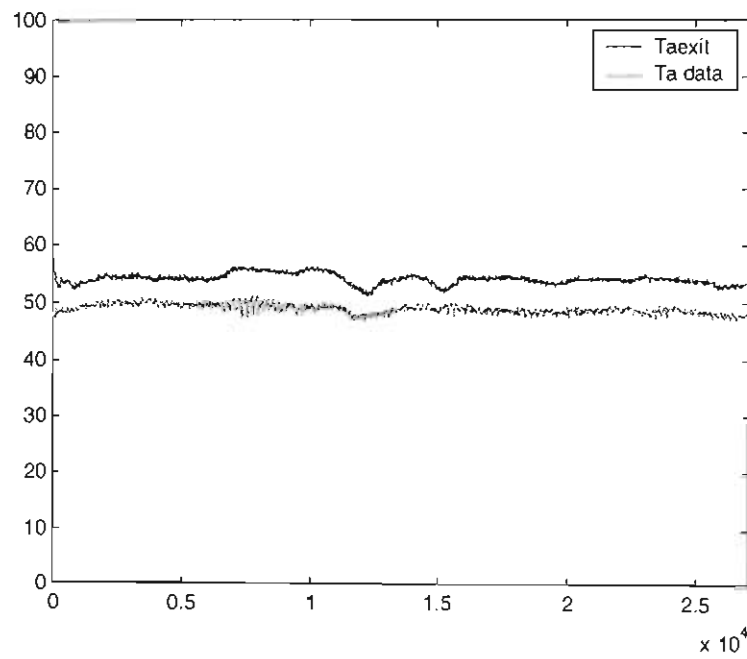


Figure D-2 : Air and sugar moisture content from the model



**Figure D-3 : Comparison of sugar temperature from the plant and the model**



**Figure D-4 : Comparison of air temperature from the plant and the model**

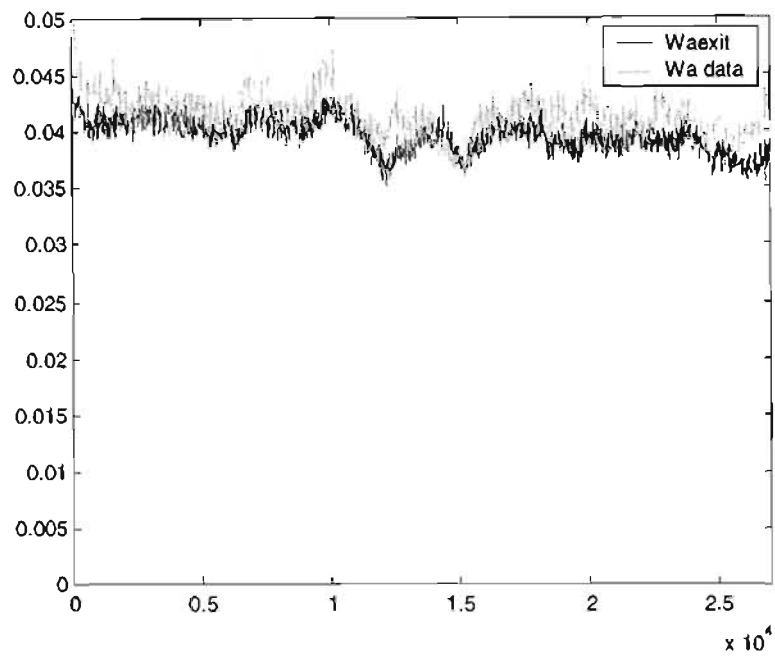


Figure D-5 : Comparison of air moisture content from the plant and the model

*D13 Closed loop response*

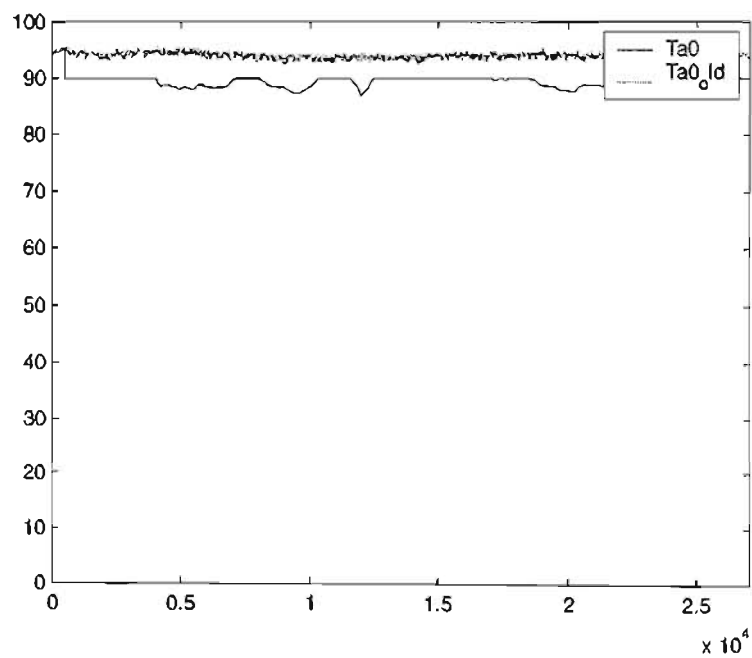


Figure D-1 : Control influence on the inlet air temperature

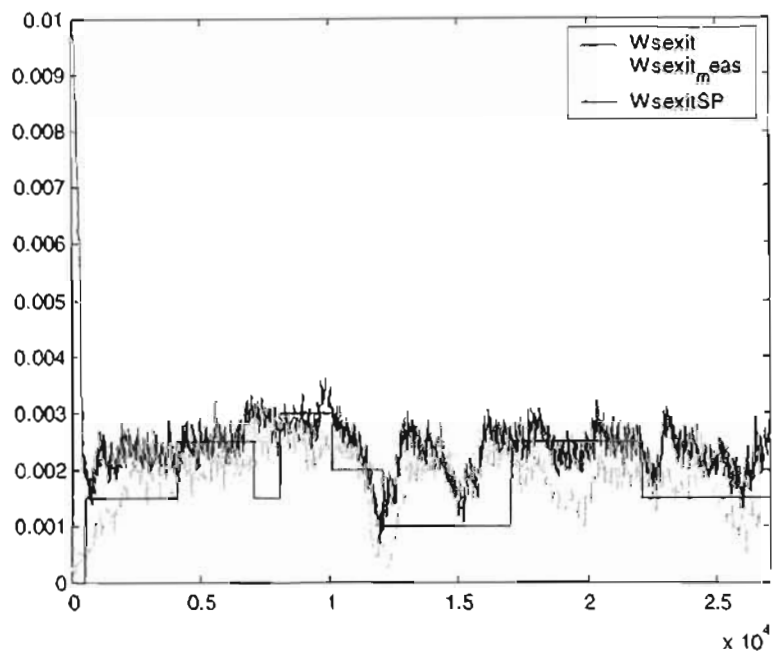


Figure D-2 : Control response on the exit sugar moisture content

## APPENDIX E PROGRAM

```

%*****
%**
%**          SUGAR DRYER MODEL with DYNAMIX MATRIX CONTROL
%**
%*****

clear all

t=0;

%Discretisation
L = 12.5; % [ m ]
n = 10;
dx = L/n; % [ m ]
dt = 0.25 ; % [ s ]
nsubstep =1;
tend=75000; % [ s ]
datastep=5;
recompute_gap=40;

%*****
%**          INIALISATION
%**
%*****

% FOR CONTROL
mnew=-9999;
mpresent=-9999;
WsnSP=-9999;
ndt=200; % no. of integration steps per control step
nopt=10; % Number of controller steps to horizon:
time=nopt*ndt*dt
scounter=ndt;
ocounter=nopt;
startflag=0;
Aso = zeros (5*n,5*n, nopt);
Bso = zeros (5*n, 3+3*n, nopt);

%-----
% FOR SUGAR AND AIR PROPERTIES
a =(6*(57e-5)^2)/(57e-5)^3; % [m2/m3 ]
Ar = 2.4; % [ m2 ]
roa = 0.9; % [kg/m3 of air]
ros = 1500; % [kg/m3 of dry sugar]
Cpa = 1.045; % [kJ/kg air.K ]
Cps = 1.25; % [kJ/kg dry sugar. K]
lambdaH2O = 2.385*10^3; % [kJ/kg water]
hs = 0.0625; % [m3 dry sugar / m3 of dryer space]
Ds = 1e-6; % [m2/s]
Da = 1e-6; % [m2/s]
MBS1dtowed=0; % Initialise air travel owed (in No. of dx's)
MBA1dtowed=0 ;

```

```

%-----
% FOR MATRIX AND VECTOR
X = zeros (5*n,1);
U = zeros (3+3*n,1);
Xo = zeros (5*n,nopt);
Uo = zeros (3+3*n,1);
I = eye(5*n,5*n);
CM=1e-30*ones(16,5);
CC=0.0*ones(16,5);      %convection coefficients
z = zeros (n,1);      %distance along dryer
for i=1:n
    z(i)=i*dx;
end
XTa=zeros(1,n);
XTs=zeros(1,n);
fa = zeros(n,1);  % [ kg/s ]
faf = zeros(n,1);
fax = zeros(n,1);
Waf = zeros(n,1);
Taf = zeros(n,1);

%-----
% FOR VECTORS FOR CALCULATION OF ALPHA, BETA and G
W=zeros(n,1);
S=zeros(n,1);
Imp=zeros(n,1);
TTs=zeros(n,1);
SOL=zeros(n,1);
SC=zeros(n,1);
SS=zeros(n,1);
PCDryS=zeros(n,1);
Bp=zeros(n,1);
pTs=zeros(n,1);
pBp=zeros(n,1);
ps=zeros(n,1);
beta=zeros(n,1);
pa=zeros(n,1);
alpha=zeros(n,1);
Ea=zeros(n,1);
G=zeros(n,1);
G0=zeros(n,1);
K2=zeros(n,1);
K4=zeros(n,1);
TaRH=zeros(n,1);
WaRH=zeros(n,1);
RH=zeros(n,1);

%-----
% FOR PLOTTING INFORMATION
dtplot = 50*dt;  % every 100 th point only
ntplot=round(tend/dtplot);
tplot=zeros(ntplot,1);
results=zeros(ntplot,19);  % for storage
tlastplot=0;
iplot=0;
nprofilemax= 6;
dtprofile = round(tend/nprofilemax);
tlastprofile=0;
iprofile=0;
Wminplot=0;
Wmaxplot=1;

```



```
tplot=zeros(ntplot,1);
Tsexit=zeros(ntplot,1);
Taexit=zeros(ntplot,1);
TaOP=zeros(ntplot,1);
TaOP_old=zeros(ntplot,1);
Tainlet=zeros(ntplot,1);
Wsexit=zeros(ntplot,1);
WsexitSP=zeros(ntplot,1);
Wsn_measP=zeros(ntplot,1);
Waexit=zeros(ntplot,1);
Gexit=zeros(ntplot,1);
Ts=zeros(n,1);
Ta=zeros(n,1);
Ws=zeros(n,1);
Wa=zeros(n,1);
Sf=zeros(n,1);
Ts_n=zeros(n,1);
Ta_n=zeros(n,1);
Ws_n=zeros(n,1);
Wa_n=zeros(n,1);
Sf_n=zeros(n,1);


%!!!!!!!!!!!!!!!!!!!!!!!!!!!!!!!!!!!!!!!!!!!!!!!!!!!!!!!!!!!!!! LOOP BEGINS !!!!!!!!!!!!!!!!!!!!!!!!!!!!!!!!!!!!!!!!!!!!!!!!!!!!!!!!

%*****
%**                               MODEL                                **
%*****

figure(1);
clf;
figure(2);
clf;
index=0;
datetime=0;
modeltime=0;
MBA1=0;
MBS1=0;
fa_factor=0;
fs_factor=0;
recompute_counter=recompute_gap;

Matrix_final_set_001213; % that opens the file with the data
index_max=4943;          % NB! MUST CHANGE FOR EACH DATA FILE

while t < tend
    recompute=0;

    t = t+dt;
    [t tend]
    modeltime=modeltime+dt;
    recompute_counter=recompute_counter+1;

%=====
%==                Present operating conditions (read from plant)        ==
%=====

if modeltime > datetime
    index=index+1;
```

```

    if index>index_max
        index=index_max;
    end
    if recompute_counter>recompute_gap
        recompute=1;
        recompute_counter=0;
    end
    datatime=datatime+datastep;
end

%%%%%%%%%%%%%%%%%%%%%%%%%%%%%%%%%%%%%%%%%%%%%%%%%%%%%%%%%%%%%%%%%%%%%%%%%%%%%%
%%%%%%%%%%%%%%%%%%%%%%%%%%%%%%%%%%%%%%%%%%%%%%%%%%%%%%%%%%%%%%%%%%%%%%%%%%%%%% BLOCK INPUT %%%%%%%%%%%%%%%%%%%%%%%%%%%%%%%%%%%%%%%%%%%%%%%%%%%%%%%%%%%%%%%%%%%%%%%%%%%%%%%
Ws0    =data_set(index,2);
Wa0    =data_set(index,3);
Ts0    =data_set(index,4);
Ta0    =data_set(index,5);
Sf0    =data_set(index,6);
fs     =data_set(index,7);
fa_in  =data_set(index,8);

%%%%%%%%%%%%%%%%%%%%%%%%%%%%%%%%%%%%%%%%%%%%%%%%%%%%%%%%%%%%%%%%%%%%%%%%%%%%%% BLOCK OUTPUT %%%%%%%%%%%%%%%%%%%%%%%%%%%%%%%%%%%%%%%%%%%%%%%%%%%%%%%%%%%%%%%%%%%%%%%%%%%%%%% from reconciliation
Wsn_meas =data_set(index,9);
Wan      =data_set(index,10);
Tsn      =data_set(index,11);
Tan      =data_set(index,12);
Sfn      =data_set(index,13);

%=====

%=====
%==                                Heat and Mass Transfer                                ==
%=====

ht= 1.35e-2 ;      % [kW / m2 K]
kg= 1.35e-9;      % [kg water / m2 s Pa]

%=====

RT=ros*Ar*L*hs/fs; %residential time
% force Super-saturation in crystal film to crystallization point
pur =98; %purity [kg sugar/ (kg sugar + kg impurity)]
If0=((100-pur)/pur)*Sf0; % kg impurity in film per kg dry sugar in
crystal

% condition of air feeds and exhausts
for i=1:n
    faf(i)=0.0;
    Waf(i)=0.0;
    Taf(i)=0.0;
    fax(i)=0.0;
end
faf(1)=fa_in;
Waf(1)=Wa0;
Taf(1)=Ta0;
% ( actually, fax(n) is reset to take care of the remaining air)

%=====

```

```

%==          Determination of the Vector flow "fa"          ==
%=====
    fain = zeros(2*n-1,1); % vector type Faf1 Fax1 ... Fafn-1 Faxn-1
Fafn
    for i=1:n-1
        fain(2*i-1)=faf(i);
        fain(2*i)=fax(i);
    end
    fain(2*n-1)=faf(n);

    Fmat1 = zeros (n,n);
    Fmat2 = zeros(n,2*n-1);

    for i=1:n-1
        Fmat1(i+1,i)=-1;
    end
    for i=1:n
        Fmat1(i,i)=1;
    end

    for i=1:n-1
        Fmat2(i,2*i)=-1;
        Fmat2(i,2*i-1)=1;
    end
    Fmat2(n,2*n-1) = 1;
    fa = inv(Fmat1)*Fmat2*fain; % vector type Fa1 ...Fan-1 Faxn

    fax(n,1) = fa(n,1);

    fa(n,1)=0;      % to be safe

    % Average of fair for MBA1
    fsum = 0;
    for i=1:n-1
        fsum = fsum + fa(i);
    end
    faverage=(fsum+ fax(n))/n;

%=====
%==          Initialisation of X and U          ==
%=====
    if t == dt
        for i=1:n
            X(i)      = Ws0;
            X(i+n)    = Wa0;
            X(i+2*n) = Cps*Ts0;
            X(i+3*n) = Cpa*Ta0;
            X(i+4*n) = Sf0;
        end
        for j=1:nopt
            Xo(:,j)=X(:);
        end
    end

    % set input vector
    U(1) = Ws0;
    U(2) = Cps*Ts0;
    U(3) = Sf0;
    for i=1:n
        U(3+i)=Waf(i);
    end

```

```

    U(3+i+2*n)=1;
    if i~=1
        U(3+i+n)= Cpa*Taf(i);    % from data file
    else
        if ((t~=dt)&(mnew~-9999))
            U(3+1+n)= mnew;        % computed on last control
calc    step late
        else
            U(3+1+n)= Cpa*Taf(1);    % from data file
        end
    end
end
end

%=====

%=====
%==                               Control computations                               ==
%=====

    Uo=U; *
    Uo(3+1+n)=U(3+1+n)+1; % Unit perturbation (only about 1C)
    scounter=scounter+1;
    if scounter>ndt
        scounter=1;
        ocounter=ocounter+1;
        if ocounter>nopt
            ocounter=1;
        end
        Xo(:,ocounter)=X(:);    % reset to present output;
    end

%=====

%=====
%==                               Axial Convection                               ==
%=====

    MBA1last=MBA1;
    MBS1last=MBS1;
    fa_factorlast=fa_factor;
    fs_factorlast=fs_factor;

    MBS2 = kg*a/ros;
    MBA2 = kg*a*hs/(roa*(1-hs));
    HBS1 = kg*a*lambdaH2O/ros;
    HBS2 = ht*a/(ros*Cpa);
    HBA1 = 1/(Ar*(1-hs)*roa*dx);
    HBA2 = a*ht*hs/(roa*Cps*(1-hs));
    MDs  = Ds/(dx*dx);
    MDa  = Da/(dx*dx);

    % Loading of A
    MBS1dtrequired = fs*dt/(Ar*hs*ros*dx);
    MBS1dtowed=MBS1dtowed+MBS1dtrequired;
    MBS1dt=max(0,round(MBS1dtowed));    % only convect in whole steps
    if MBS1dt>1
        error = 'dx/dt too small for sugar flow !!!!!'
        halt;
    end
    MBS1dtowed=MBS1dtowed-MBS1dt;
    MBS1=MBS1dt/dt;

```

```

if MBS1dt == 0
    fs_factor=0;
else
    fs_factor = MBS1dt / MBS1dtrequired;
end

MBA1dtrequired = faverage*dt/((1-hs)*Ar*roa*dx);
MBA1dtowed=MBA1dtowed+MBA1dtrequired;
MBA1dt=max(0,round(MBA1dtowed)); % only convect in whole steps
if MBA1dt>1
    error = 'dx/dt too small for air flow !!!!!'
    halt;
end
MBA1dtowed=MBA1dtowed-MBA1dt;
if MBA1dt == 1
    MBA1 = MBA1dt/dt;
    fa_factor = MBA1dt / MBA1dtrequired;
else
    MBA1=0;
    fa_factor=0;
end

if ((MBA1 ~= MBA1last)|(fa_factor ~= fa_factorlast))
    recompute=1;
end

if ((MBS1 ~= MBS1last)|(fs_factor ~= fs_factorlast))
    recompute=1;
end

if t==dt
    recompute=1;
end

%=====

%=====
%==                                     Tuning of A & B matrices                               ==
%=====

for o=1:(nopt+1)
    A = zeros (5*n,5*n); % reset all matrices to zero
    AC= zeros (5*n,5*n); % convection matrix
    B = zeros (5*n, 3+3*n);
    BC = zeros (5*n, 3+3*n); % convection matrix
    if o<=nopt
        Xt= Xo(:,o); % temporary 'X' versions with various
delays
    else
        Xt= X; % do the actual solution last so
solution values stay in arrays
    end
    if recompute % only do this if necessary
        %-----
        %Tuning of Vectors alpha , beta and G
        for i=1:n
            W(i)= Xt(i)*fs;
            S(i)= Xt(4*n+i)*fs;
            Imp(i)=If0;
            TTs(i)=Xt(2*n+i)/Cps;

```

```

        SOL(i)=64.407+0.07251*TTs(i)+0.0020569*TTs(i)^2-
9.035*10^-6*TTs(i)^3;
        Ea(i)=62.86-0.84*(TTs(i)-60);
        K2(i)=-(Ea(i)/8.314e-3)*(1/(273.16+TTs(i))-1/333.16);
        K0=0.005;
        K5=0.08;
        SC(i)= 1-K5*Imp(i)/W(i);
        SS(i) = (S(i)/W(i))*(100-SOL(i))/(SOL(i)*SC(i));
        K1=0.00000087;
        K3=1.75;
        PCDryS(i)=100*(S(i)+Imp(i))/(S(i)+Imp(i)+W(i));
        Bp(i)=100+2*PCDryS(i)/(100-PCDryS(i));
        pTs(i)=1367.6-132.54*TTs(i)+9.635*TTs(i)^2-
0.115*TTs(i)^3+0.00132*TTs(i)^4;
        T100=100;
        p100=1367.6-132.54*T100+9.635*T100^2-
0.115*T100^3+0.00132*T100^4;
        pBp(i)=1367.6-132.54*Bp(i)+9.635*Bp(i)^2-
0.115*Bp(i)^3+0.00132*Bp(i)^4;
        ps(i)=pTs(i)*p100/pBp(i)*min(1,1/SS(i));
        pa(i)=101325*(Xt(n+i)/18)/(Xt(n+i)/18 + 1/29);
        WaRH(i)=Xt(n+i);
        TaRH(i)=Xt(3*n+i)/Cpa;
        RH(i) = 100*1.01/(10^(5.083-
1665.6/(TaRH(i)+228)))*(0.62/WaRH(i)+1));
        G(i) =1* K1*(SS(i)-(1+K0))*exp(K2(i)-K3*Imp(i)/W(i));
        beta(i)=ps(i)/Xt(i);
        alpha(i)=pa(i)/Xt(n+i);
    end
    %-----

    for i=1:n
        if i==1
            ffaiml=0;
        else
            ffaiml=fa_factor*fa(i-1);
        end
        if i==n
            ffaip1=0;
        else
            ffaip1=fa_factor*fa(i+1);
        end
        ffax=fa_factor*fax(i);
        ffaf=fa_factor*faf(i);
        ffa=fa_factor*fa(i);

        %-----
        % Building of CM matrix
        %dWs/dt
        CM(1,1) = MDs; CC(1,1)= MBS1; %Wsi-1
        CM(2,1) = -2*MDs -MBS2*beta(i); CC(2,1)= - MBS1; %Wsi
        CM(3,1) = MDs ; %Wsi+1
        CM(5,1) = MBS2*alpha(i); %Wai

        %dWa/dt
        CM(2,2) = MBA2*beta(i); %Wsi
        CM(4,2) = MDa; CC(4,2) = ffaiml*HBA1; %Wai-1
        CM(5,2) = -2*MDa - MBA2*alpha(i); CC(5,2)= - ffax*HBA1 - ffa*HBA1; %Wai
        CM(6,2) = MDa; %Wai+1
        CM(16,2) = 0; CC(16,2)= ffaf*HBA1; %force
    end

```

```

% d(CpsTs)/dt
CM(2,3) = -HBS1*beta(i); %Wsi
CM(5,3) = HBS1*alpha(i); %Wai
CM(7,3) = MDs ; CC(7,3) = MBS1; %CpsTsi-1
CM(8,3) = -2*MDs - HBS2*Cpa/Cps ; CC(8,3) = - MBS1; %CpsTsi
CM(9,3) = MDs; %CpsTsi+1
CM(11,3) = HBS2; %CpaTai
CM(16,3) = 0; CC(16,3) = ffaf*HBA1; %force

% d(CpaTa)/dt
CM(8,4) = HBA2; %CpsTsi
CM(10,4) = MDa; CC(10,4) = ffaim1*HBA1; %CpaTai-1
CM(11,4) = -2*MDa - (Cps/Cpa)*HBA2; CC(11,4) = - ffax*HBA1 - ffa*HBA1; %CpaTai
CM(12,4) = MDa ; %CpaTai+1
CM(16,4) = 0; CC(16,4) = ffaf*HBA1; %force

% d(Sf)/dt
CM(13,5) = MDs; CC(13,5) = MBS1; %Sfi-1
CM(14,5) = -2*MDs; CC(14,5) = - MBS1; %Sfi
CM(15,5) = MDs ; %Sfi+1
CM(16,5) = -a*G(i); %force

for j=1:5
    ii=(j-1)*n+i;% row in full vector
    for k=1:5 % block order to be Ws,Wa,CpsTs,CpaTa,Sf
        jjoff = (k-1)*n;
        % A & AC ; B & BC matrix additions
        for m=1:3
            coeff = CM((k-1)*3+m,j);
            coeffC = CC((k-1)*3+m,j);
            ij=i+m-2;
            if ij<1
                if ((k~=2)&(k~=4))
                    kk=(k+1)/2;
                    B(ii,kk)= B(ii,kk) + coeff; % forcing boundary
                    conditions
                    BC(ii,kk)= BC(ii,kk) + coeffC; % forcing boundary
                    conditions
                end;
            else
                if ij>n
                    A(ii,k*n)= A(ii,k*n) + coeff; % sets flat
                    prifile at 'n'
                    AC(ii,k*n)= AC(ii,k*n) + coeffC; % sets flat
                    prifile at 'n'
                else
                    jj = jjoff+ij;
                    A(ii,jj)= A(ii,jj) + coeff;
                    AC(ii,jj)= AC(ii,jj) + coeffC;
                end
            end
        end
    end
end
% B matrix additions
if j==2
    B(ii,3+i) = B(ii,3+i) + CM(16,j);
    BC(ii,3+i) = BC(ii,3+i) + CC(16,j);
else
    if j==4
        B(ii,3+n+i) = B(ii,3+n+i) + CM(16,j);
        BC(ii,3+n+i) = BC(ii,3+n+i) + CC(16,j);
    end
end

```

```

        else
            if j==5
                B(ii,3+2*n+i) = B(ii,3+2*n+i) + CM(16,j);
                BC(ii,3+2*n+i) = BC(ii,3+2*n+i) + CC(16,j);
            end
        end
    end
end
end
end

%=====
%==                                Integration                                ==
%=====
% for singular A use series to find "expmAdt_IdivA" = [expm(A*dt)-
I]*A^-1
    subdt = dt/nsubstep;
    tolerance=1e-10;
    change=99;
    expmAdt_IdivA=subdt*I;
    * changemat=subdt*I;
    Adt=A*subdt;

    k=1;
    while change>tolerance
        k=k+1;
        changemat=(changemat*Adt)/k;
        change=sum(sum(abs(changemat))); % makes a 1-by-n vector
with the sum of the columns as its entries
        expmAdt_IdivA=expmAdt_IdivA+changemat;
    end;

    if o<=nopt
        Aso(:, :, o)=expmAdt_IdivA*Adt+I;
        Bso(:, :, o)=expmAdt_IdivA*B;
    else
        As=expmAdt_IdivA*Adt+I;
        Bs=expmAdt_IdivA*B;
    end
end
end

% Now integrate rest using matrix exponential over substeps

% Operator - splitting : First do convection step by Euler
if o<=nopt
    Xo(:, o) = Xo(:, o) + dt*(AC*Xo(:, o) + BC*Uo);
else
    X = X + dt*(AC*X + BC*U);
end

for i=1:nsubstep
    if o<=nopt
        Xo(:, o) = Aso(:, :, o)*Xo(:, o) + Bso(:, :, o)*Uo;
    else
        X = As*X + Bs*U;
    end
end
end
end

%*****
%**                                DYNAMIC MATRIX CONTROL ALGORITHM                                **
%*****

```



```

if t==dt % first step
    DM=zeros(nopt,nopt); % Dynamic Matrix (use a simple
                        % square system)
    DMol=zeros(nopt,nopt); % Openloop Matrix
    DM0=zeros(nopt,nopt); % Measurement Offset Matrix
    % Initialise counter for Control Time Steps
    ncount=0;
    % Initilaise vector of previous control moves
    dmpast=zeros(nopt,1);
    % Set up Tuning Matrices WW & Lam
    WW=zeros(nopt,nopt);
    for i=1:nopt
        WW(i,i)=60000000;
    end
    Lam=1;
    % Limits for Output
    mmax=Cpa*90; % allow a max air temperature of 90C
    mmin=Cpa*30; % allow a min air temperature of 30C
    % Flag value for control action as warning that it is not yet
    % available
    mnew=-9999;
end

if scounter==ndt % Time for a control step
    if ocounter==nopt % have done ndt steps since the nopt
                    % perturbation now allow control
        startflag=1;
    end
    ControlSwitch=1;
    if ((ControlSwitch==1) & (startflag==1)) % use this to switch
the controller on at a particular time
        % Make Dynamic Matrix DM
        for i=1:nopt
            for jj=1:i
                kk=ocounter-jj+1;
                if kk<1
                    kk=kk+nopt; % wrap around
                end
                j=i-jj+1;
                DM(i,j)=Xo(n,kk)-X(n); % only the difference
caused by the unit shift in input
            end
        end
        % Make Openloop Matrix DMol & Offset Measurement Matrix DM0
        for i=1:nopt
            for j=1:nopt
                jj=min(nopt,nopt+i-j+1);
                DMol(i,j)=DM(nopt,nopt+1-jj); % pick off
backwards along bottom line of DM
                jjj=nopt-j+1;
                DM0(i,j)=DM(nopt,jjj);
            end
        end
    end

%=====
%==                               Set point                               ==
%=====

    if t>0
        WsnSP=0.0015;
    end

```

```

if t>4000
    WsnSP=0.0025;
end
if t>7000
    WsnSP=0.0015;
end
if t>8000
    WsnSP=0.0030;
end
if t>10000
    WsnSP=0.0020;
end
if t>12000
    WsnSP=0.0010;
end
if t>16000
    WsnSP=0.0015;
end
if t>17000
    WsnSP=0.0025;
end
if t>22000
    WsnSP=0.0015;
end
if t>28000
    WsnSP=0.0070;
end
if t>30000
    WsnSP=0.0020;
end
if t>38000
    WsnSP=0.0010;
end
if t>40000
    WsnSP=0.0015;
end
if t>46000
    WsnSP=0.006;
end
if t>47000
    WsnSP=0.0015;
end
if t>52000
    WsnSP=0.0030;
end
if t>56000
    WsnSP=0.0020;
end
if t>58000
    WsnSP=0.0010;
end
if t>62000
    WsnSP=0.0015;
end
if t>64000
    WsnSP=0.0025;
end
if t>67000
    WsnSP=0.0015;
end
if t>68000

```

```

        WsnSP=0.0030;
    end
    if t>70000
        WsnSP=0.0070;
    end
    if t>72000
        WsnSP=0.0010;
    end

%=====

    Wsn=X(n); % Actual value

    eol=ones(nopt,1)*(Wsn-WsnSP)+(DMol-DM0)*dmpast;
    % only one move, so only 1st col of DM
    DMs=DM(:,1);
    % only do least squares part, not constrained search
    dmopt=-inv(DMs'*WW*DMs+Lam)*DMs'*WW*eol;
    mpresent=U(3+n+1);
    * mnew=mpresent+dmopt;
    % Clip externally to limits
    mnew=min(mmax,max(mmin,mnew)); % actual new absolute
control action to be used
    dmused=mnew-mpresent;
    else
        mnew=-9999; % back off line
        WsnSP=-9999;
        if mpresent~-9999
            dmused=U(3+n+1)-mpresent; % keep the moves that are
going on "manually" will help control
            mpresent=U(3,n,1);
        else
            dmused=0;
        end
    end
    % Update past moves vector
    for i=1:(nopt-1)
        dmpast(i)=dmpast(i+1);
    end
    dmpast(nopt)=dmused; % newest move at bottom of vector
end

%*****
%** Store for plotting and plotting **
%*****

% store points for time-plot if time is right
if (t-tlastplot)>=dtplot
    iplot=iplot+1;
    tplot(iplot)=t;
    Wsexit(iplot)=X(n);
    Waexit(iplot)=X(2*n);
    Tsexit(iplot)=X(3*n)/Cps;
    Taexit(iplot)=X(4*n)/Cpa;
    Tainlet(iplot)=X(3*n+1)/Cpa;
    Gexit(iplot) = G(n);

    Wa_n(iplot)=Wan;
    Ts_n(iplot)=Tsn;
    Ta_n(iplot)=Tan;
    Sf_n(iplot)=Sfn;

```

```

if mnew==-9999
    Ta0P(iplot)=Ta0;
    Ta0P_old(iplot)=Ta0;
else
    Ta0P(iplot)=mnew/Cpa;
    Ta0P_old(iplot)=Ta0;
end;
WsexitSP(iplot)=WsnSP;
Wsn_measP(iplot)=Wsn_meas;

% store results
results(iplot,1)=t;
results(iplot,2)=fs;
results(iplot,3)=fa_in;
results(iplot,4)=Ws0;
results(iplot,5)=Wa0;
results(iplot,6)=Ts0;
if mnew==-9999
    * results(iplot,7)=Ta0;
else
    results(iplot,7)=mnew/Cpa;
end;
results(iplot,8)=Sf0;
results(iplot,9)=X(n);
results(iplot,10)=Wan;
results(iplot,11)=Tsn;
results(iplot,12)=Tan;
results(iplot,13)=Sfn;
results(iplot,14)=X(n);
results(iplot,15)=X(2*n);
results(iplot,16)=X(3*n)/Cps;
results(iplot,17)=X(4*n)/Cpa;
results(iplot,18)=X(5*n);
results(iplot,19)=WsnSP;

tlastplot=t;
end;

for i=1:n
    Ws(i)=X(i);
    Wa(i)=X(n+i);
    Ts(i)=X(2*n+i)/Cps;
    Ta(i)=X(3*n+i)/Cpa;
    Sf(i)=X(4*n+i);

end

% plot chosen profiles if time is right
if (t-tlastprofile)>=dtprofile
    iprofile=iprofile+1;
    if iprofile<=nprofilemax

        figure(1);
        subplot(2,nprofilemax/2,iprofile);
        plot(z,Ts,'b',z,Ta,'r');
        axis ([0 z(n) 0 100]);
        legend('Ts','Ta');
        title(t)
    end
end

```

```

        figure(2);
        subplot(2,nprofilemax/2,iprofile);
        plot(z,Ws,'b',z,Wa,'r');
        axis ([0 z(n) 0 0.1]);
        legend('Ws','Wa');
        title(t)

    end
    tlastprofile=t;
end

RHn = 100*1.01/(10^(5.083-1665.6/(Ta(n)+228))*(0.62/Wa(n)+1));

end % of time loop

%Save Results
save results.dat results -ascii -tabs;

% final profiles
figure (3);
clf;
subplot(2,2,1);
plot(z,Ws,'r');
axis ([0 z(n)0 0.02]);
legend('Ws');

subplot(2,2,2);
plot(z,Wa,'r');
axis ([0 z(n)0 0.05]);
legend('Wa');

subplot(2,2,3);
plot(z,Ts,'b');
axis ([0 z(n) 0 100]);
legend('Ts');

subplot(2,2,4);
plot(z,Ta,'k');
axis ([0 z(n) 0 100]);
legend('Ta');

% time variations
figure (4);
clf;
plot
(tplot(1:iplot),Tsexit(1:iplot),'b',tplot(1:iplot),Taexit(1:iplot),'g'
);
axis ([0 tplot(iplot) 0 100]);
legend('Tsexit','Taexit');

figure (5);
clf;
plot
(tplot(1:iplot),Wsexit(1:iplot),'r',tplot(1:iplot),Waexit(1:iplot),'y'
)
axis ([0 tplot(iplot) 0 0.04]);
legend('Wsexit','Waexit');

```

```

figure (6);
clf;
plot
(tplot(1:ipplot),Wsexit(1:ipplot),'r',tplot(1:ipplot),Wsn_measP(1:ipplot),
'y',tplot(1:ipplot),WsexitSP(1:ipplot),'b')
axis ([0 tplot(ipplot) 0 0.01]);
legend('Wsexit','Wsexit_meas','WsexitSP');

figure (7);
clf;
plot
(tplot(1:ipplot),Waexit(1:ipplot),'r',tplot(1:ipplot),Wa_n(1:ipplot),'y')
axis ([0 tplot(ipplot) 0 0.05]);
legend('Waexit','Wa data');

figure (8);
clf;
plot
(tplot(1:ipplot),Tsexit(1:ipplot),'b',tplot(1:ipplot),Ts_n(1:ipplot),'g');
axis ([0 tplot(ipplot) 0 100]);
legend('Tsexit','Ts data');

figure (9);
clf;
plot
(tplot(1:ipplot),Taexit(1:ipplot),'b',tplot(1:ipplot),Ta_n(1:ipplot),'g');
axis ([0 tplot(ipplot) 0 100]);
legend('Taexit','Ta data');

figure (10);
clf;
plot
(tplot(1:ipplot),Ta0P(1:ipplot),'b',tplot(1:ipplot),Ta0P_old(1:ipplot),'g'
);
axis ([0 tplot(ipplot) 0 100]);
legend('Ta0','Ta0_old');

eq_Ts = Ts(n)
eq-Ta = Ta(n)
eq_Wa = Wa(n)
eq_Ws = Ws(n)
eq_RH = 100*1.01/(10^(5.083-1665.6/(Ts(n)+228))*(0.62/Wa(n)+1))
eq_Sf = Sf(n)

save LASTRUN;

```